Ion Optics of Fragment Separators

Helmut Weick, GSI Helmholtz Center

NUSYS School, Zhuhai 28th July 2024

1. Basic Ion Optics Decription
   (transfer map, lenses, phase space ellipse, beam envelopes)
2. Ion Optics of Separators
3. Separation with Degrader -> Fragment separator

break

4. Higher Order Optics, Large Apertures, Fringe-Fields
5. Modern Fragment Separator Systems
6. FAIR Facility Status

1. Basic Ion Optics Description

Ion Optical Coordinates

We look at beamline, use coordinates relative to the nominal optical axis.

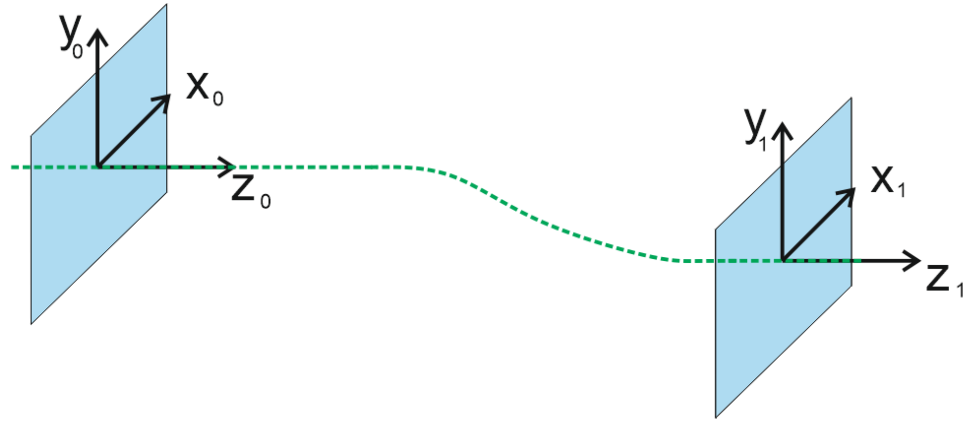

Transverse motion:

$x' = dx / dz$

$y' = dy / dz$

Often defined as derivative in path with coordinates of single ions.

$a = p_x / p_0$

$b = p_y / p_0$

With common constant p_0 we can use a normal Hamiltonian.

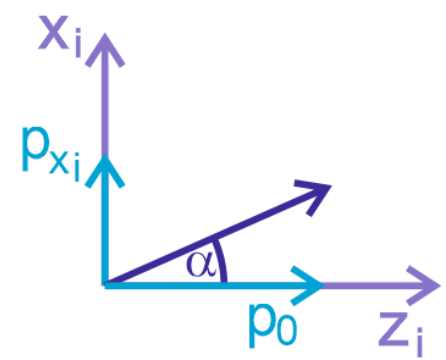

for same forward momentum $x' = a$,
for small angles $x' = a = \tan(\alpha) \sim \alpha$

Magnetic Rigidity ($B\rho$)

$B\rho := p / q$

p = momentum

q = charge

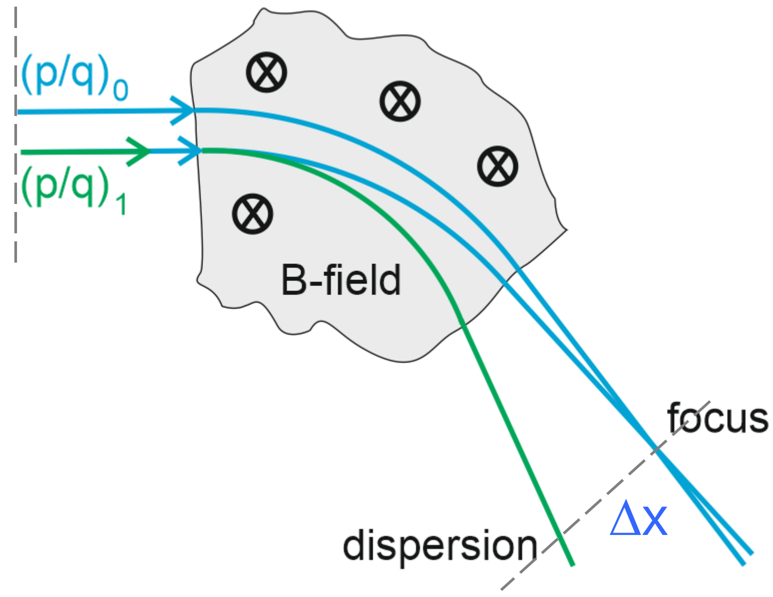

In a homogenous field with flux density B perpendicular to the direction of motion, ions of magnetic rigidity $B\rho$ are bend on a radius ρ.

Ions with relative deviation in $\delta := \Delta B\rho / B\rho_0$ from given reference arrive at a shifted position on the detector. Shift Δx per δ is called dispersion coefficient $(x|\delta)$.

In magnets not mass, charge or velocity are important only $B\rho$.

Similar definition for in electrostatic fields $E\rho := mv^2 / q$

Optical Elements – Dipole Magnets

Dipole magnets to deflect the beam.
We want a homogeneous magnetic field to bend the beam on a constant radius --> sector magnets of H shape.

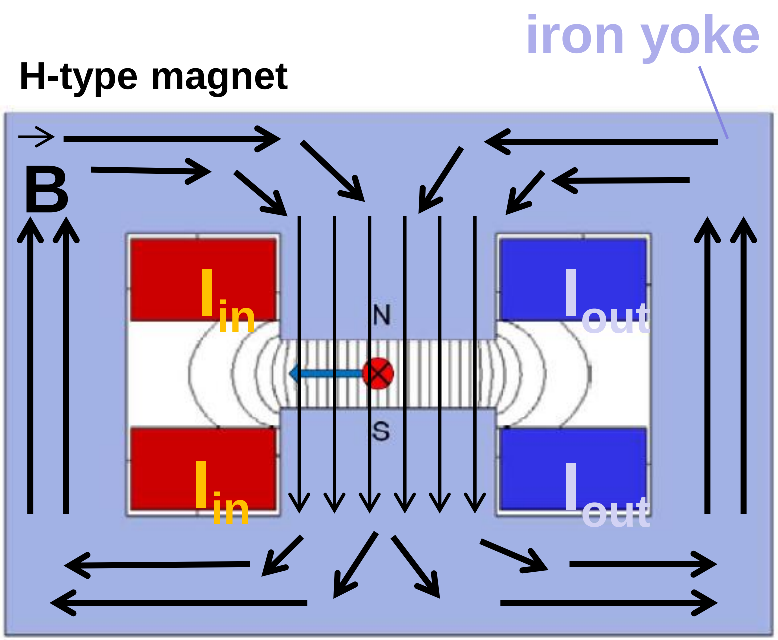

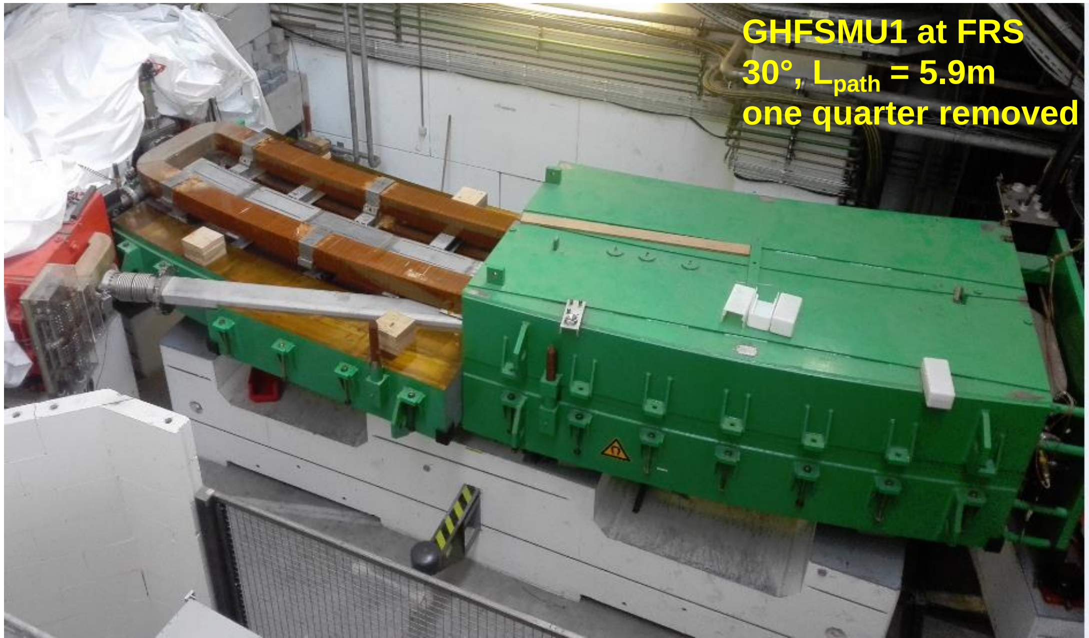

Transfer Matrix Description

Transfer function on vector of coordinates

In practise use Taylor expansion of this function, $(x,a) = \dfrac{\partial x_f}{\partial a_i}$

1st order transfer matrix T :

$$
\begin{pmatrix} X \\ a \\ Y \\ b \\ \delta \end{pmatrix}_f = \left(\begin{array}{ccccc} (X,X) & (X,a) & \multicolumn{2}{c}{\boxed{=0}} & (X,\delta) \\ (a,X) & (a,a) & & & (a,\delta) \\ \multicolumn{2}{c}{\boxed{=0}} & (Y,Y) & (Y,b) & \boxed{=0} \\ & & (b,Y) & (b,b) & \\ \multicolumn{4}{c}{\boxed{=0}} & \boxed{=1} \end{array}\right) \begin{pmatrix} X \\ a \\ Y \\ b \\ \delta \end{pmatrix}_i
$$

Det (T) = 1
Liouville's theorem

with bending only in one plane
only forces in x or y direction
momentum conservation

Full system $T_{tot} = T_n * \ldots * T_3 * T_2 * T_1$

Transfer Matrix Example

focusing with one thin lens

$$\begin{pmatrix} x(z) \\ a(z) \end{pmatrix} = \begin{pmatrix} (x|x) & (x|a) \\ (a|x) & (a|a) \end{pmatrix} \begin{pmatrix} x_1 \\ a_1 \end{pmatrix}$$

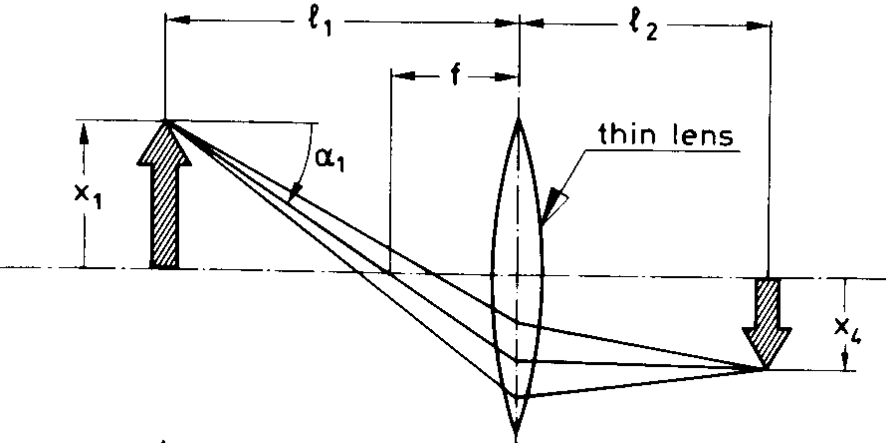

Transfer matrices for:

free space with length l_1

$x \rightarrow x + l_1 \tan(\alpha)$

$$T_{21} = \begin{pmatrix} 1 & l_1 \\ 0 & 1 \end{pmatrix}$$

thin lens with focal length f

$$T_{32} = \begin{pmatrix} 1 & 0 \\ -1/f & 1 \end{pmatrix}$$

free space with length l_2

$$T_{43} = \begin{pmatrix} 1 & l_2 \\ 0 & 1 \end{pmatrix}$$

combined system:

$$\begin{pmatrix} x_4 \\ \tan\alpha_4 \end{pmatrix} = \begin{pmatrix} 1 & l_2 \\ 0 & 1 \end{pmatrix} \begin{pmatrix} 1 & 0 \\ -1/f & 1 \end{pmatrix} \begin{pmatrix} 1 & l_1 \\ 0 & 1 \end{pmatrix} \begin{pmatrix} x_1 \\ \tan\alpha_1 \end{pmatrix}$$

$$= \begin{pmatrix} 1 - l_2/f & =0 \\ -1/f & 1 - (l_1/f) \end{pmatrix} \begin{pmatrix} x_1 \\ \tan\alpha_1 \end{pmatrix}$$

image (point to point) when $(x|a) = 0$

magnification

$(x|x) = 1 - l_2/f \quad \rightarrow -1 \quad (\text{for } f = l_2/2)$

H. Wollnik, optics of charged particles, Academic Press (1987).

Focusing Elements

perfect linear lens

$\tan(\alpha) \propto x$

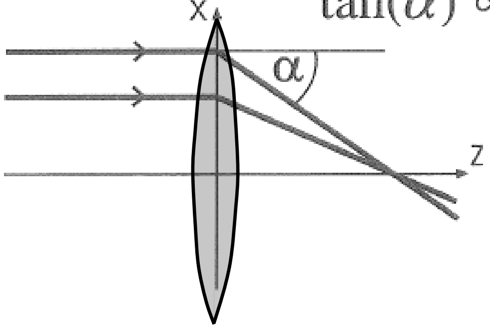

requires force F_x proportional to x

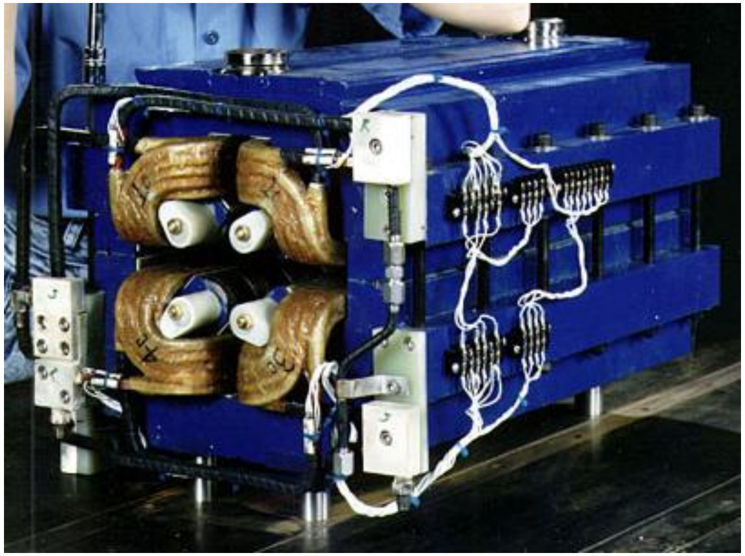

realisation as quadrupole magnet

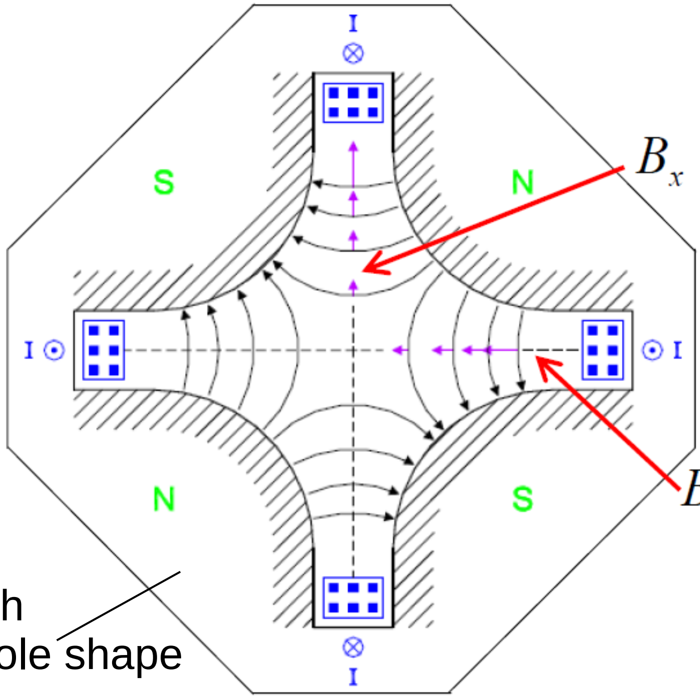

$$B_x = g \cdot y \quad \Rightarrow \quad F_y = g \cdot y$$

defocusing

$$B_y = -g \cdot x \quad \Rightarrow \quad F_x = -g \cdot x$$

focusing !

iron yoke with
hyperbolic pole shape

Focusing Elements

one quadrupole does
not solve the problem

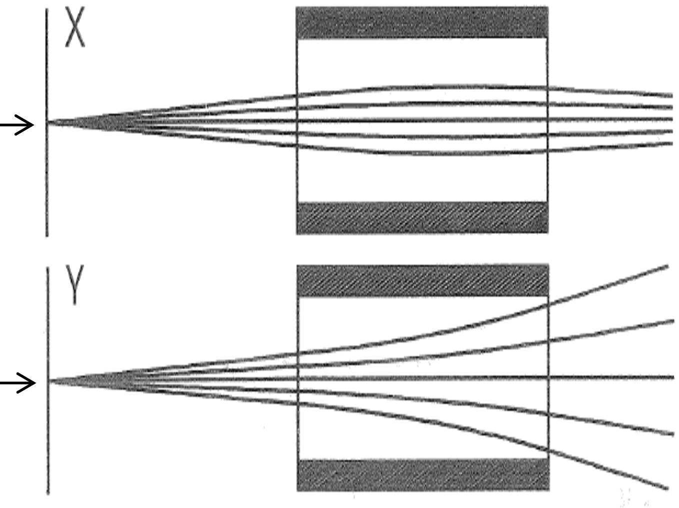

many quadrupole magnets
combined can focus in x and y

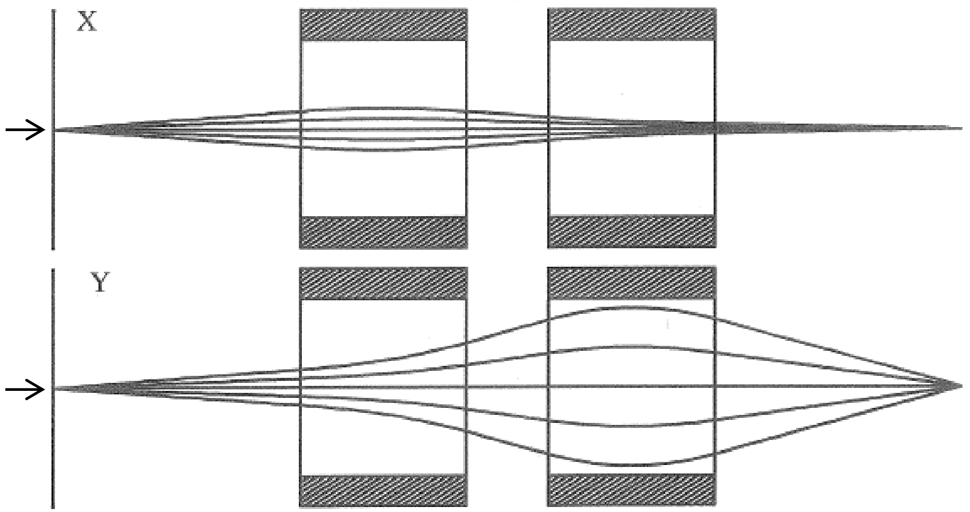

quadrupole channel with
different trajectories

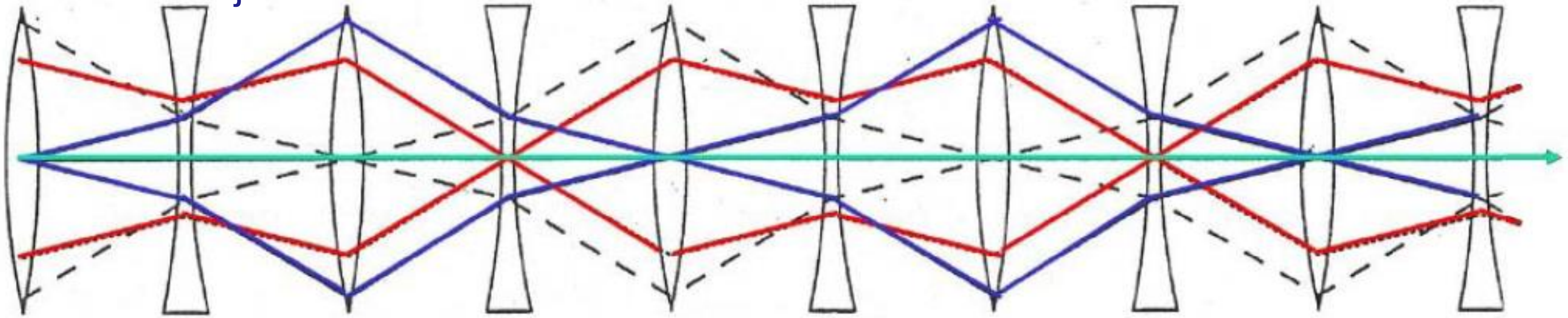

How to Describe a Beam

Beam emittance

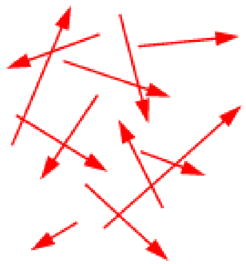

plasma

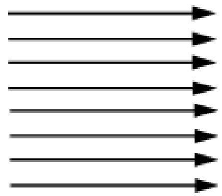

beam

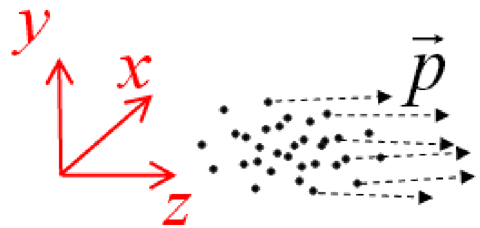

real beam

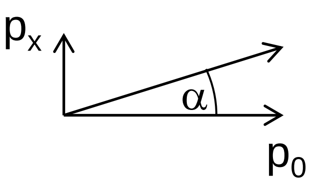

Phase space diagram

$$\frac{p_x}{p_0} = \tan(\alpha) = a$$

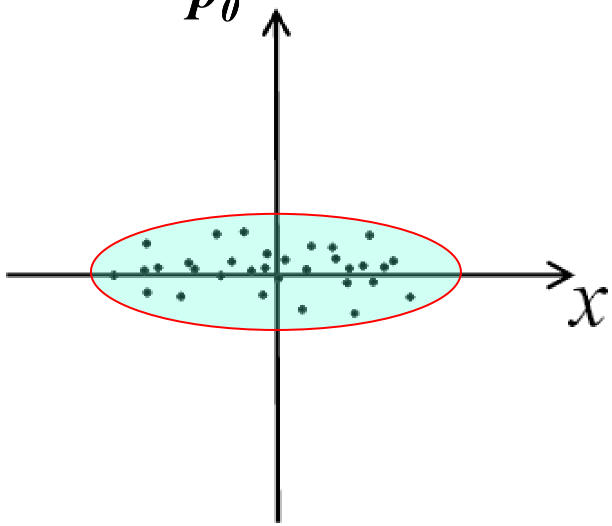

Area is often described well by an ellipse.

emittance ε = ellipse area / π

same with y, b and in longitudinal (z) direction
$\delta_p = \Delta p_z/p_0$ vs. z, or
$\delta_E = \Delta E/E_0$ vs. time t.

Definition of Phase-Space Ellipse

Described by beam parameters* α, β, γ and emittance ε.
Under linear transformation ellipse stays ellipse.

$$\gamma x^2 + 2\alpha\, xa + \beta\, a^2 = \varepsilon$$

Any linear transformation again leads to an ellipse.

$$\begin{pmatrix} x \\ a \end{pmatrix}_f = \begin{pmatrix} (x,x) & (x,a) \\ (a,x) & (a,a) \end{pmatrix} \cdot \begin{pmatrix} x \\ a \end{pmatrix}_i$$

Beam diameter defined by parameter β, scales with emittance ε, i.e. $\beta\gamma - \alpha^2 = 1$

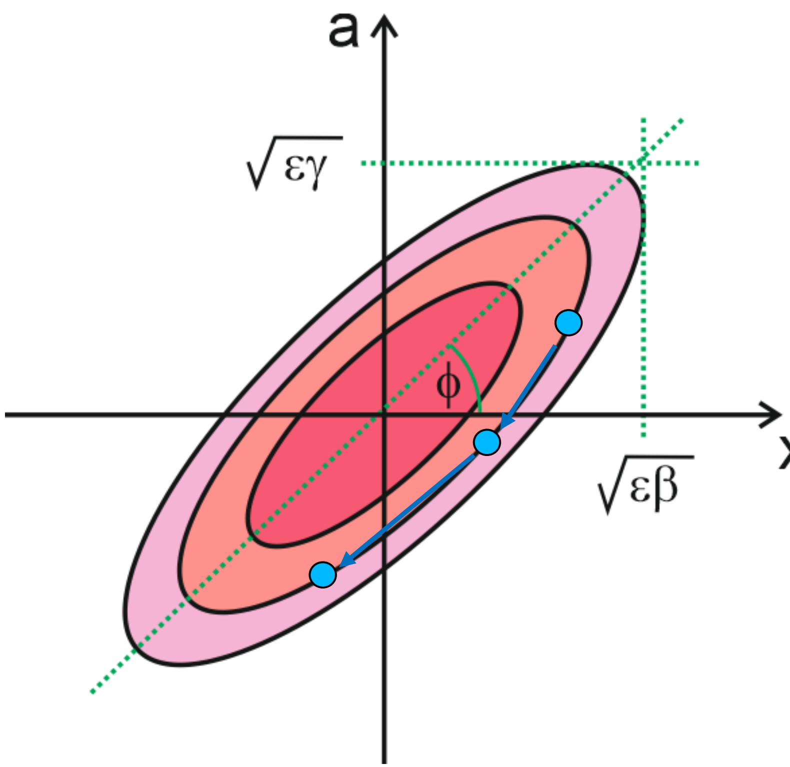

Emittance is constant (Liouville in const. electro-magn. fields), valid also for subellipses.
$\Rightarrow$ ions travel on ellipse, back and fourth.

In systems with independent planes use separate ellipses for x and y

* first used by Courant & Snyder 1953, sometimes also called Twiss parameters.

Dynamics of Phase-Space Ellipse

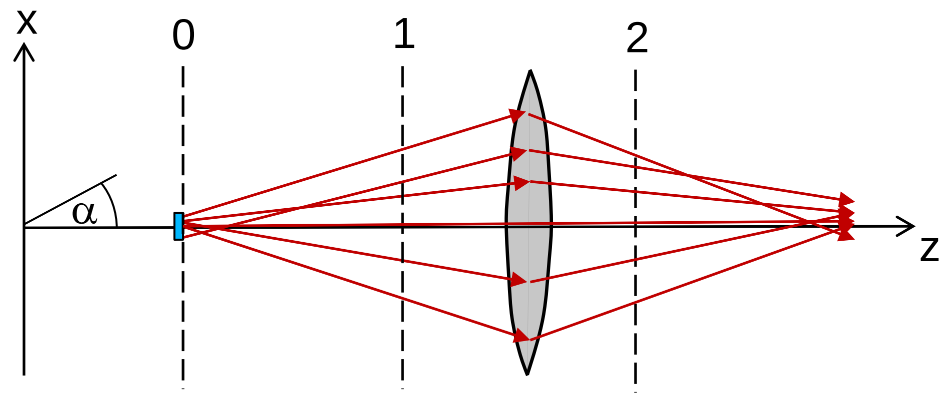

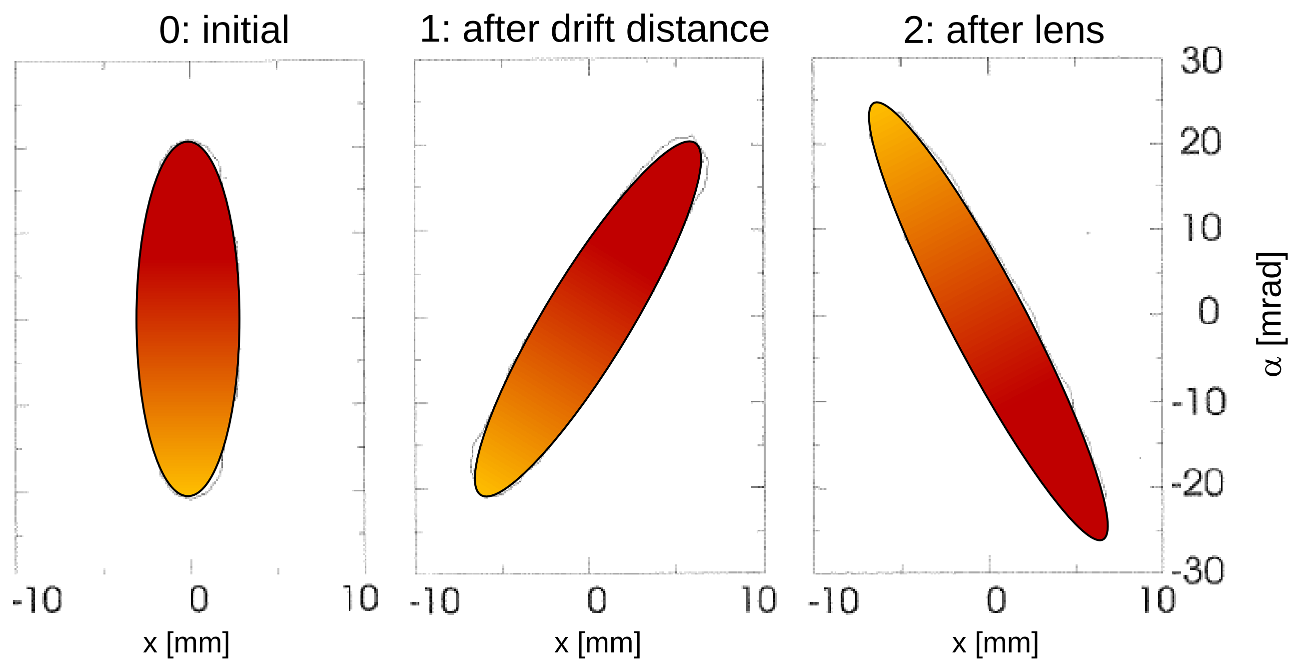

Old TSR storage ring in Heidelberg

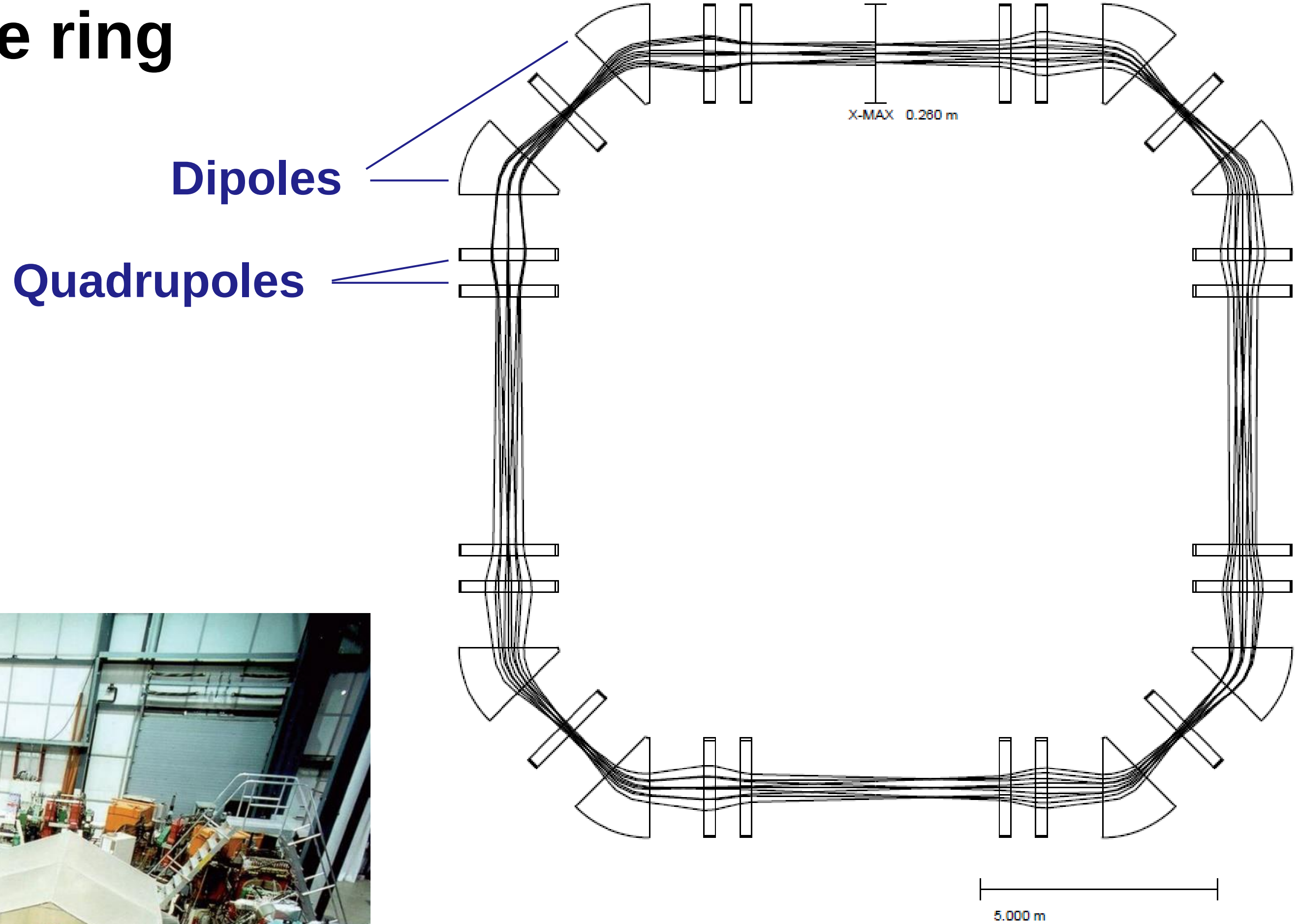

TSR storage ring beam ellipses

ε = 100 mm mrad

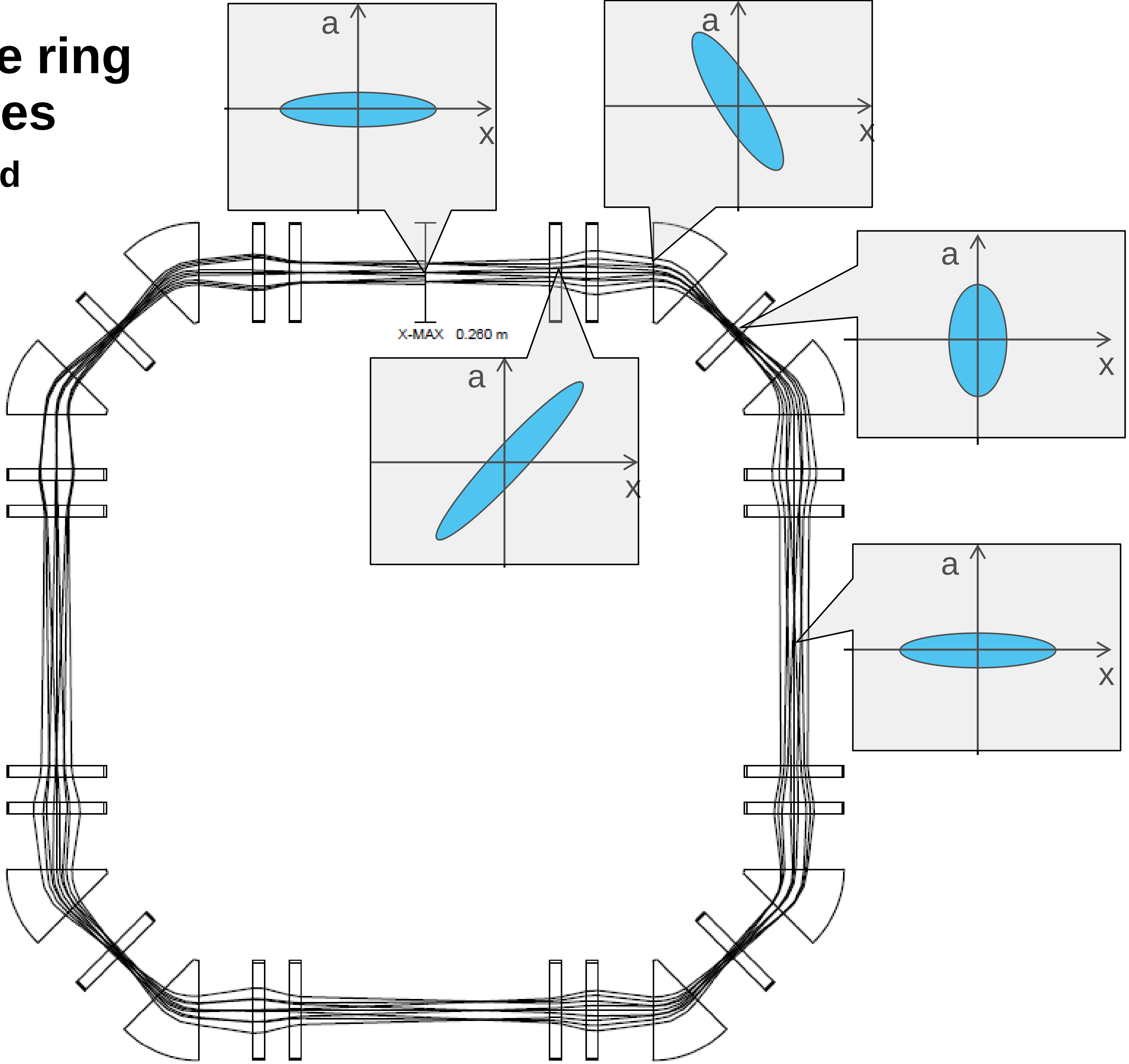

Beam envelopes in TSR storage ring

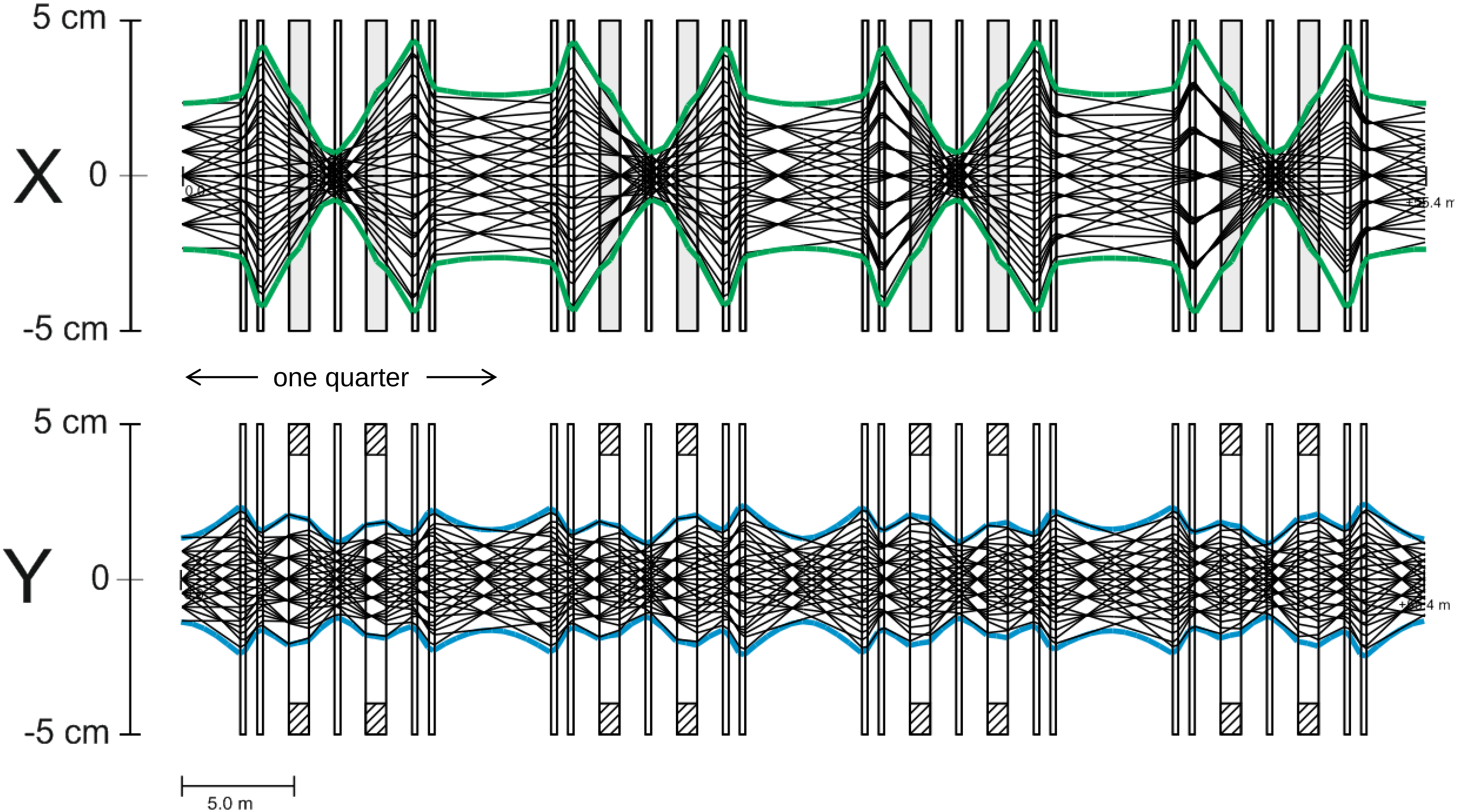

Periodic structure, will envelope stay within fixed limits or diverge?
Elliptic or hyberbolic solution of 2nd order ODE.
Stable when for single cell: Trace(**T**) = |(x,x)+(a,a)| ≤ 2

2. Ion Optics of Separators

Resolution of Separator

Resolving power $$R = \frac{(x,\delta)}{\Delta x_f} = \frac{(x,\delta)}{(x,x)\,\Delta x_i}$$

High R needed to separate not only by mass number but also by binding energy, R > 10 000.
Use dipole magnet most effectively.
In an almost parallel beam small changes of deflection angle are most sensitive.
➔ stretch phase space, make beam very wide.

$$R = \frac{1}{x_0\, a_0} \int \frac{\vec{B}(s)}{B\rho}\, d\vec{f}$$

maximize area in dipoles

DESIR-HRS @ GANIL

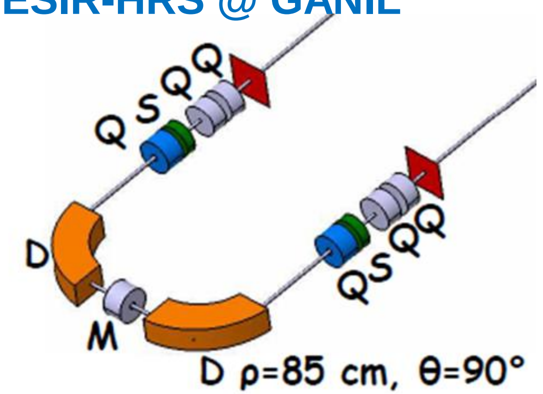

T. Kurtukian-Nieto et al., NIM B (2013) 317

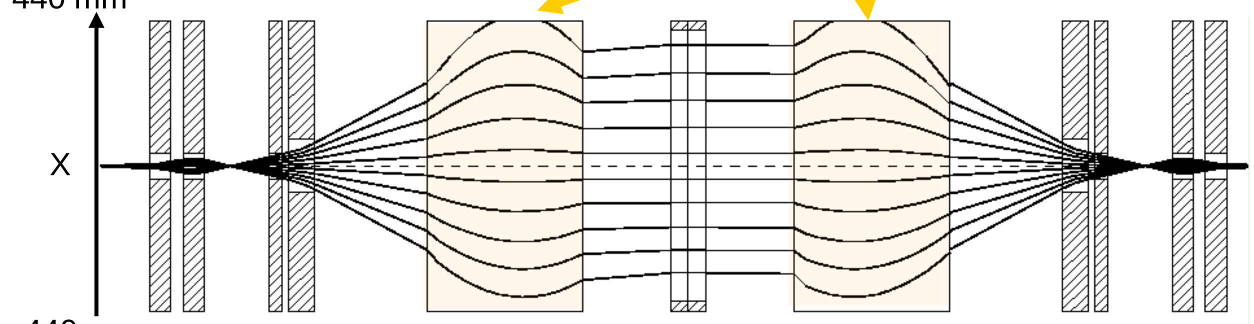

trajectories

$x_0\, a_0$ = 0.5mm x 7 mrad

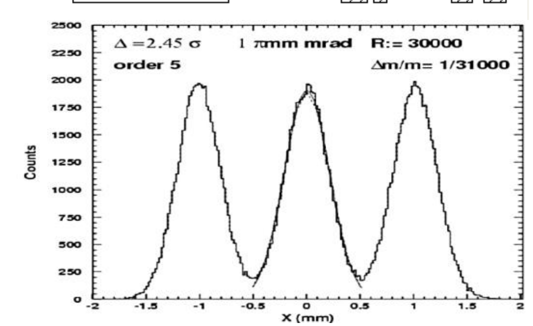

Small emittance of course helps (beam cooling).

Beam Interaction

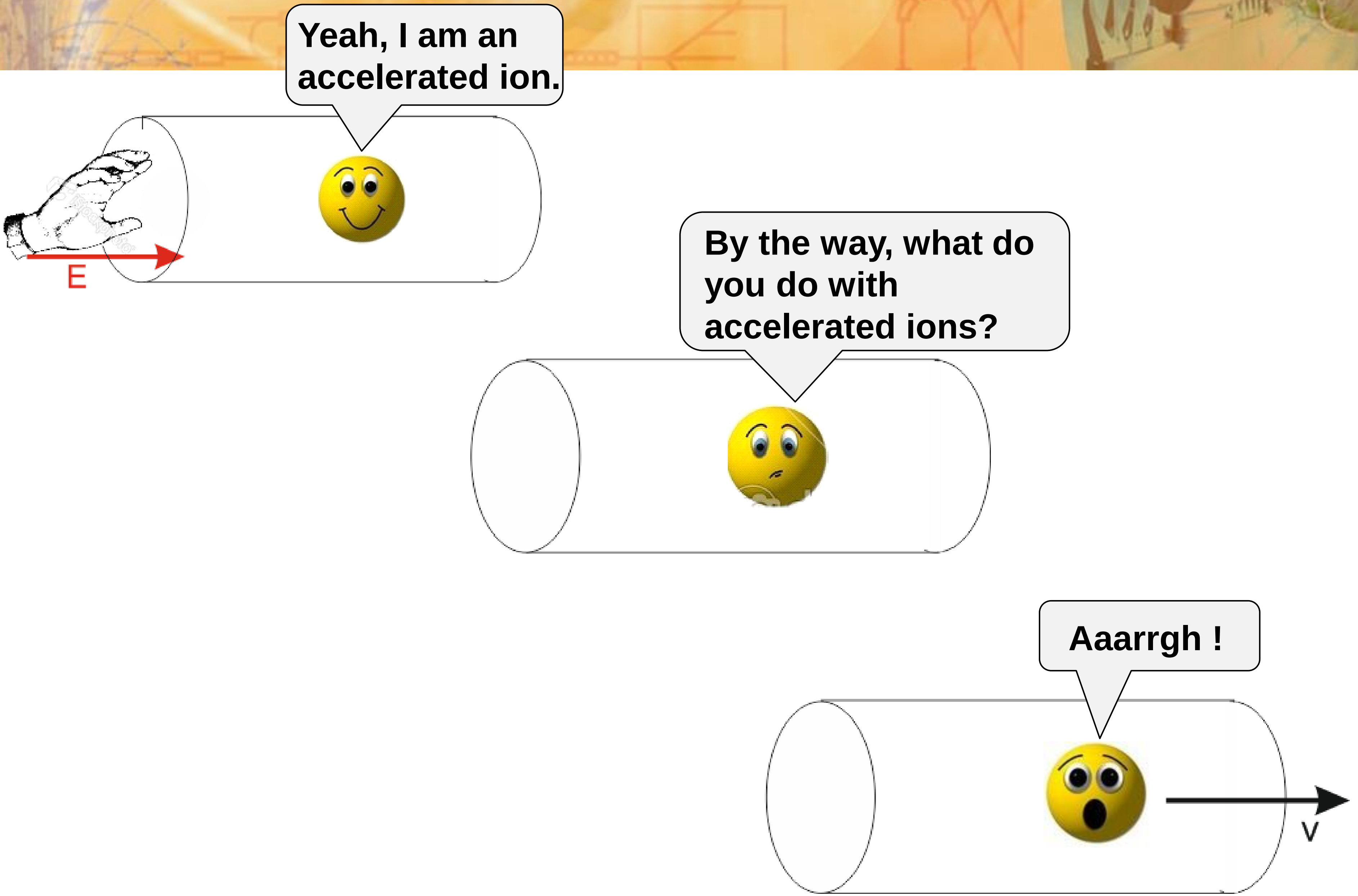

Emittance Growth with Targets

Momentum transfer by reaction in target increases transverse momentum spread, but in a thin target Δx does not change much.

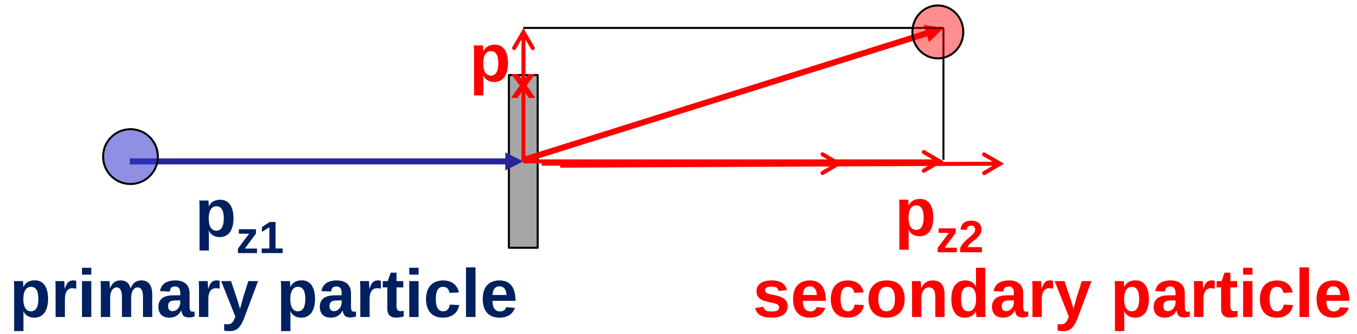

Make small beam spot to avoid large emittance for secondary beam

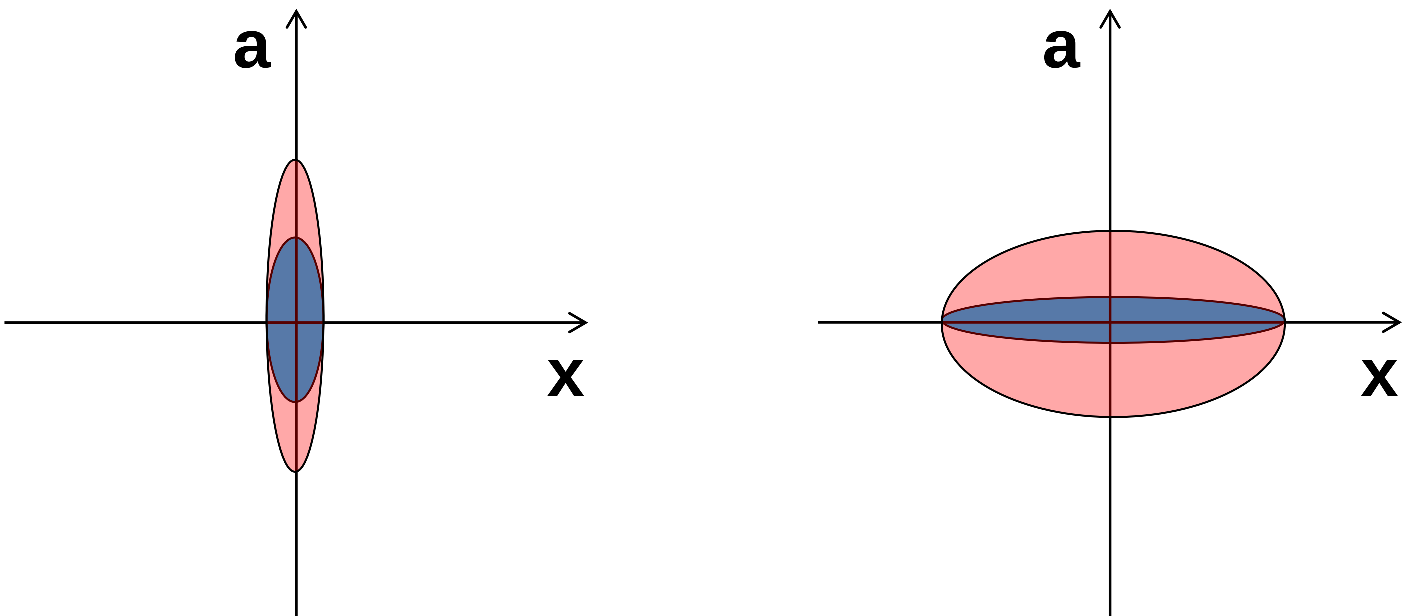

Fragmentation and Fission as source of rare isotopes

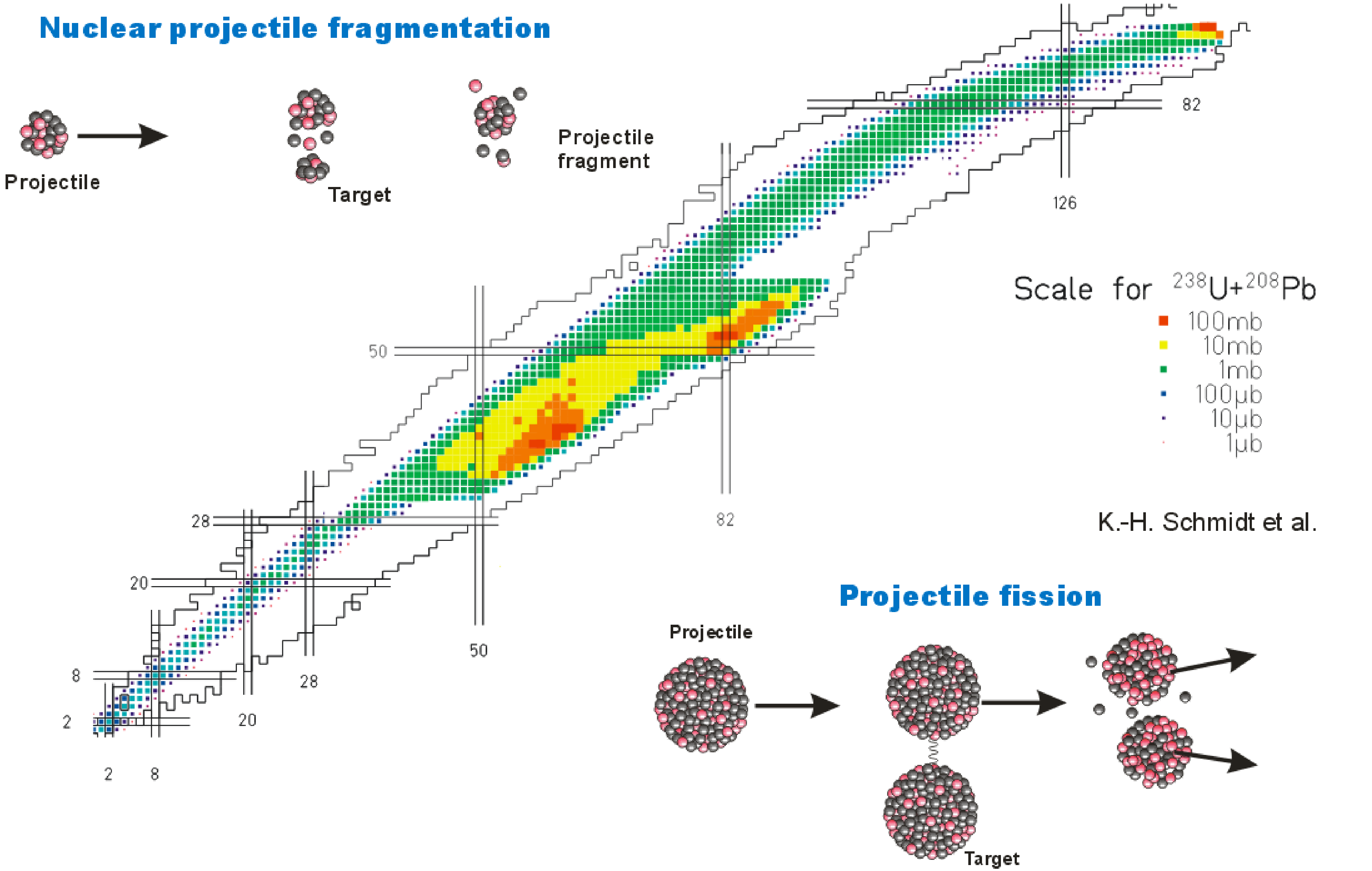

3. Separation with Degrader

select ions by mass and charge separately
→ fragment separator

Principle: Bρ-ΔE-Bρ Separation

Achromatic in velocity, but dispersive in mass and charge

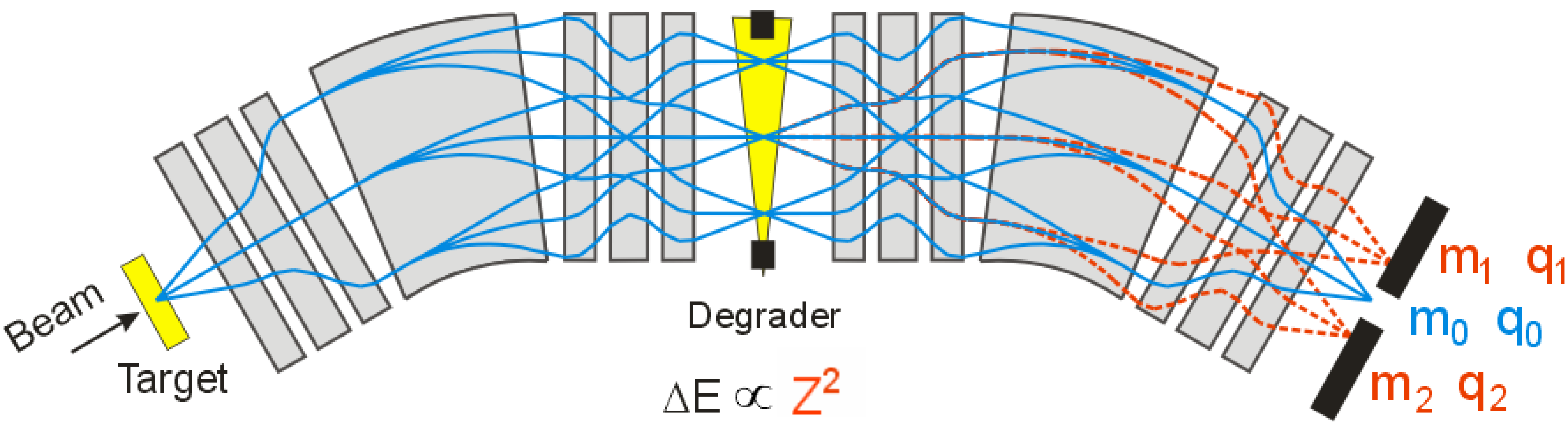

shaped to keep overall system achromatic

Degrader Wedge

→ wedge shape **(δ|x)**
for symmetric wedge **(δ|a)=0**

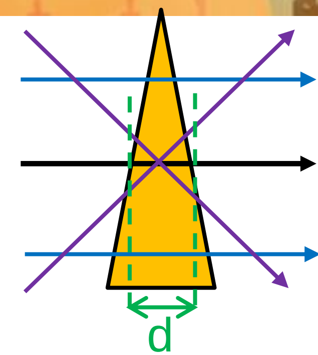

Physics limitation by energy-loss straggling in stochastic process
of many atomic collisions: $\sigma_E^2 = \underbrace{d\Omega^2/dz}_{\text{from atomic physics}}\; d$ --> δ_{str} ~ 2e-3 .. 2e-4
ultimate limitation of technique

Real wedges are thin metal plates. Combine many plates for easy adjustment.
Shape and surface flatness must be very precise, on the level of wanted resolution.

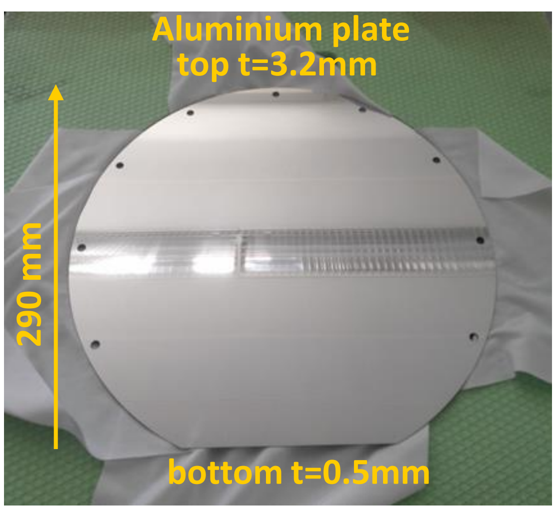

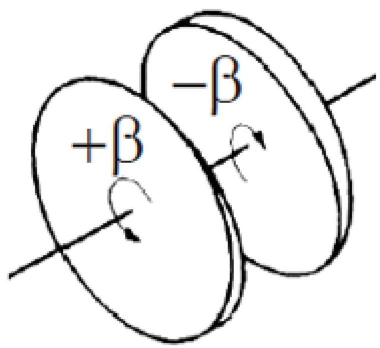

deviation from wedge shape
area: 280 mm x 134 mm

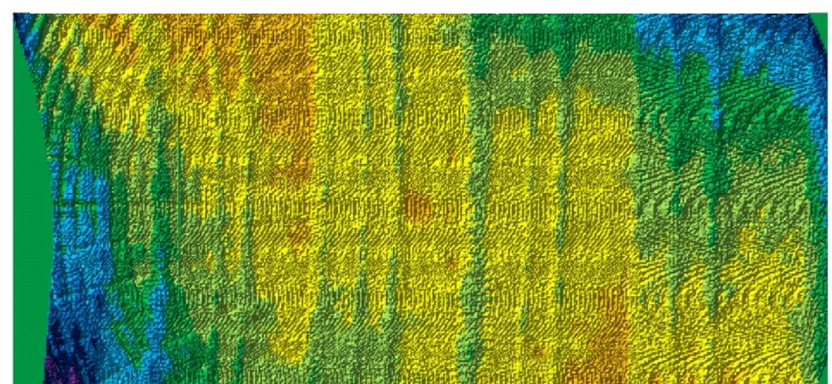

Transfer Matrix Description

ion-optical coordinates

$$x,\ a=p_x/p_0\ ,\ y,\ b=p_y/p_0\ ,\ \delta=\Delta B\rho/B\rho_0$$

$$B\rho = c_0\beta\gamma\ \ m/q = \nu\ m/q$$

$$\delta_m=\Delta m/m\ ,\ \delta_q=\Delta q/q\ ,\ \delta_\nu=\Delta\nu/\nu_0$$

Separator stage, D

$$\begin{pmatrix} x \\ a \\ \delta_m \\ \delta_q \\ \delta_\nu \end{pmatrix}_f = \begin{pmatrix} (x|x) & \cancel{(x|a)} & (x|\delta) & -(x|\delta) & (x|\delta) \\ (a|x) & (a|a) & (a|\delta) & -(a|\delta) & (a|\delta) \\ 0 & 0 & 1 & 0 & 0 \\ 0 & 0 & 0 & 1 & 0 \\ 0 & 0 & 0 & 0 & 1 \end{pmatrix} \begin{pmatrix} x \\ a \\ \delta_m \\ \delta_q \\ \delta_\nu \end{pmatrix}_i$$

Degrader wedge W

$$\begin{pmatrix} x \\ a \\ \delta_m \\ \delta_q \\ \delta_\nu \end{pmatrix}_f = \begin{pmatrix} 1 & 0 & 0 & 0 & 0 \\ 0 & 1 & 0 & 0 & 0 \\ 0 & 0 & 1 & 0 & 0 \\ 0 & 0 & 0 & 1 & 0 \\ (\delta_\nu|x) & (\delta_\nu|a) & (\delta_\nu|\delta_m) & (\delta_\nu|\delta_q) & (\delta_\nu|\delta_\nu) \end{pmatrix} \begin{pmatrix} x \\ a \\ \delta_m \\ \delta_q \\ \delta_\nu \end{pmatrix}_i$$

Full system $= \mathbf{D_2 \,.\, W \,.\, D_1}$

require $(x|\delta_\nu)_{tot} = 0,\ (a|\delta_\nu)_{tot} = 0$

Transfer Matrix Description

H. Geissel et al, NIM B247 (2006) 368.

Momentum resolving power of one half

$$R = \frac{(x|\delta)}{\Delta x_f} \quad \sim 1000 \,..\, 2000$$

Energy-loss straggling

$$\delta_{\nu,str} \sim 1e\text{-}3 \,..\, 3e\text{-}3$$

Resolution in mass, charge

$$R_m = \frac{(x|\delta_m)}{\Delta x_f} \qquad R_q = \frac{(x|\delta_q)}{\Delta x_f}$$

for achromatic separator $(x|\delta_\nu)_{tot} = 0$

$$R_m = \frac{[(\delta_\nu|\delta_m) + 1 - (\delta_\nu|\delta_\nu)] \,/(\delta_\nu|\delta_\nu)}{\sqrt{1/R^2 + (\delta_{\nu,str}/(\delta_\nu|\delta_\nu))^2}} = R \frac{\overbrace{[(\delta_\nu|\delta_m) + 1 - (\delta_\nu|\delta_\nu)]}^{<1}}{\underbrace{(\delta_\nu|\delta_\nu)}_{>1}}$$

for $\delta_{\nu\, str} \to 0$

$$R_q = \frac{[(\delta_\nu|\delta_q) - 1 + (\delta_\nu|\delta_\nu)] \,/(\delta_\nu|\delta_\nu)}{\sqrt{1/R^2 + (\delta_{\nu,str}/(\delta_\nu|\delta_\nu))^2}} = R \frac{[(\delta_\nu|\delta_q) - 1 + (\delta_\nu|\delta_\nu)]}{(\delta_\nu|\delta_\nu)}$$

$\sim 0 \,..\, 200$

Bρ-ΔE-Bρ Separation Method in FRS

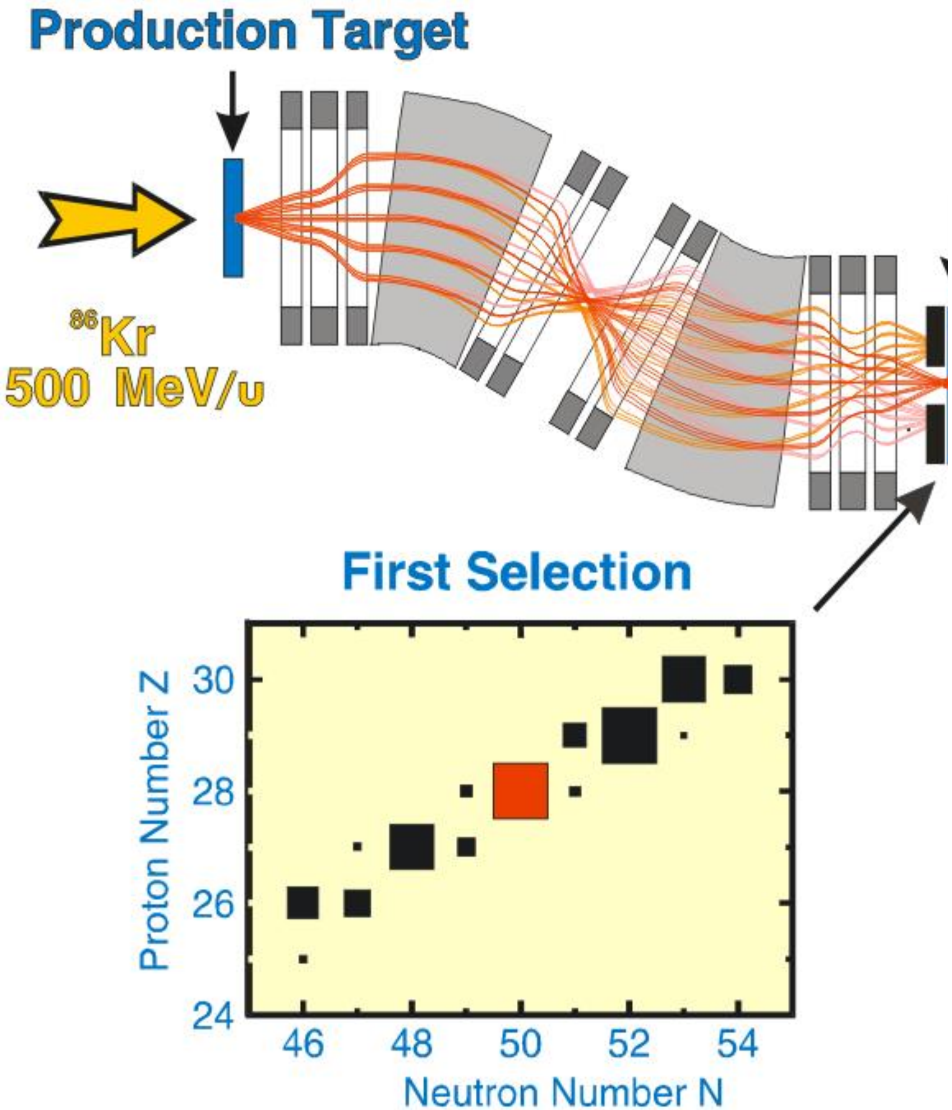

Bρ-ΔE-Bρ Separation Method

scheme of FRS @ GSI, L=72m

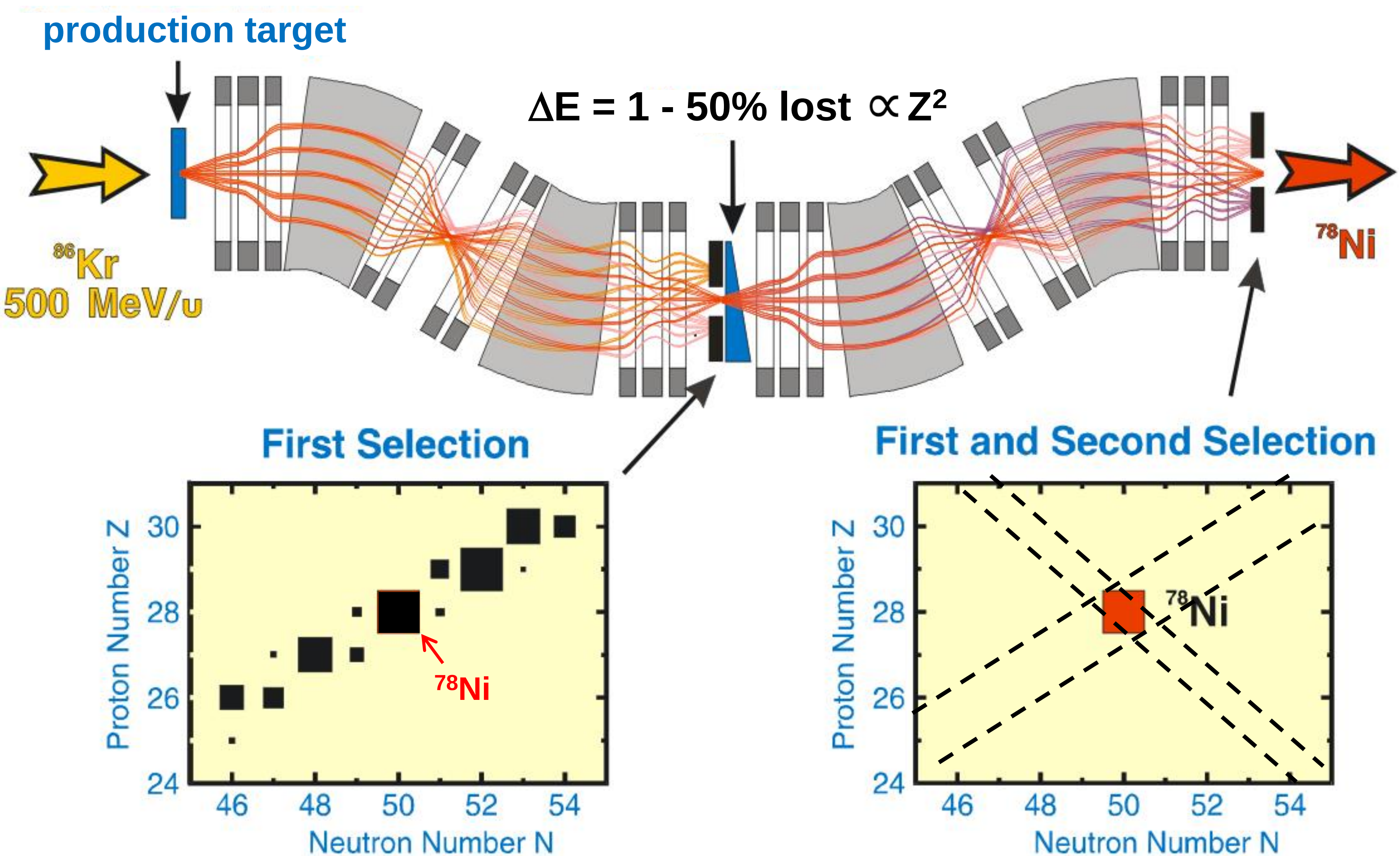

Optics Mode FRS

Ions starting with different angles and momenta

$\delta = \pm 1\%$, $a = \pm 5, \pm 10$ mrad, $b = \pm 7.5, \pm 15$ mrad

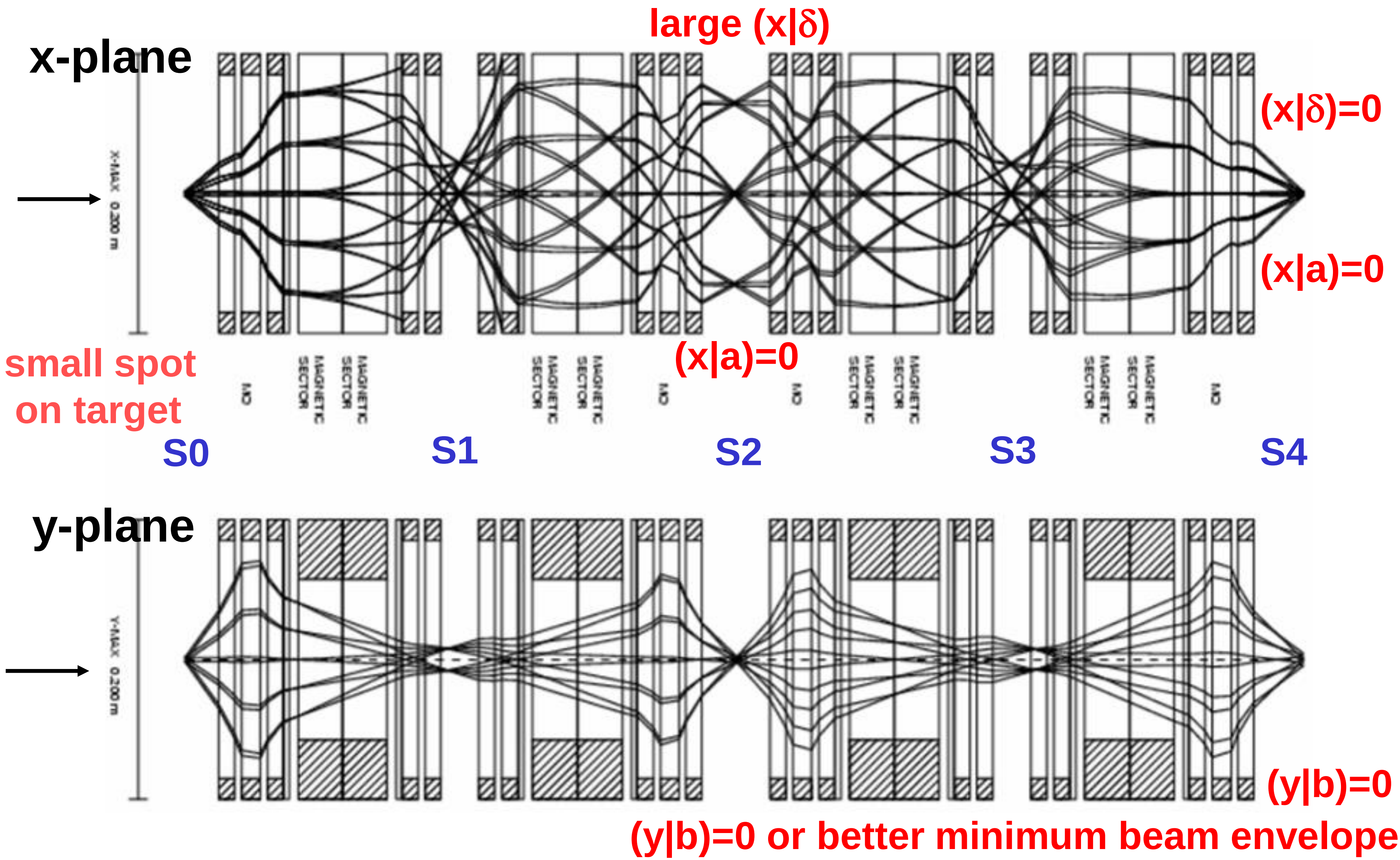

Slowing Down in Matter

Accelerator

longitudinal momentum change

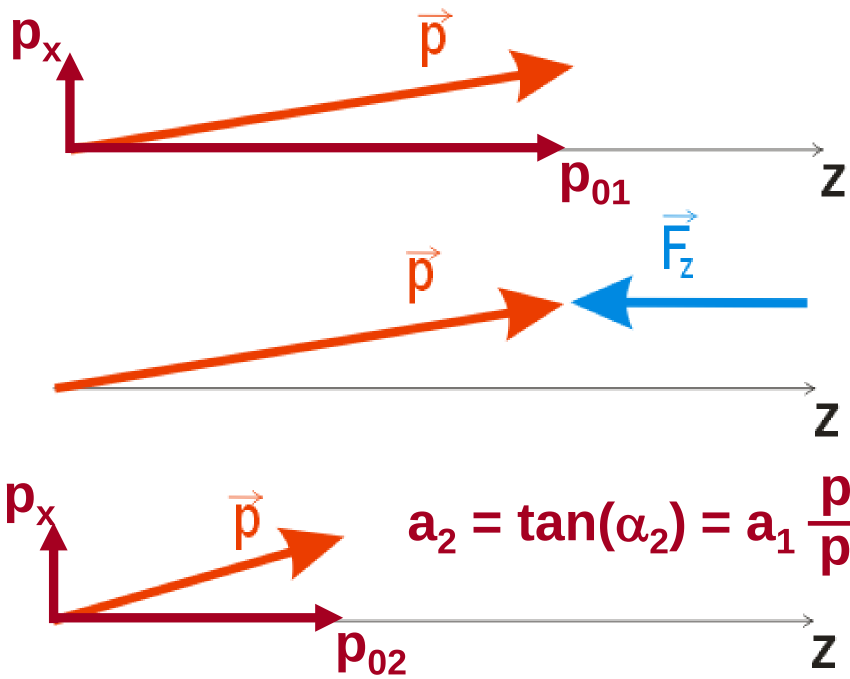

$$a_2 = \tan(\alpha_2) = a_1 \frac{p_{01}}{p_{02}}$$

in Matter

Average Force (dE/ds) opposite to direction of motion.

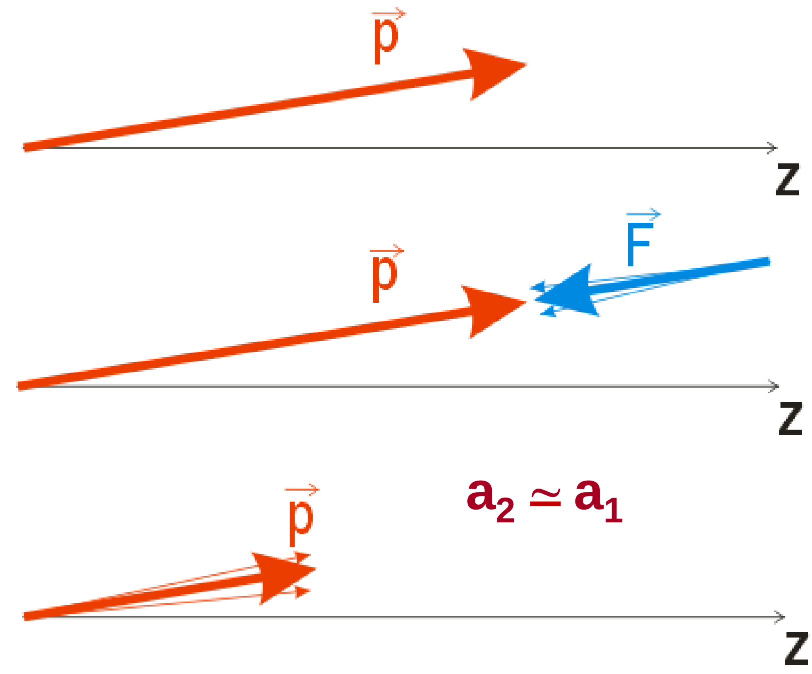

$$a_2 \simeq a_1$$

Large emittance growth in accelerator, less in matter.

Large changes require a new reference $p_{02} = p_{01} \dfrac{\beta_1 \gamma_1}{\beta_2 \gamma_2}$

$\delta_1 = \Delta p_{z1}/p_{01}$ –> $\delta_2 = \Delta p_{z2}/p_{02}$ **, to preserve a symmetric separator** $\delta_1 = \delta_2$

Energy-Loss of Heavy Ions

No closed system (non-Liouvillean), $(\delta|\delta)$ does not just depend on beam momenta p_{01}, p_{02}.

Slowing down depends on the atomic processes described by average stopping force.

different energy loss within peak
=> stretching of distribution

stopping force in matter

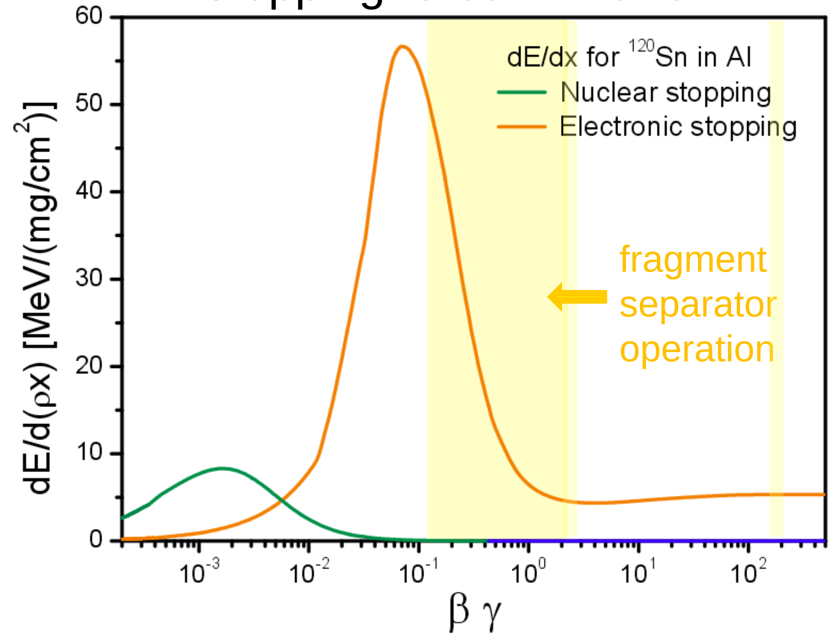

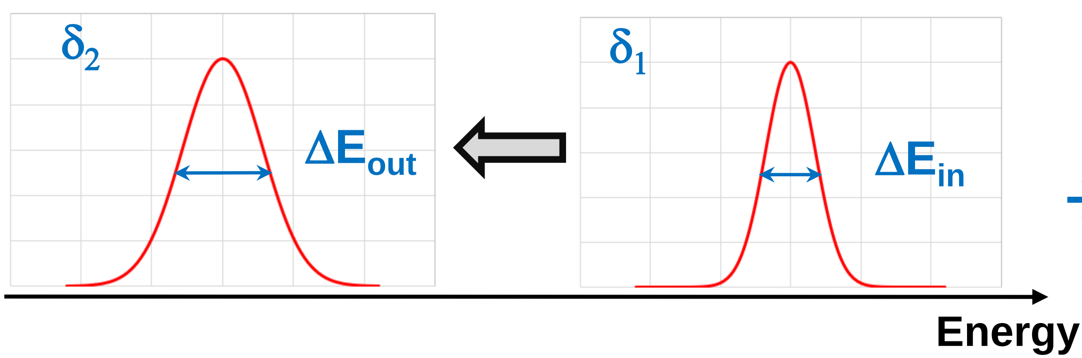

$$\frac{\Delta E_{in}}{\Delta E_{out}} = \frac{(dE/d\rho x)_{in}^2}{(dE/d\rho x)_{out}^2}$$

→ **additional contribution to $(\delta|\delta)$**

$$\delta_E = \delta_p\,(1+1/\gamma)$$

Effect of degrader at different velocity

fragment ^{190}W in achromatic FRS
with Al degrader d/r=0.5
transmission

1st slits at $\pm 2\sigma_x$

2nd slits at $\pm 2\sigma_x$

both slits at $\pm 2\sigma_x$

MOCADI simulation

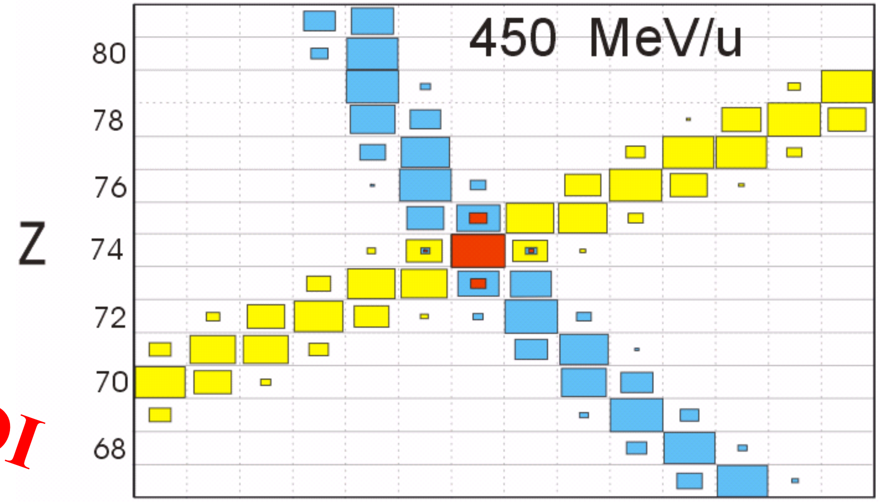

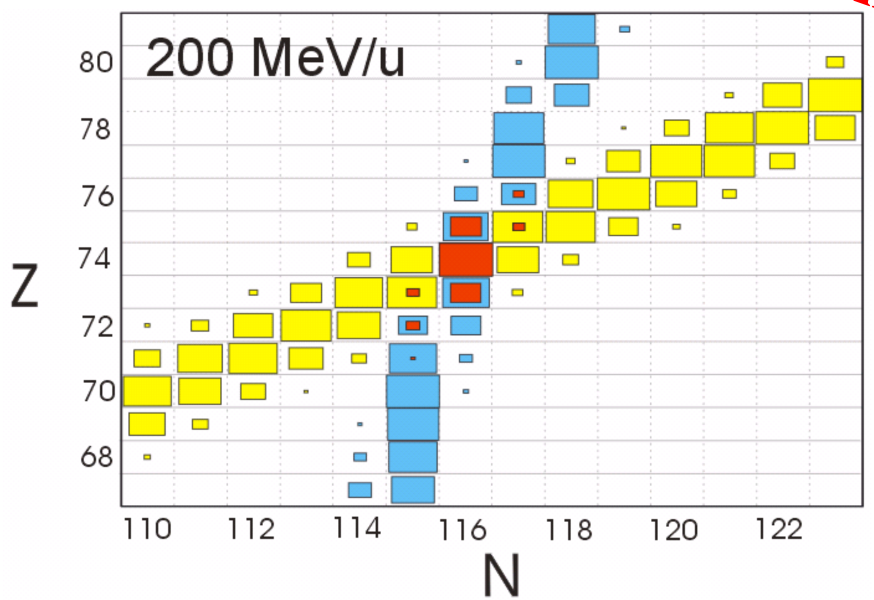

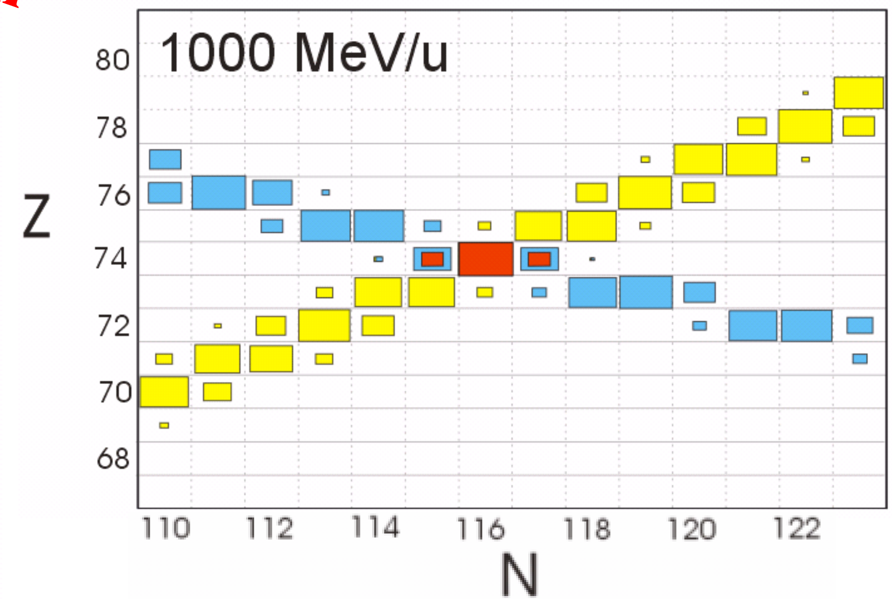

Phase Space Consideration

Determinant of transfer matrix is a measure of phase space volume.
For overall achromatic system imaging in each stage, (x|a)=0.

transverse, 2-dim

$$\mathrm{Det}_t = (x|x)_{tot}\,(a|a)_{tot}$$

$$= -(\delta_\nu|\delta_\nu)\,\frac{(x|\delta)_2}{(x|x)_2\,(x|\delta)_1} \neq 1$$

Non-Liouvillean

longitudinal, 2-dim

$$\mathrm{Det}_l = (\delta_\nu|\delta_\nu)\,\underbrace{(\Delta z|\Delta z)}_{=1} = -\,\frac{(x|x)_2\,(x|\delta)_1}{(x|\delta)_2}$$

no time dependence

combined, 4-dim.

$$\mathrm{Det}_{comb} = \mathrm{Det}_t\;\mathrm{Det}_l = (\delta_\nu|\delta_\nu) \;\text{-->}\; 1$$

quasi Liouvillean

for dE/dz (ν) = const.
Neglecting straggling

Wedge shaped degrader couples transverse and longitudinal motion.
One increased by factor, the other reduced by same factor.

4. Large Apertures, Higher Order Optics Fringe Fields

Large Aperture Optical Elements

Emittances of secondary beams are large, e.g. after RIB production.
Magnets with large aperture compared to their lengths are required.

➔ Fringe fields cannot be neglected.

Often a division into drifts, fringe fields (FF) and main field is possible.
Main field with effective length (same integral along axis) and short fringe field maps describe the deviation to a real soft edge.

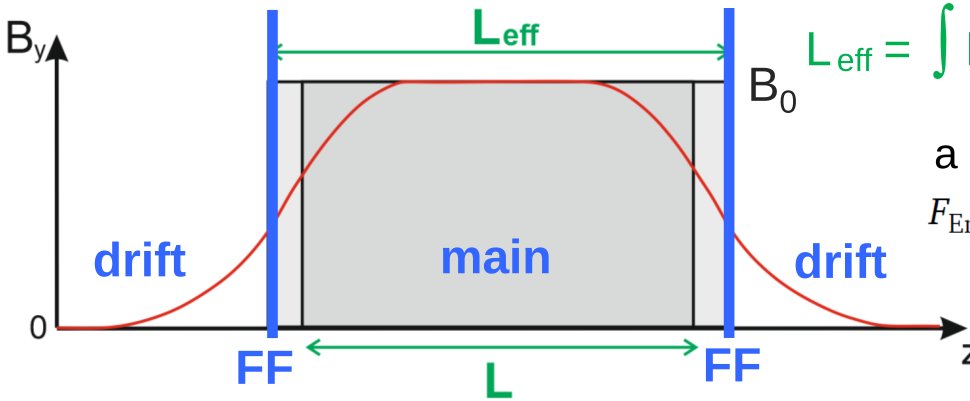

$L_{eff} = \int B_y(z)\,dz \;/\; B_0$

a typical approximation:

$$F_{\mathrm{Enge}}(z) = \frac{1}{1+\exp(a_1 + a_2\cdot(z/D) + \ldots + a_6\cdot(z/D)^5)}$$

Sharp drops violate Maxwell's equations. A field curvature along axis requires similar opposite curvature in transverse direction. Fringe fields will always contain transverse non-linear components. For a given multipole symmetry the distribution along the axis defines the transverse distribution.

Field derived from potential (outside and const. in time):

$$\vec{E} = \vec{\nabla}\Phi, \quad \Delta\Phi = 0$$

$$\vec{B} = \vec{\nabla}\times\vec{A}, \quad \vec{\nabla}\cdot\vec{A} = 0$$

Quadrupole with Fringe Fields

Main field has analytical solution.

$$\mathbf{Q} = \begin{bmatrix} (x,x) & (x,a) \\ (a,x) & (a,a) \end{bmatrix} = \begin{bmatrix} \cos(k_0 L) & \sin(k_0 L)/k_0 \\ -k \sin(k_0 L) & \cos(k_0 L) \end{bmatrix}$$

$$\text{with } k_0^2 = \frac{B_0}{r_0 B\rho}, \quad L \rightarrow L_{eff}$$

Use approximate solutions for fringe fields.
For example by step-wise integration (Picard iteration).

$$\mathbf{FF} = \begin{bmatrix} (x,x) & (x,a) \\ (a,x) & (a,a) \end{bmatrix} \sim \begin{bmatrix} 1 \pm k_0 I_1 & -2k_0 I_2 \\ 0 & 1 \mp k_0 I_1 \end{bmatrix}$$

$I_1, I_2, \ldots$ = fringe field integrals

$$I_1 = \frac{1}{k_0} \iint k(z)\, d^2z - z_b^2/2$$

$$I_2 = \frac{1}{k_0} \iint k^2(z)\, d^2z - z_b^3/2$$

Matsuda, Wollnik, NIM 102 (1972) 117.

Integrals depend only on shape, different weighting with k(z), can later be scaled with r_0
Some are even independent of the detailed shape, e.g. $(x,xxx) \sim k_0/12$, $(x,xyy) \sim k_0/4$
→ Any fringe field is better than none, typical ones often are good enough.

For very hard cases, e.g. no main field can be defined, use numerical integration directly of algebraic expressions of matrix elements (differential algebra). Is relatively fast and avoids problem of differences of differences on higher order optics coefficients. → COSY INFINITY

M. Berz, AIP Conf. Proc. 177, 275–300 (1988)

Effective Length of FRS Sextupole

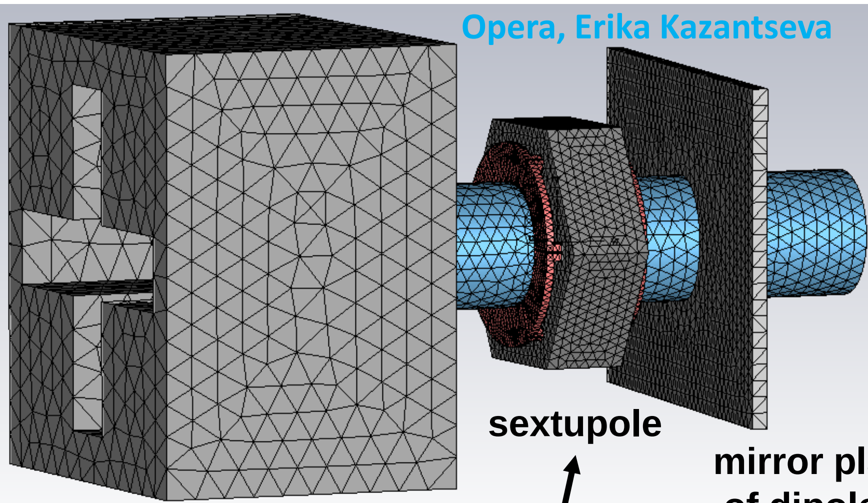

pole-tip radius = 125mm.

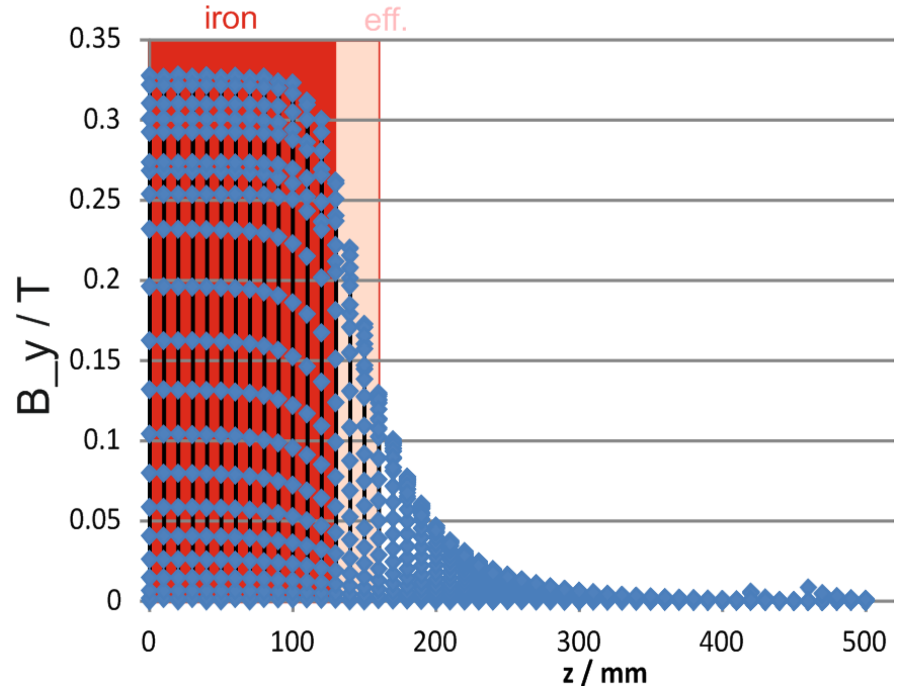

L_iron_geometric = 260 mm
L_eff (standalone) = 330 mm (measured)
L_eff (combined) = 319 mm (calculated)

Higher Order Aberrations

Described by higher order coefficients of transfer map (Taylor expansion)

$$x_2 = (x,x)\,x + (x,a)\,a + (x,\delta)\,\delta$$

$$+ \underbrace{(x,xx)\,x^2 + (x,xa)\,xa + (x,aa)\,a^2 + (x,bb)b^2}_{\text{geometric}} + ..$$

$$+ \underbrace{(x,a\delta)\,a\delta + (x,x\delta)\,x\delta}_{\text{chromatic}} + .. + \underbrace{(x,\delta\delta)\,\delta^2}_{\text{non-lin. dispersion}}$$

$$+ (x,xxx)\,x^3 + .. + (x,a\delta\delta)\,a\delta^2 + .. + (x,\delta\delta\delta)\,\delta^3$$

$$+ \ldots$$

Chromaticity at FRS:
Wide angle test beam with shifted Bρ, δ = -0.6%, 0%, +0.6%

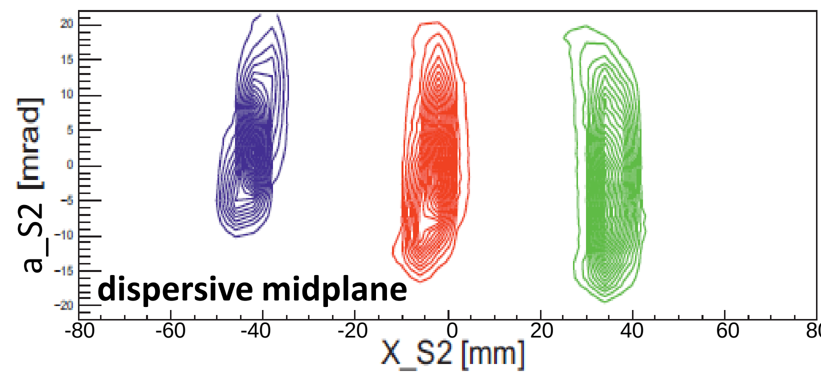

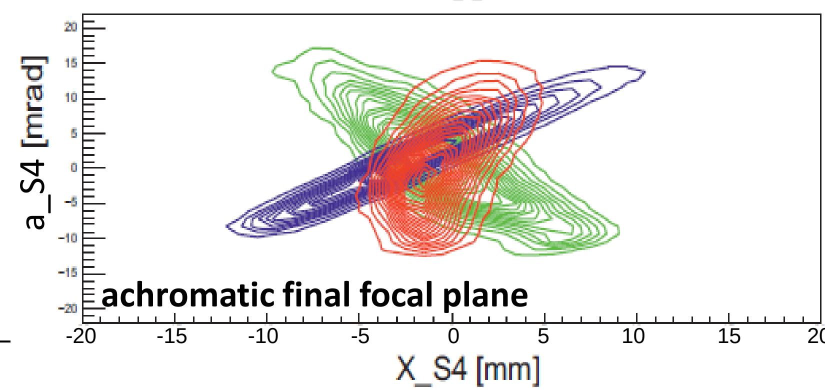

high Bρ is focused less -> natural chromaticity

Higher Order Corrections

schematic sextupole

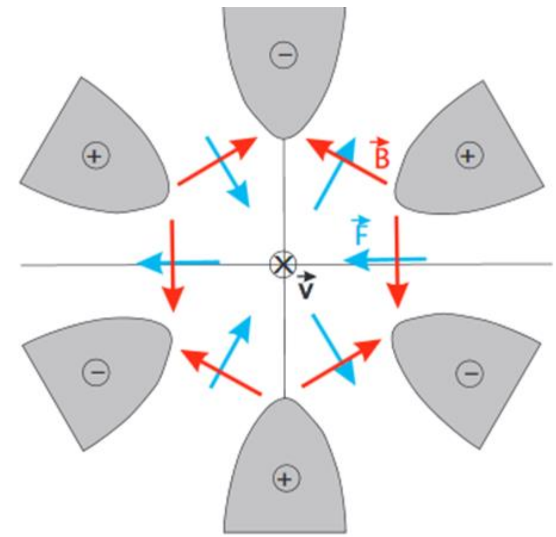

(a,xx)>0 for q>0 ions

Compensate by non-linear fields at the right positions.
Use magnets with defined multipole order.

$$B_y(x,y) + iB_x(x,y) = B_0 \sum_{n=1}^{\infty} (b_n + ia_n) \left(\frac{x+iy}{r_0} \right)^{n-1}$$

- n=1, dipole , 2 poles, $B_y(x) = B_0 = \text{const.}$
- n=2, quadrupole , 4 poles, $B_y(x) = B_0\, b_2\, (x/r_0)$
- n=3, sextupole , 6 poles, $B_y(x) = B_0\, b_3\, (x/r_0)^2$
- n=4, octupole , 8 poles, $B_y(x) = B_0\, b_4\, (x/r_0)^3$
- n multipole 2n poles, $B_y(x) = B_0\, b_n\, (x/r_0)^{n-1}$

Terms of different orders are linear independent,
For n^{th} order multipole matrix with order n<0 is like drift,
$\Rightarrow$ An n^{th} order multipole magnet can only change the overall transfer map of order ≥ n.

Effect of one excited sextupole in FRS positioned where the beam is wide. (a,xx) of the sextupole leads to a parabolic deformation of phase space.

B''L = 3.24 T/m at Bρ=8.7 Tm

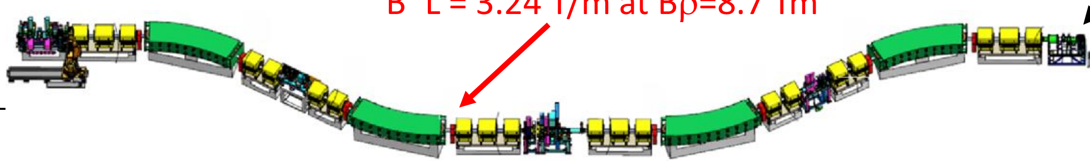

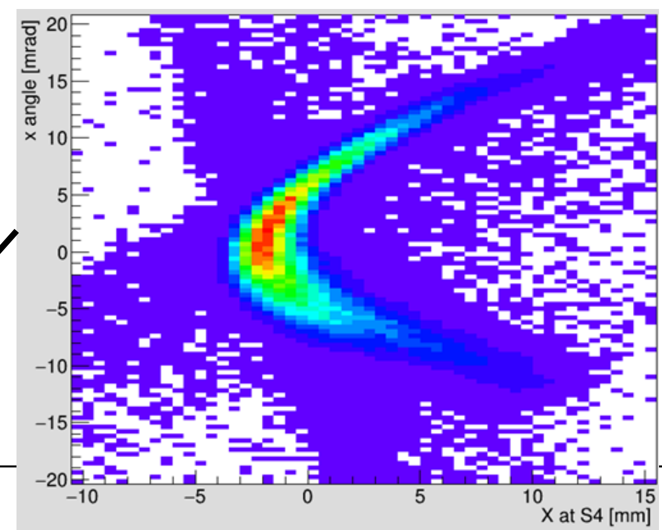

FRS 2nd Order Correction

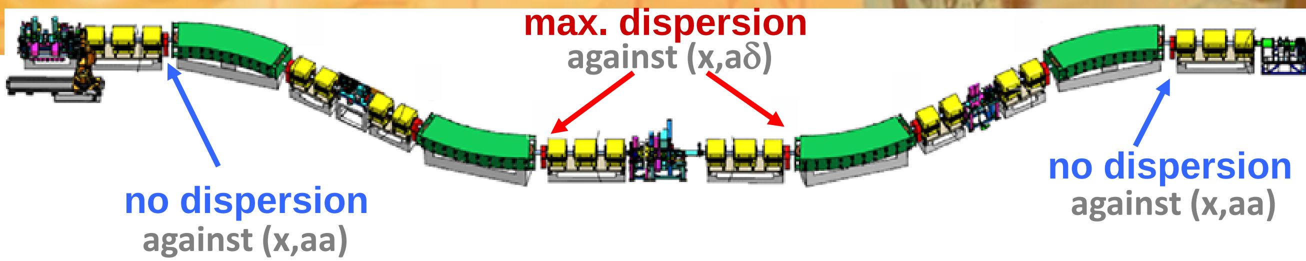

Ta-6045 mg/cm² target
in 600 MeV/u ^{12}C beam,
FRS scaled by ±0.6%

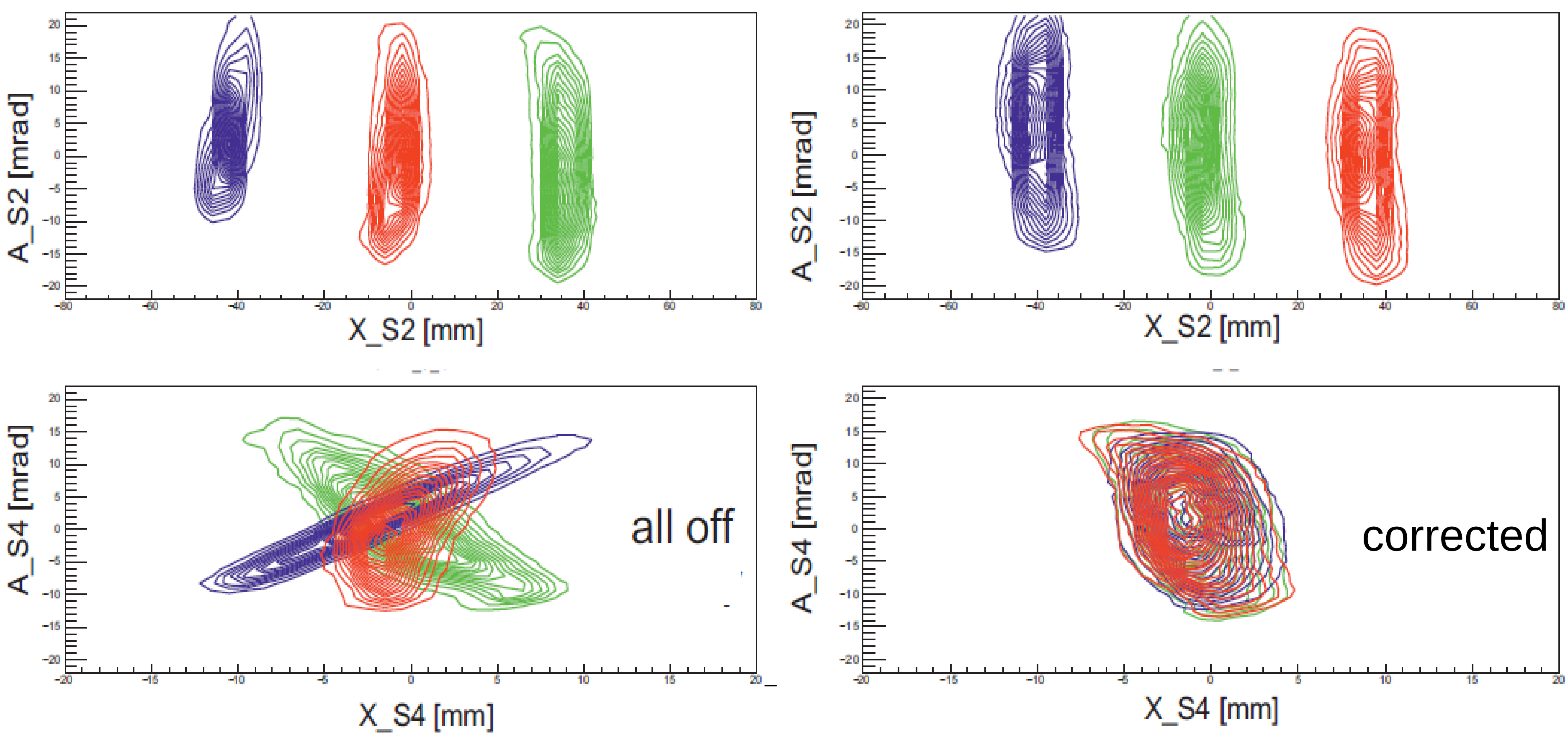

Ion Optics Codes

only the most wide spread

fixed formulas | integration

only magnetic | electric +magnetic | more general field definition

Transport 2nd order

MIRKO

WinAGILE

MAD-8, MAD-X

fringe field integrals

TRIO

GIOS 3rd order

GICOSY 5th order

MaryLie

extended fringe fields

ZGOUBY

COSY-infinity nth order

mainly accelerator design | mainly for spectrometers | general

Many add-ons exist:
e.g. for tracing ions
in Monte-Carlo mode

PTC, Trace-3D
Turtle, Raytrace

MOCADI (includes matter in beamline)
LISE++ (convolution method incl. matter)

Field computation codes
can trace single ions:

Simion (arbitrary electrode geometry)
Opera, ANSYS, COMSOL, …

BDSIM, GEANT4beamline and FLUKA focus on interaction

4.5. Fragment Identification in Flight

Identification In-Flight

$B\rho = \beta\gamma c_0\ m / q$

$v = \beta c_0 = L / ToF$

$B\rho$ from deflection in dipoles

$q \sim Z$ from ΔE in MUSIC

$\Longrightarrow m, Z$

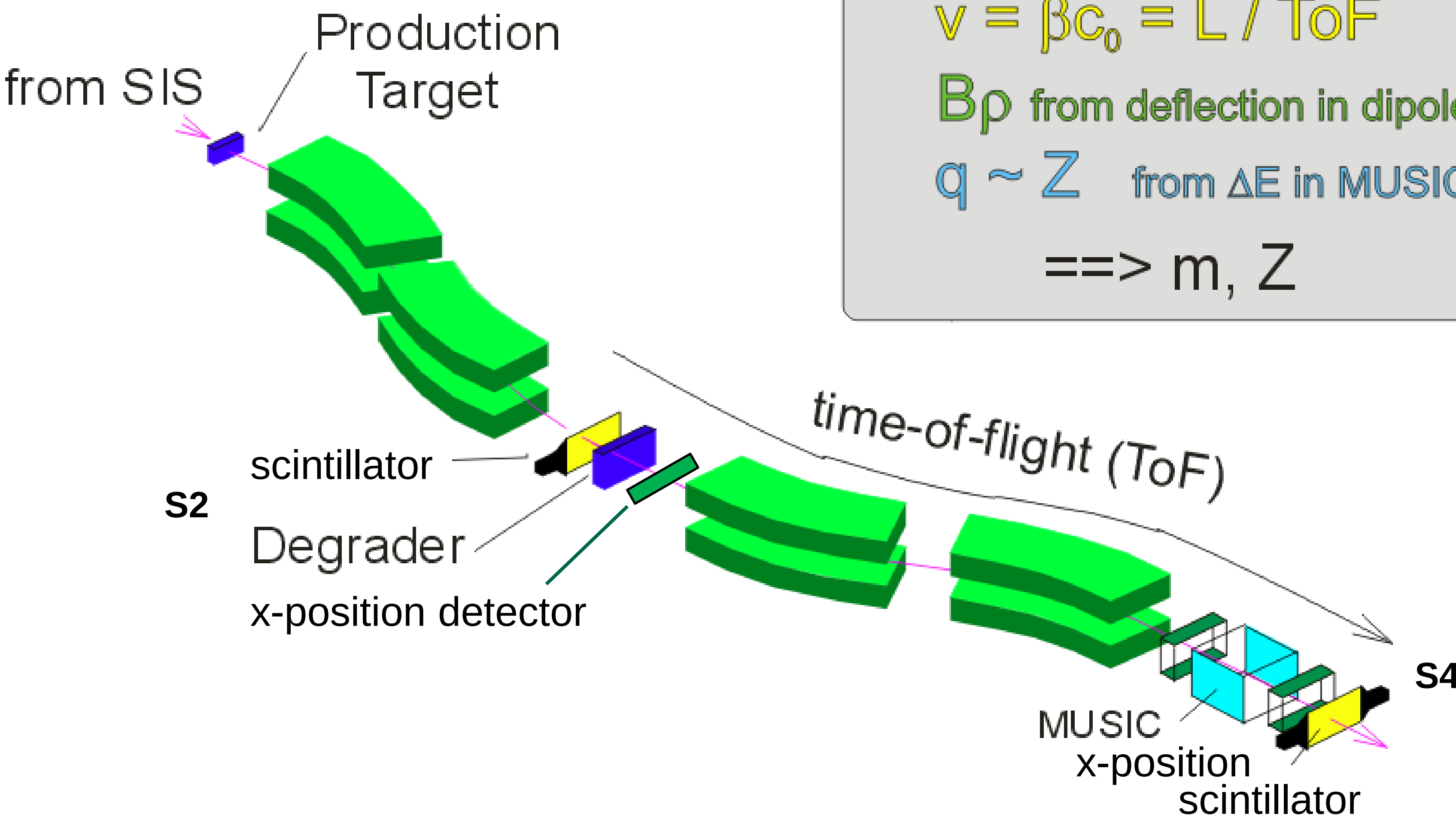

Identification In-Flight

$$B\rho = m/q\ \beta\gamma\ c_0$$

- $B\rho$ from magnet setting and position detectors at focal planes

$$B\rho = B\rho_0 \left[1 + \frac{x_{S4} - (x|x)\, x_{S2}}{(x|\delta)} \right]$$

- velocity from ToF between two scintillators at S2 and S4.

$$\beta = L(\alpha,\delta) / ToF / c_0$$

- MUSIC: average all anodes

$$Z = Z_0 * \sqrt{\frac{\Delta E_{ADC}}{Polynomial(\beta)}}$$

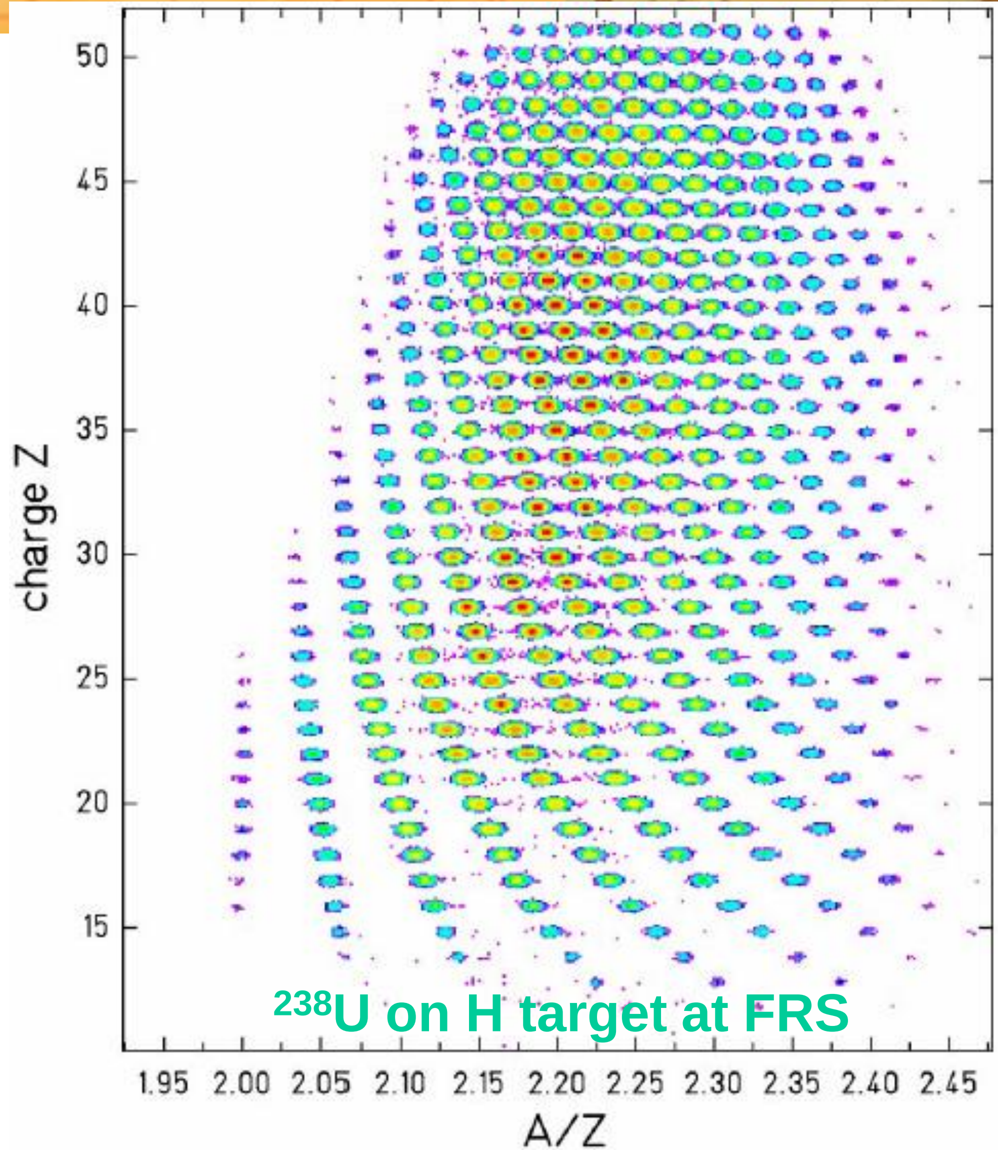

thesis V. Henzl, CTU Prague 2005.

5. Modern Fragment Separator Systems

Built for much higher beam intensities.
Selectivity up to of 1 out of 10^{20}
at efficiency ~ 50%

Production of RIBs In-Flight

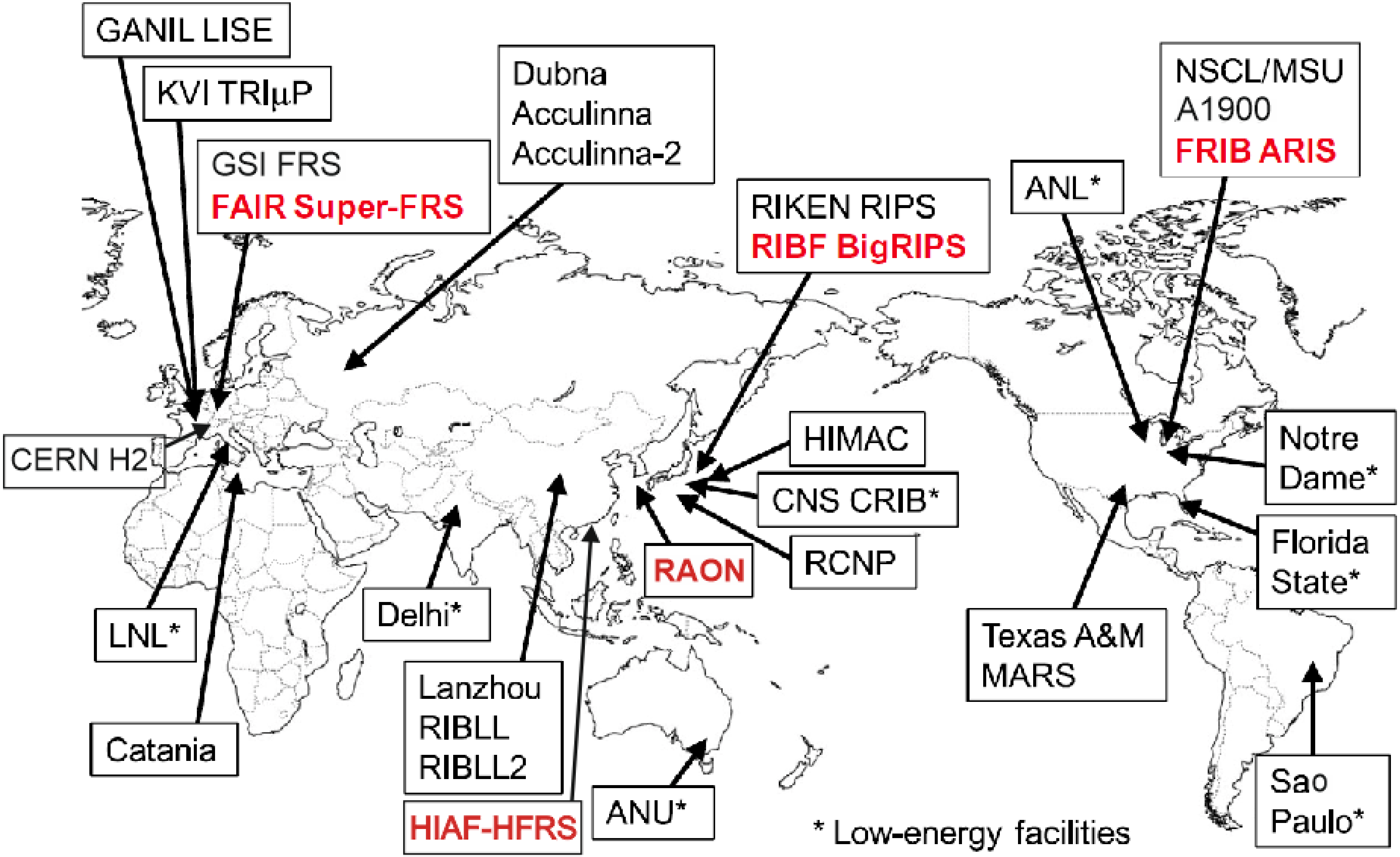

update of T. Kubo, NIM B 376,102 (2016)

Super-FRS

after thick shaped degraders
Δa, Δb ~ ± 20 mrad, $\Delta p/p$ = ± 2.5%
but $\varepsilon_{x,y}$ ~ 100-300 mm mrad

Initial acceptance:
Δa = ± 40 mrad
Δb = ± 20 mrad
$\Delta p/p$ = ± 2.5%
x_0 = 0.5 - 4 mm

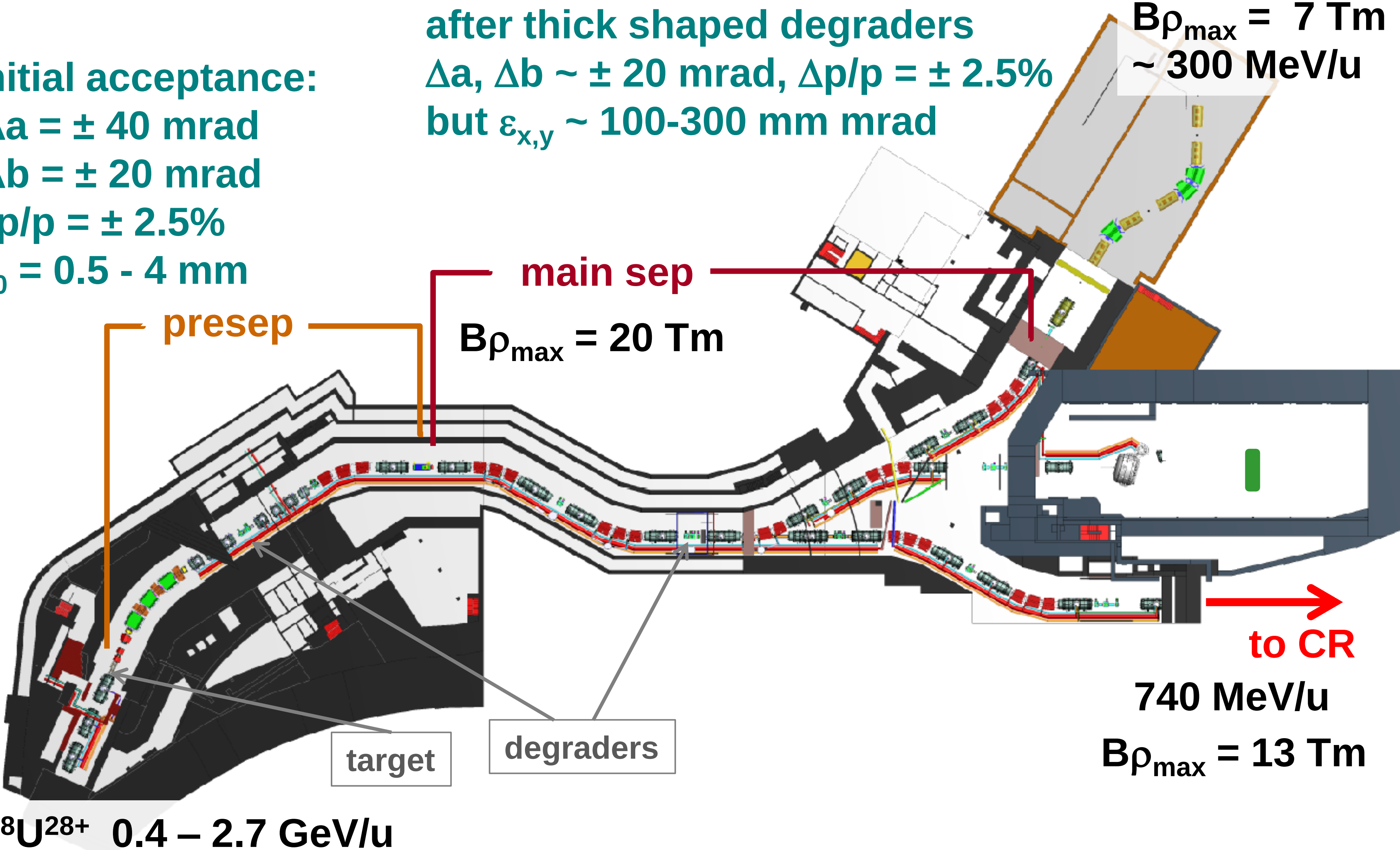

$^{238}U^{28+}$ 0.4 – 2.7 GeV/u

Super-FRS in Higher Order

field shapes in nc-dipoles
in reality full 3D distribution

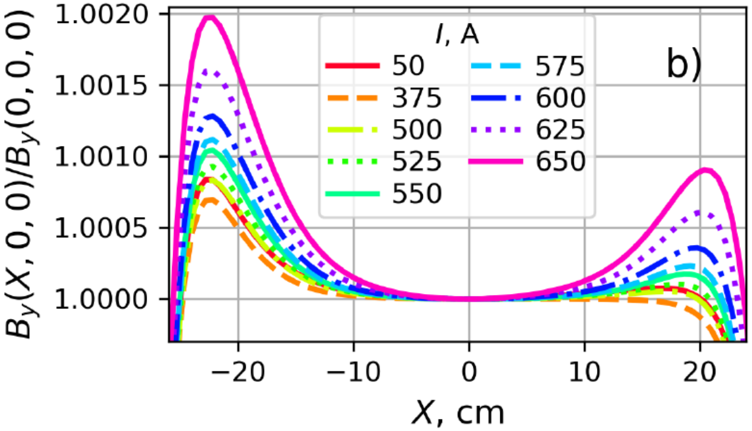

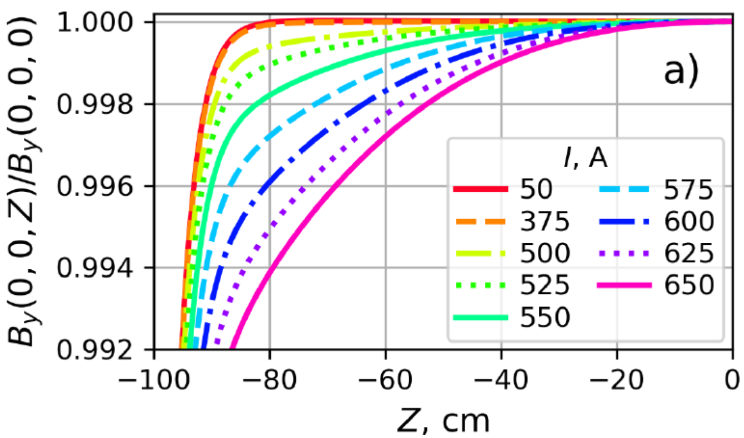

Simulation in COSY infinity 13th order with two different descriptions of dipole field. Corrections up to octupoles (3rd order).

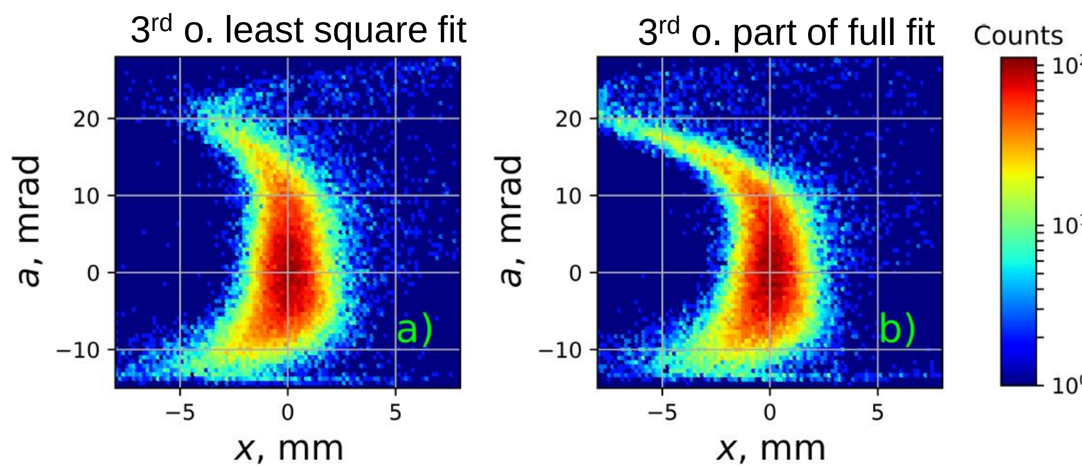

Different effective field lengths and shapes depending on magnetic field strength, due to iron saturation. No exact prediction possible, but find a scheme for correction.

E. Kazantseva, thesis TU Darmstadt 2019

Optics of Super-FRS at FAIR

1.1 A GeV ^{238}U on 4 g/cm^2 C target, two Al degraders d/R=0.3, d/R=0.7

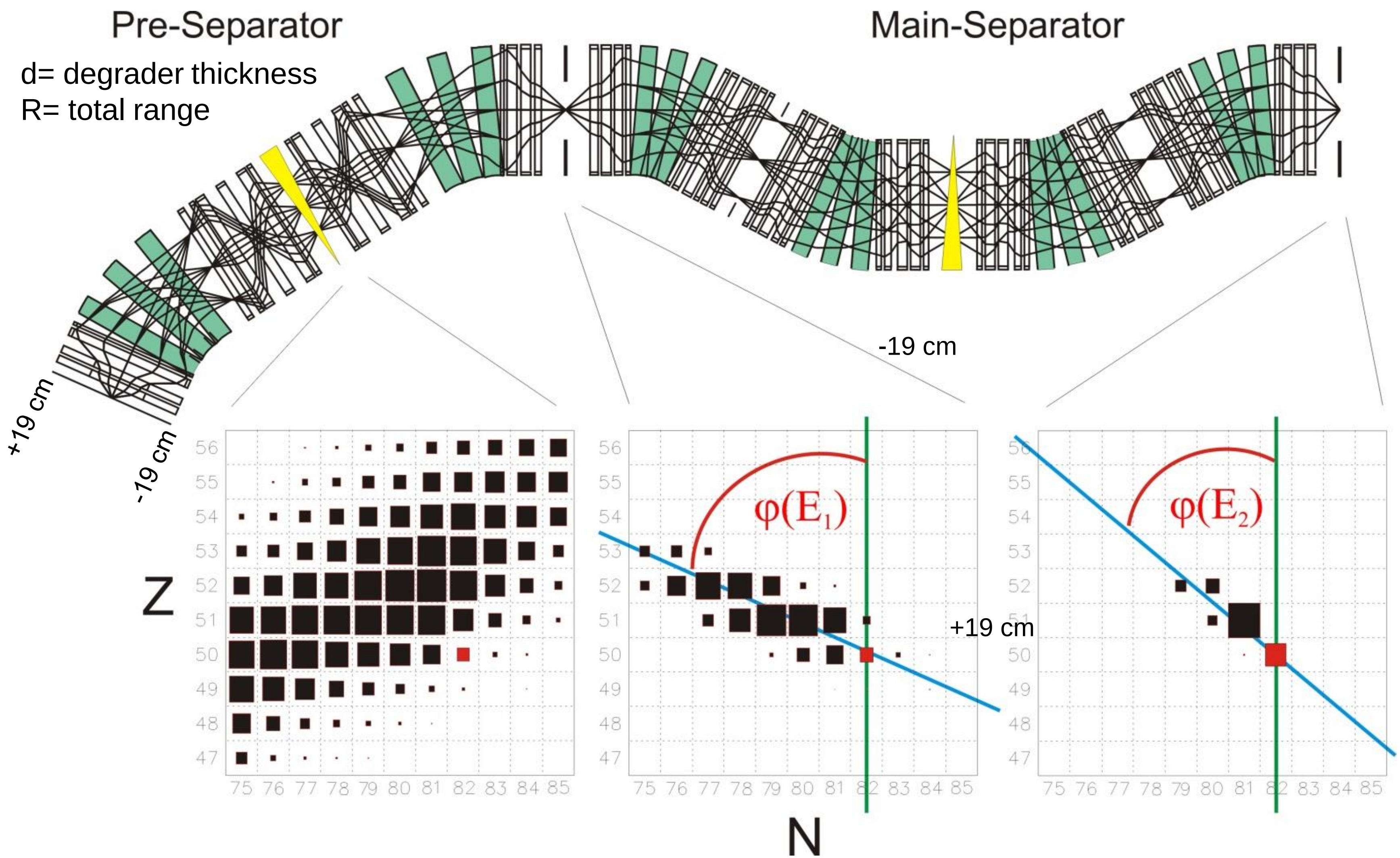

1.1 A GeV ^{238}U on 4 g/cm^2 C target, two Al degraders d/R=0.3, d/R=0.7

For fission fragments separation is difficult, other beams more pure.

Coupling of many Stages

Wide momentum spread after reaction, simple Bρ cut not selective enough.
What helps? Two achromatic degraders at different energy.

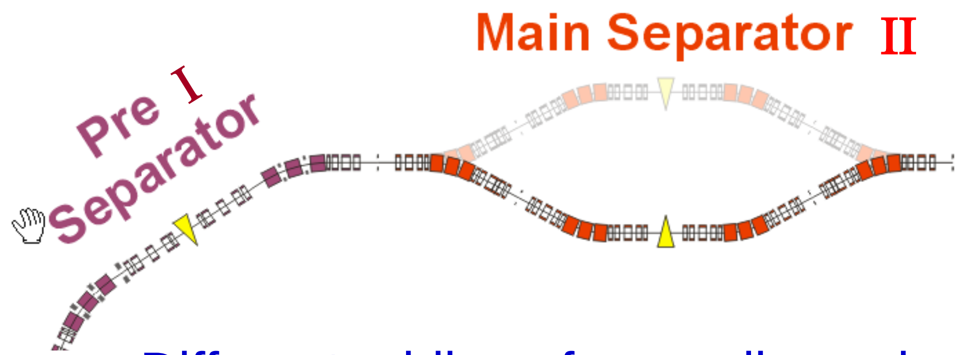

Example ^{78}Ni with degrader matter distributed to two degraders in pre (I) + main(II) separator, both d/R = 0.5

Different adding of m, q -dispersion

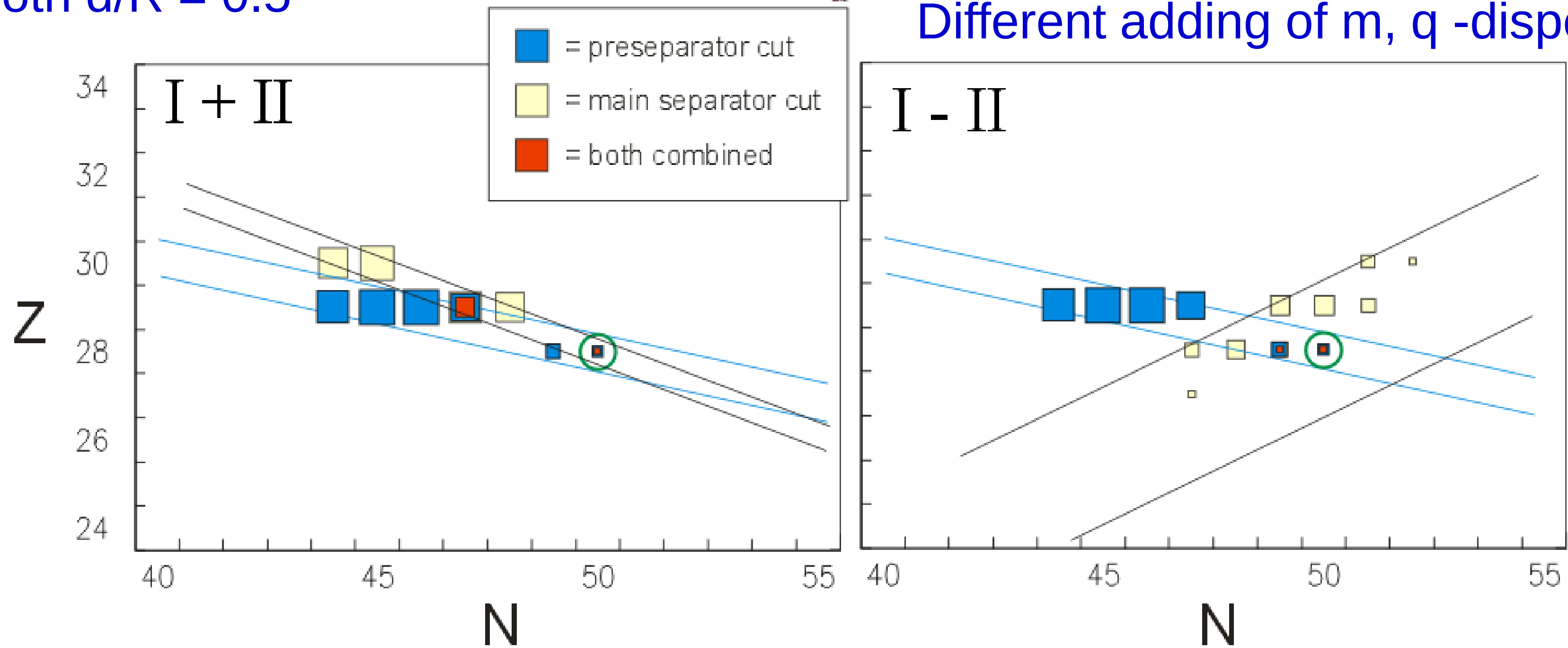

Fragments from Degrader
BigRIPS Comissioning at RIKEN

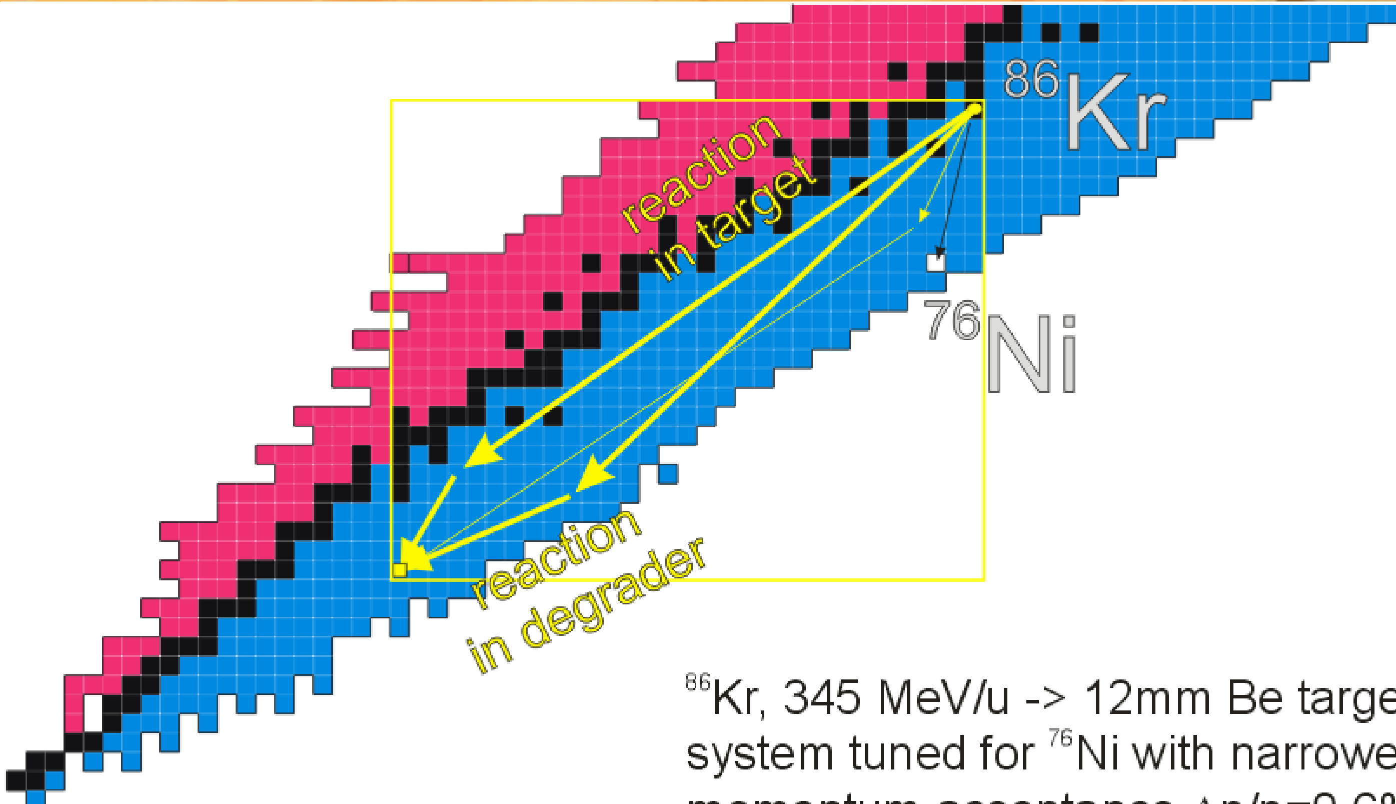

^{86}Kr, 345 MeV/u -> 12mm Be target system tuned for ^{76}Ni with narrowed momentum acceptance $\Delta p/p$=0.6%, a **6mm Al** degrader at F1 was used.

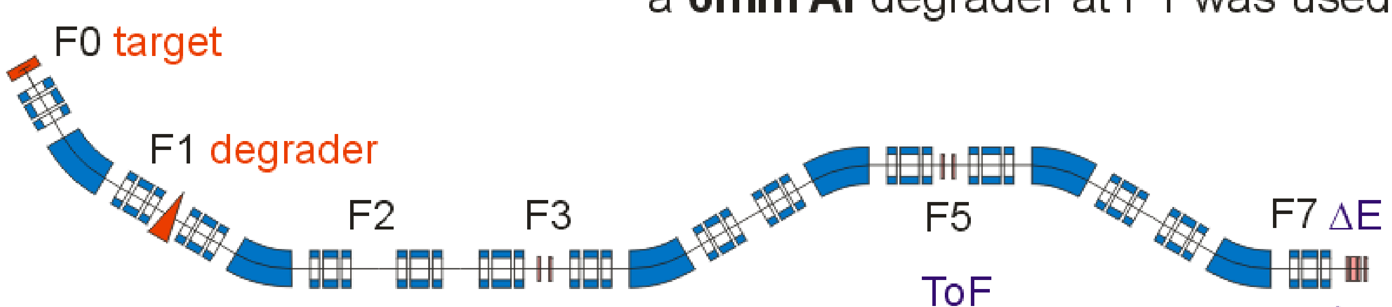

BigRIPS Commissioning in 2006
Setting $^{86}Kr \rightarrow {}^{76}Ni$

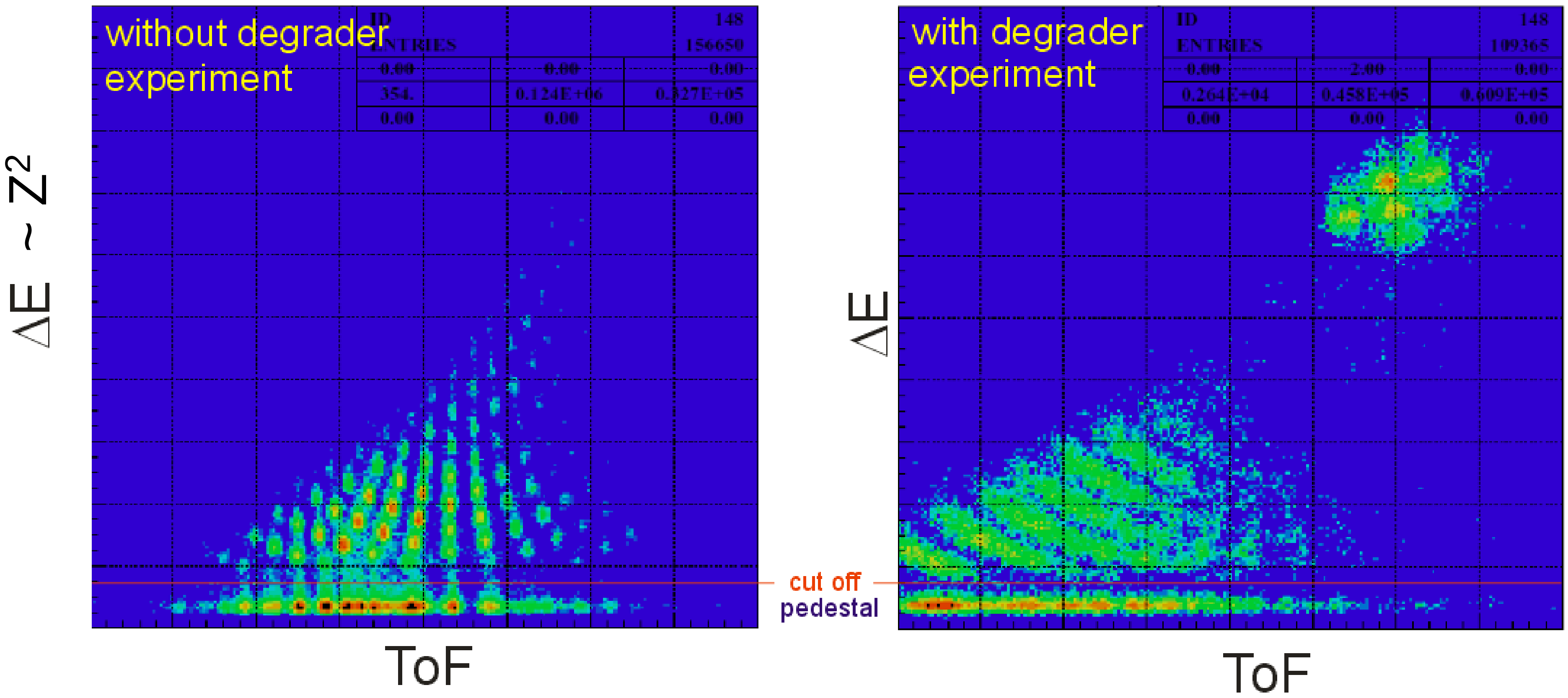

Without degrader ^{76}Ni region not visible,
with degrader still lots of lighter fragments.

BigRIPS ^{86}Kr -> ^{76}Ni
Simulation with LISE^{++}

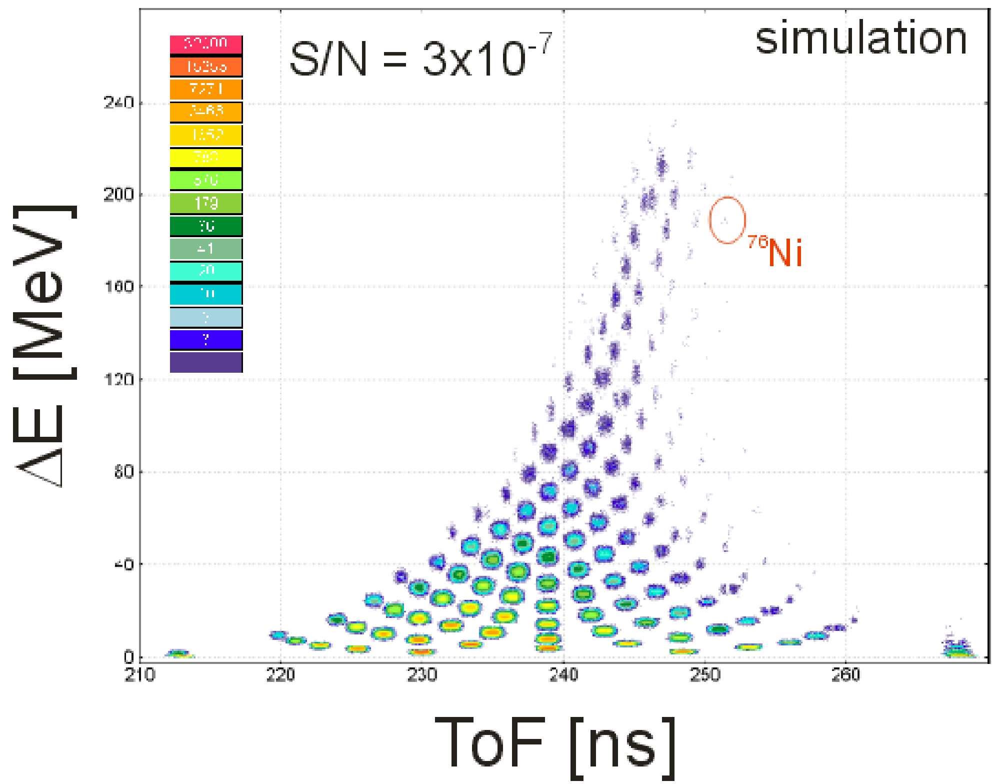

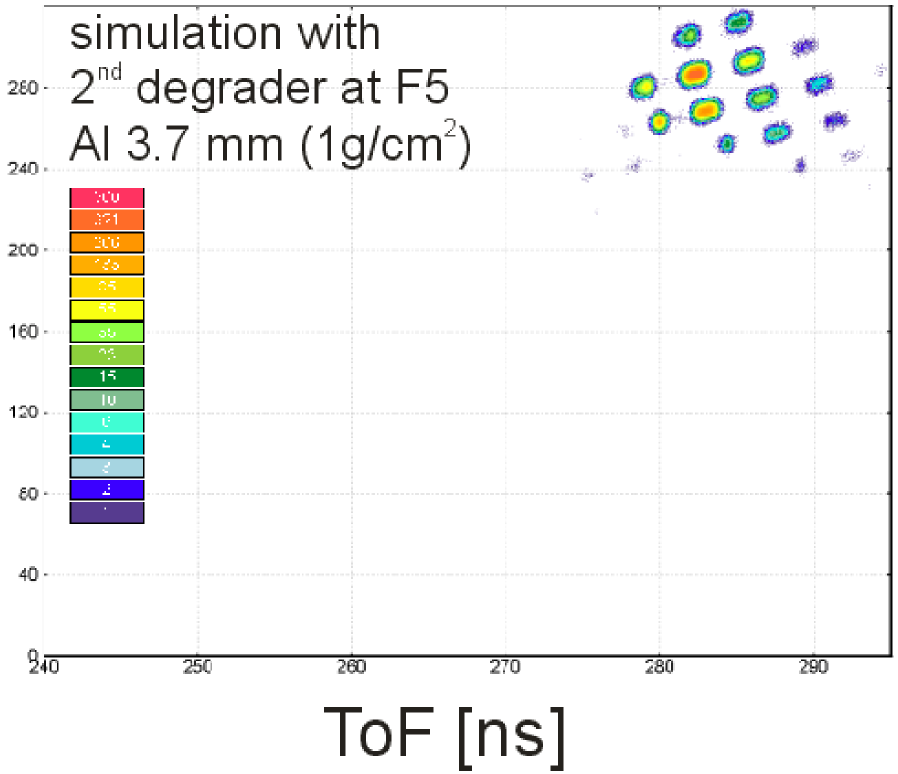

Ratio: total rate / ^{76}Ni rate (=S/N).

FRIB Separator

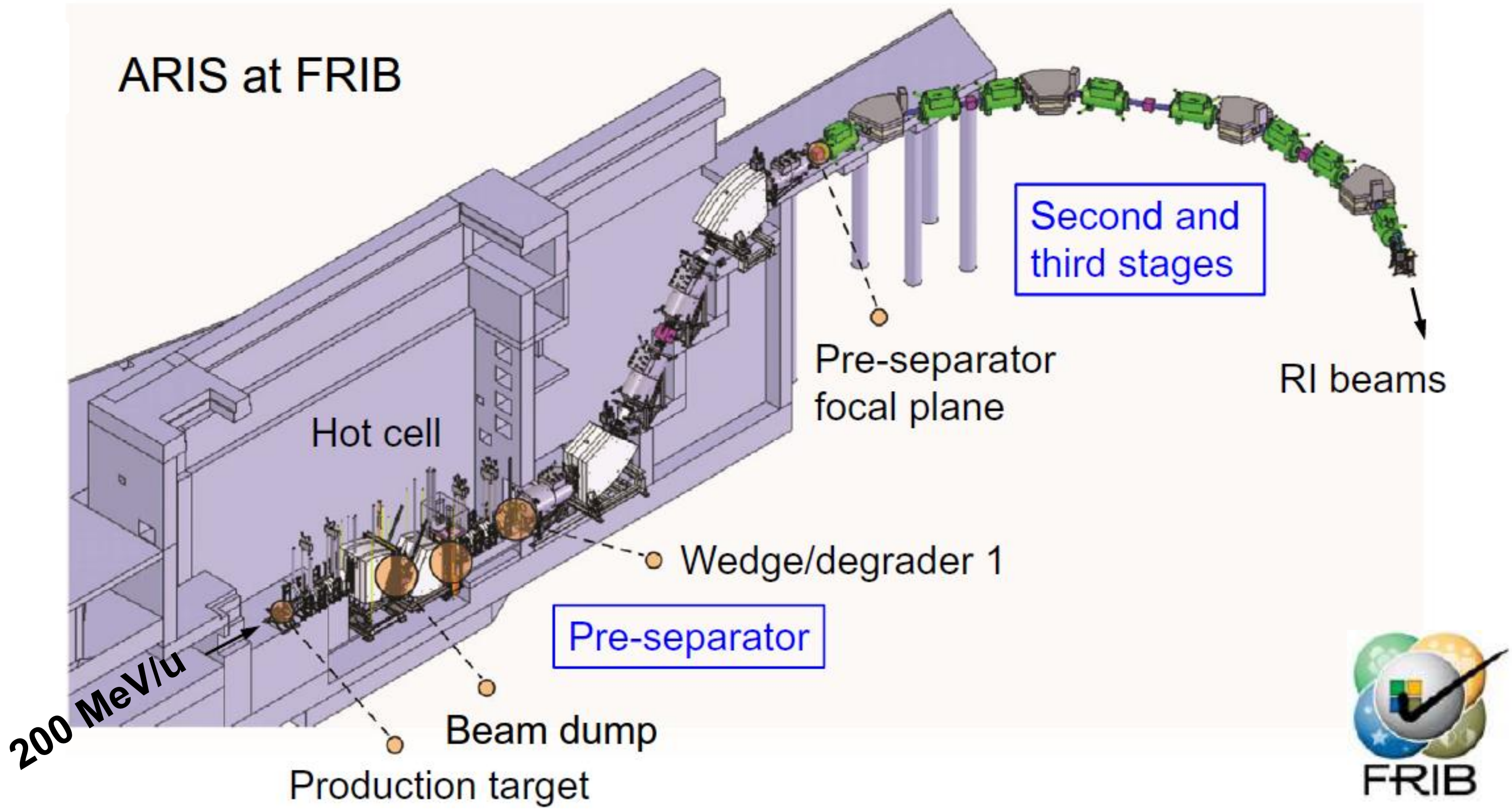

- Asymmetric pre-separator to compress Bρ spread by factor 3
- Pre and main separator in different planes

M. Hausmann, M. Portillo, C. Wilson et al.

Q-State Effect on Separator

Separation of ^{213}Fr

optimum combination of q-states and stripper materials at different energy, FRS with achromatic S2 degrader in LISE^{++}

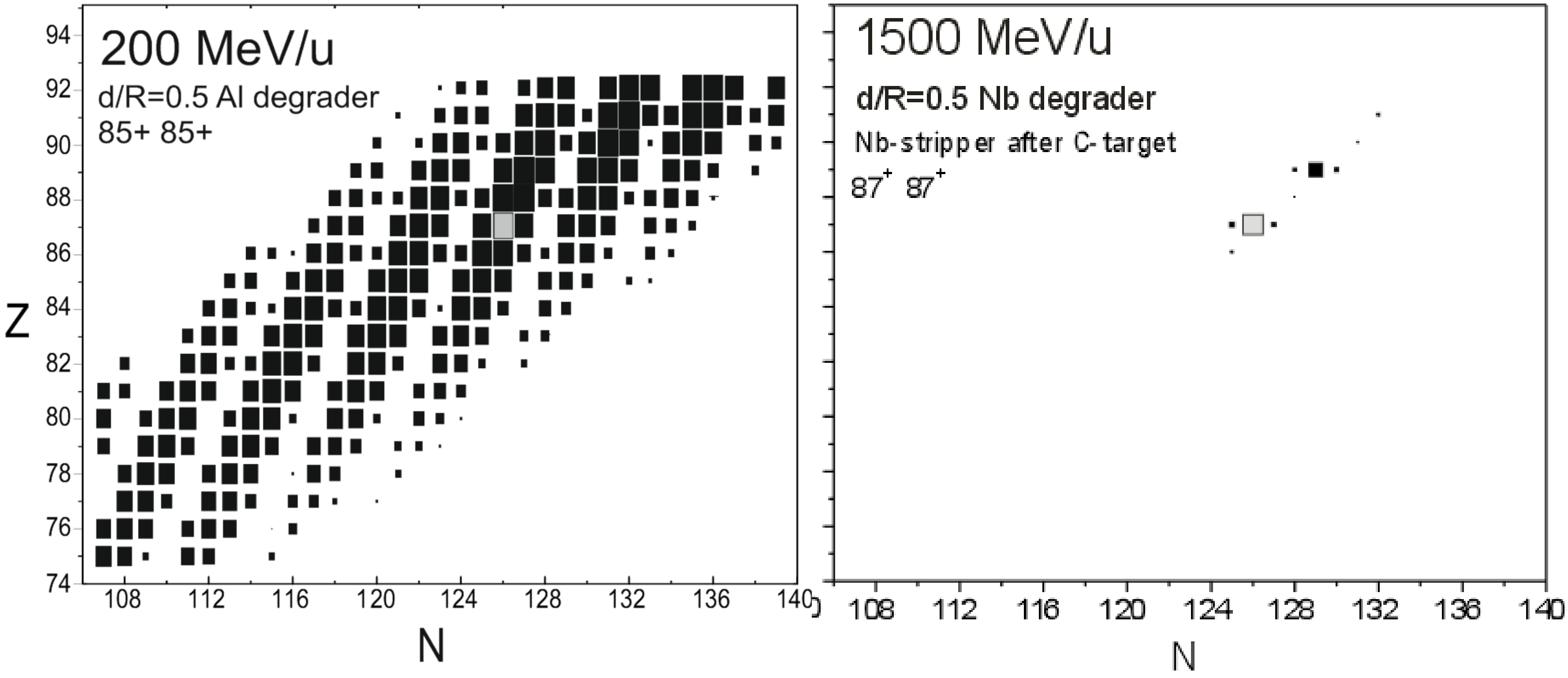

Change in q in degrader fools the Bρ-ΔE-Bρ separation

Separator Comparison

			in LAB			normalized to Bρ =18 Tm for m/q = 2.56		
		[Tm]	[mrad]	[mrad]	[%]	[mrad]	[mrad]	[%]
	stages	Brho	a	b	dp/p	a	b	dp/p
FRS	1	18	11	17	1.2	11.0	17.0	1.2
A1900-MSU	1	6	30	50	2.9	10.0	16.7	1.7
BigRIPS	2	9	55	40	3.0	27.5	20.0	2.2
Super-FRS	2	20	40	20	2.5	44.4	22.2	
ARIS-FRIB	3	7	40	40	4.5	15.6	15.6	2.9
HFRS	2	12.75-25 limited by BRing	30	25	2.0	21-42	18-35	

Forward focusing (Lorentz transformation)

transverse: $a = p_x / p_0$

longitudinal: $\Delta p_z/p = \gamma \; p_z / p_0$

	[mm] x0	$R=\frac{(x\|\delta)}{2(x\|x)x_0}$	[m^2] dipole area*
FRS	1.2	3385	2.36
A1900-MSU	1.0	1480	0.68
BigRIPS	0.5	2850	1.28
Super-FRS	1.0	2900	4.08
ARIS-FRIB	0.5	1300	0.96
HFRS	1.0	1100	

Resolution limit by energy-loss straggling in half range thickness degrader, R ~ 800.

One can also use large area dipoles for high-resolution physics experiments, spectrometer for secondary beam.

* for 2 dipole stages

Range Bunching
Monoenergetic Degrader

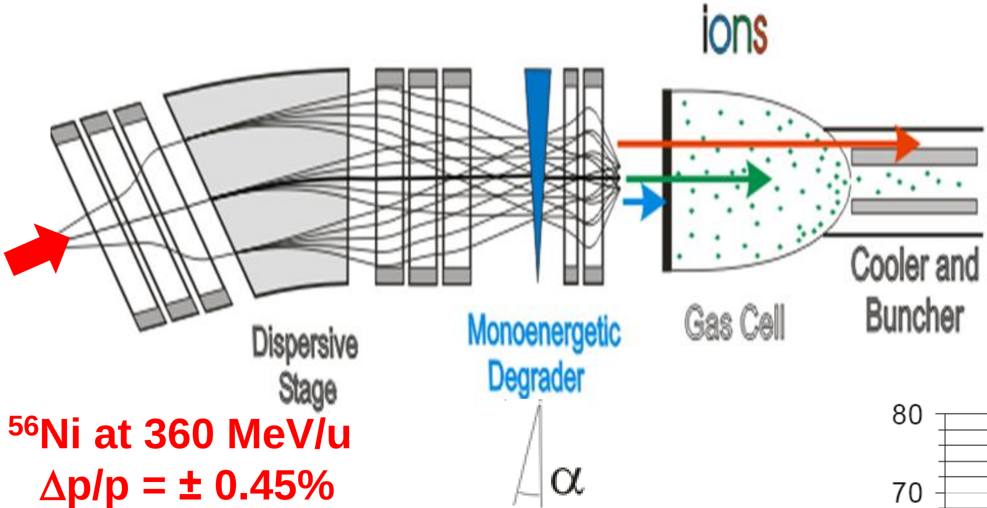

^{56}Ni at 360 MeV/u
$\Delta p/p = \pm\ 0.45\%$

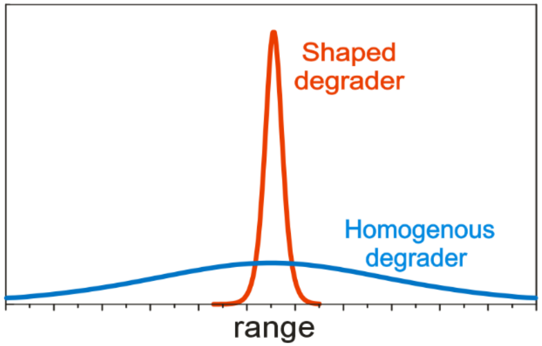

Limit by energy-loss straggling

σ_R = 9.2 mg/cm^2 Al

a typical sheet of paper is 8 mg/cm^2

momentum compression

$\sigma_p/p < 5\times10^{-4}$

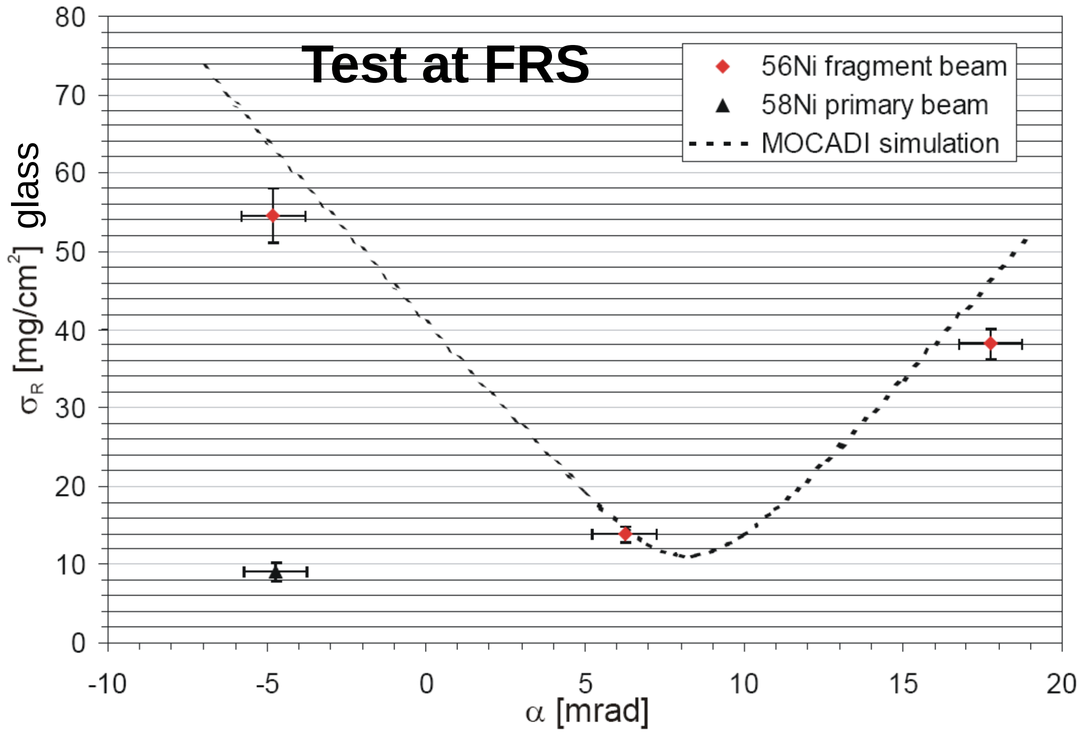

PhD thesis Michael Maier, JLU Giessen 2004

Separation in Range

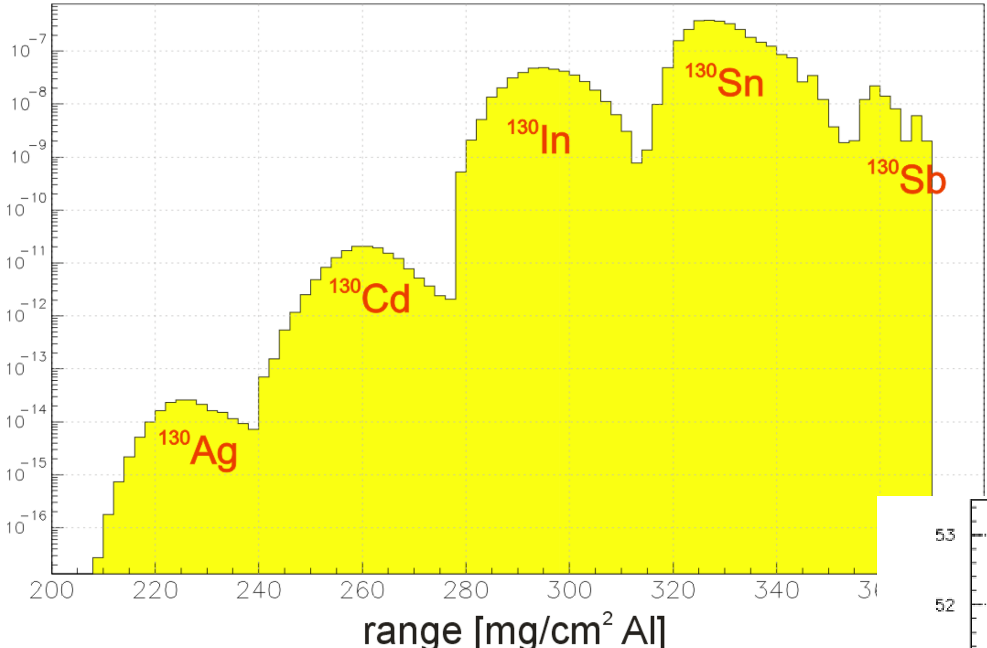

Separation of isobars in range for stopping in gas cell.

σ_R (^{130}Cd) = 7.5 mg/cm^2

Separation in range also not hindered by transverse emittance increase.

MOCADI simulation with extra stage behind Super-FRS.

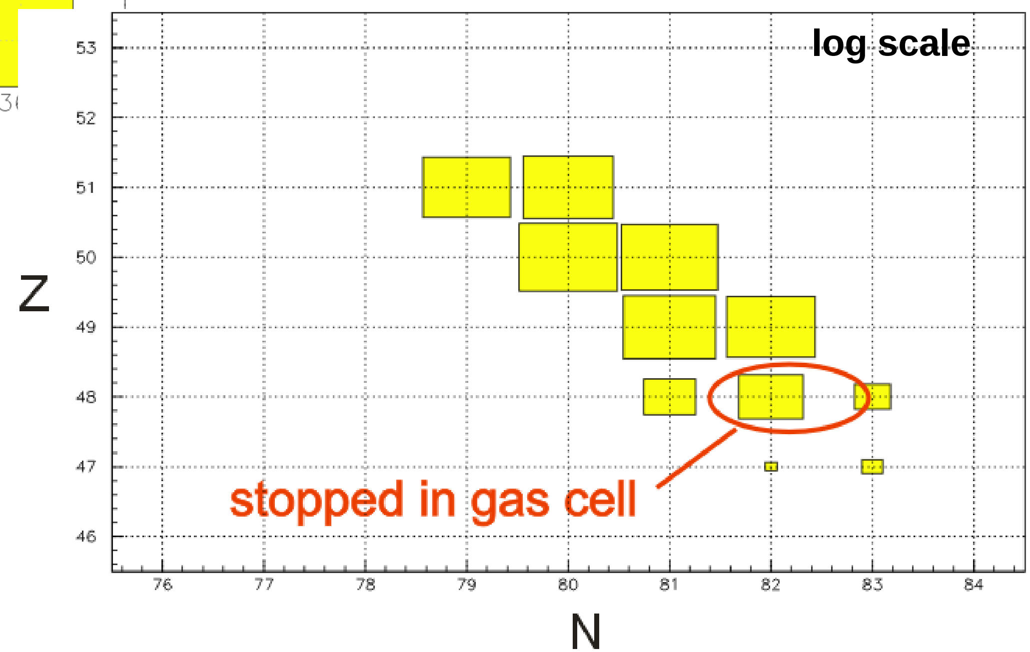

Influence of Degrader Shape

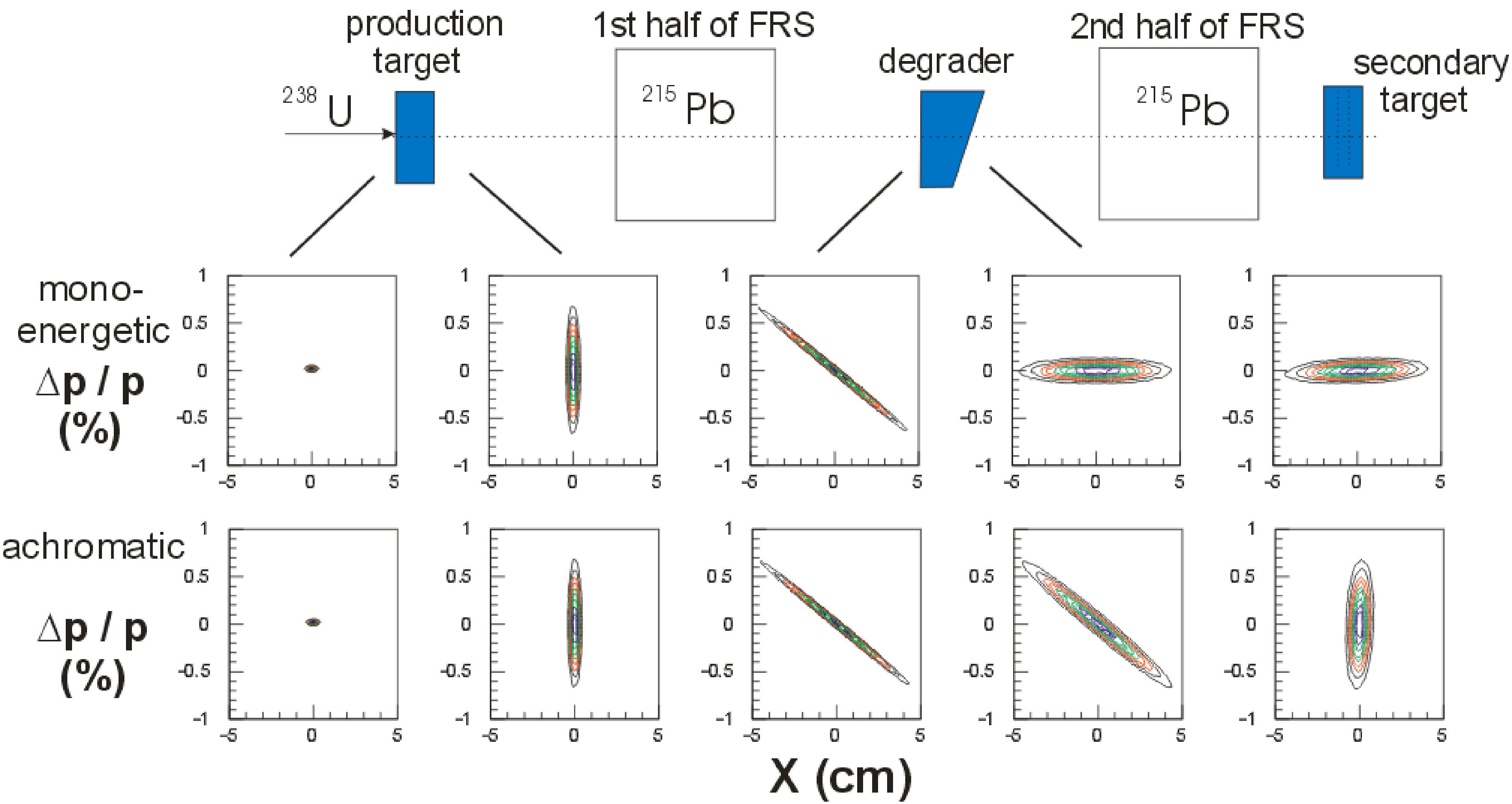

6. FAIR Status

FAIR - Facility for Antiproton and Ion Research

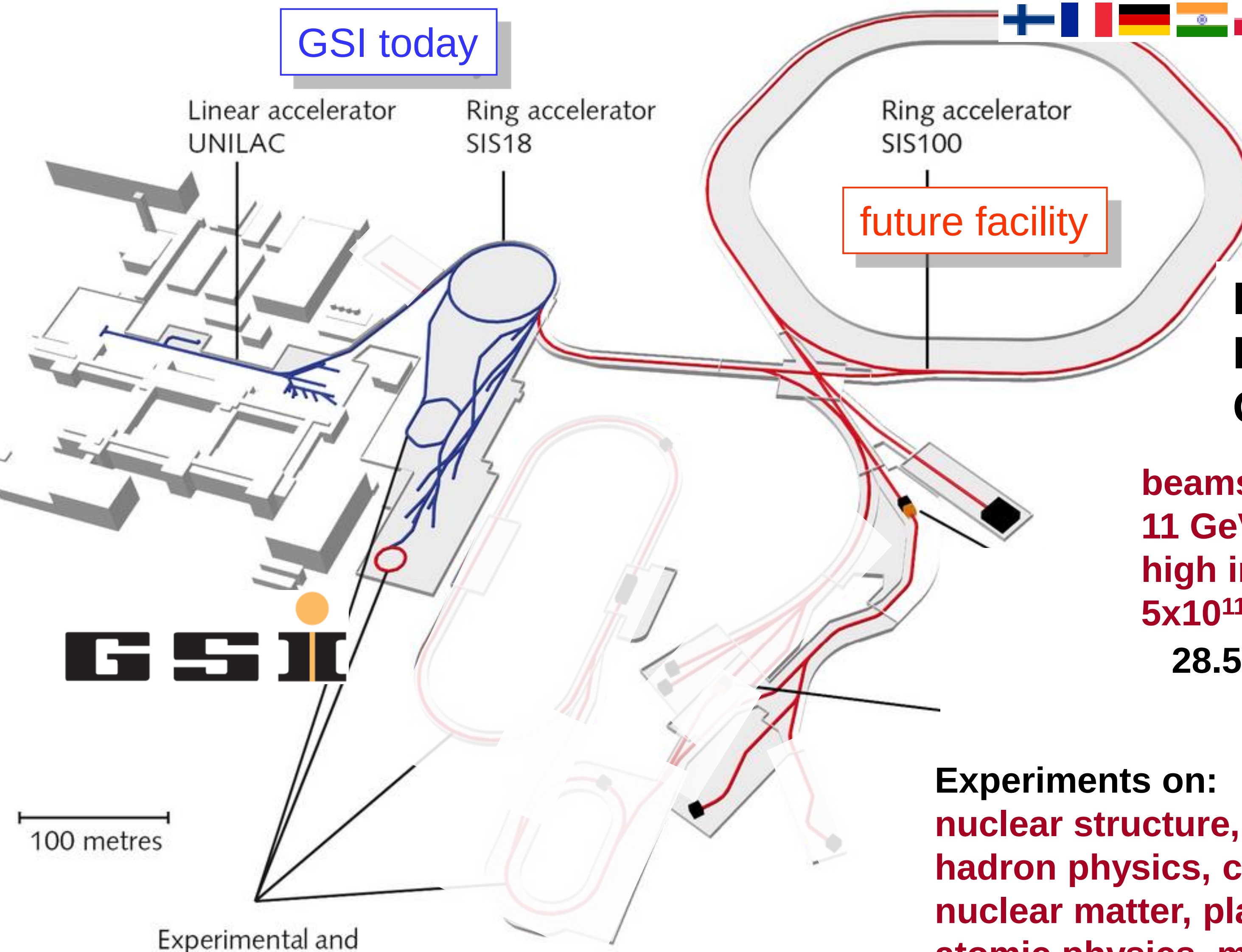

FAIR Gmbh

International Partners 8+2, Germany >50%

beams with energies of 11 GeV/u ^{238}U, 27 GeV p
high intensity up to 5×10^{11} U Ions/pulse
28.5 kJ per pulse

Experiments on:
nuclear structure, astro physics hadron physics, compressed nuclear matter, plasma physics atomic physics, material science, bio physics

FAIR civil construction

SIS-100

Ion synchrotron for p - U **$B\rho_{max}$ = 100 Tm**

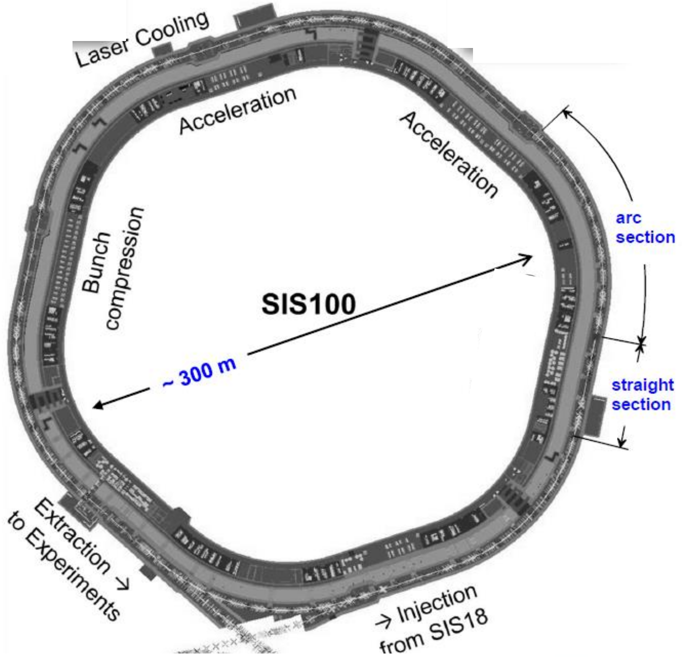

Acelerate U^{28+} to avoid space charge and one stripper. UHV in danger by beam losses. Cryogenic catchers for ions changing charge.

FODO cells but asymmetric.

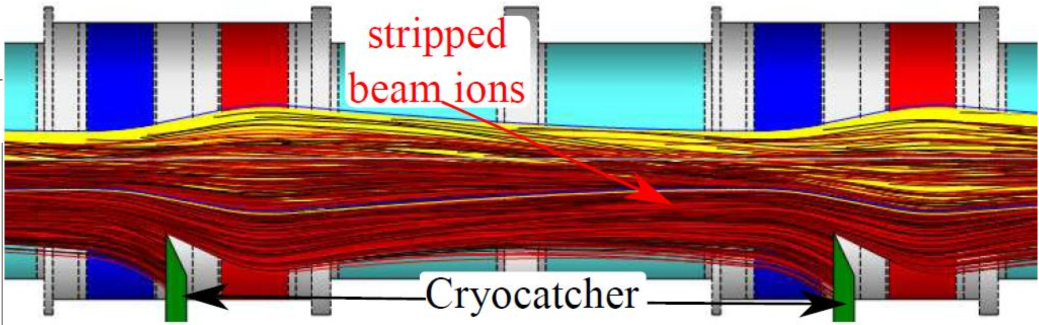

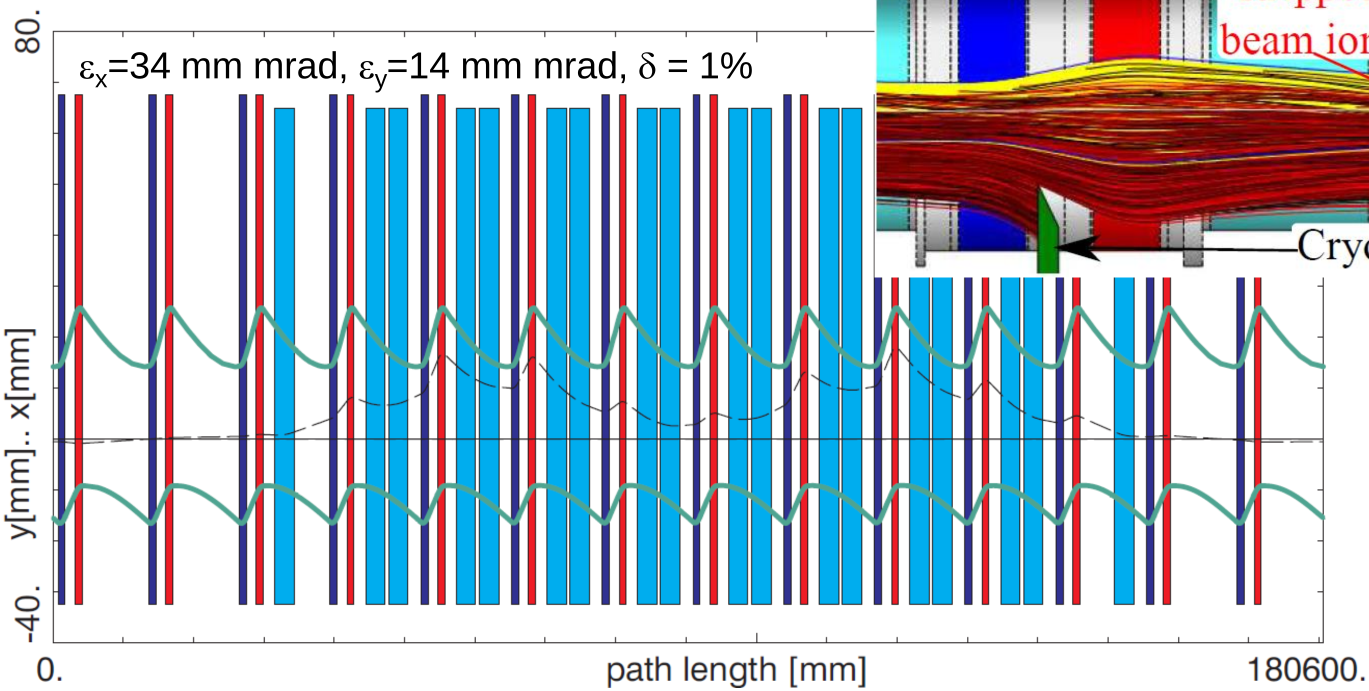

1/6 of total 1084 m.

a little bit of separator

J. Stadlmann et al., EPAC 2006
L. Bozyk et al., EuCARD 2012

Building Construction Super-FRS

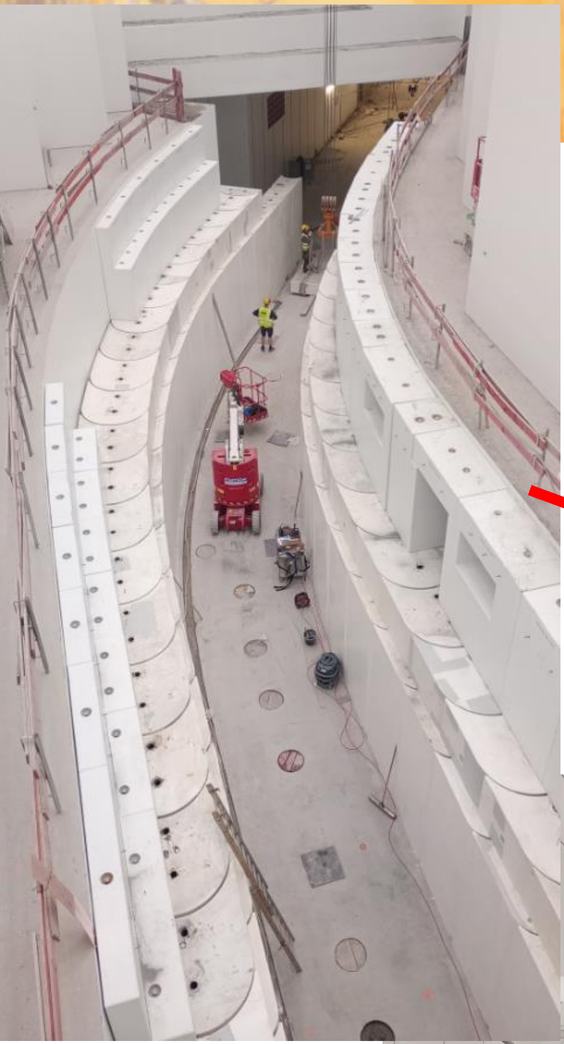

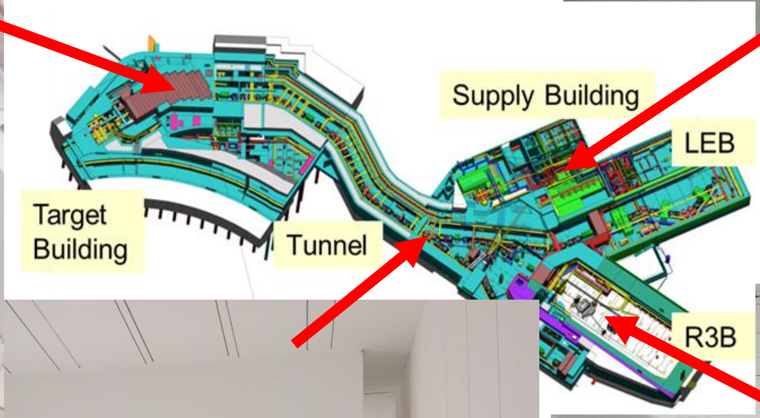

FAIR Magnets

external storage hall, beamline magnets

SIS100 sc magnets

big rad. hard dipole 95 t

sc multiplets
for SuperFRS

BE42 storage at GSI

Pre-assembly place at GSI

in SIS100 tunnel

The END

7. Simulation

Input for Simulation

<u>nuclear physics:</u>

reaction kinematics
production cross sections
nuclear absorption

codes:

MOCADI
LISE++

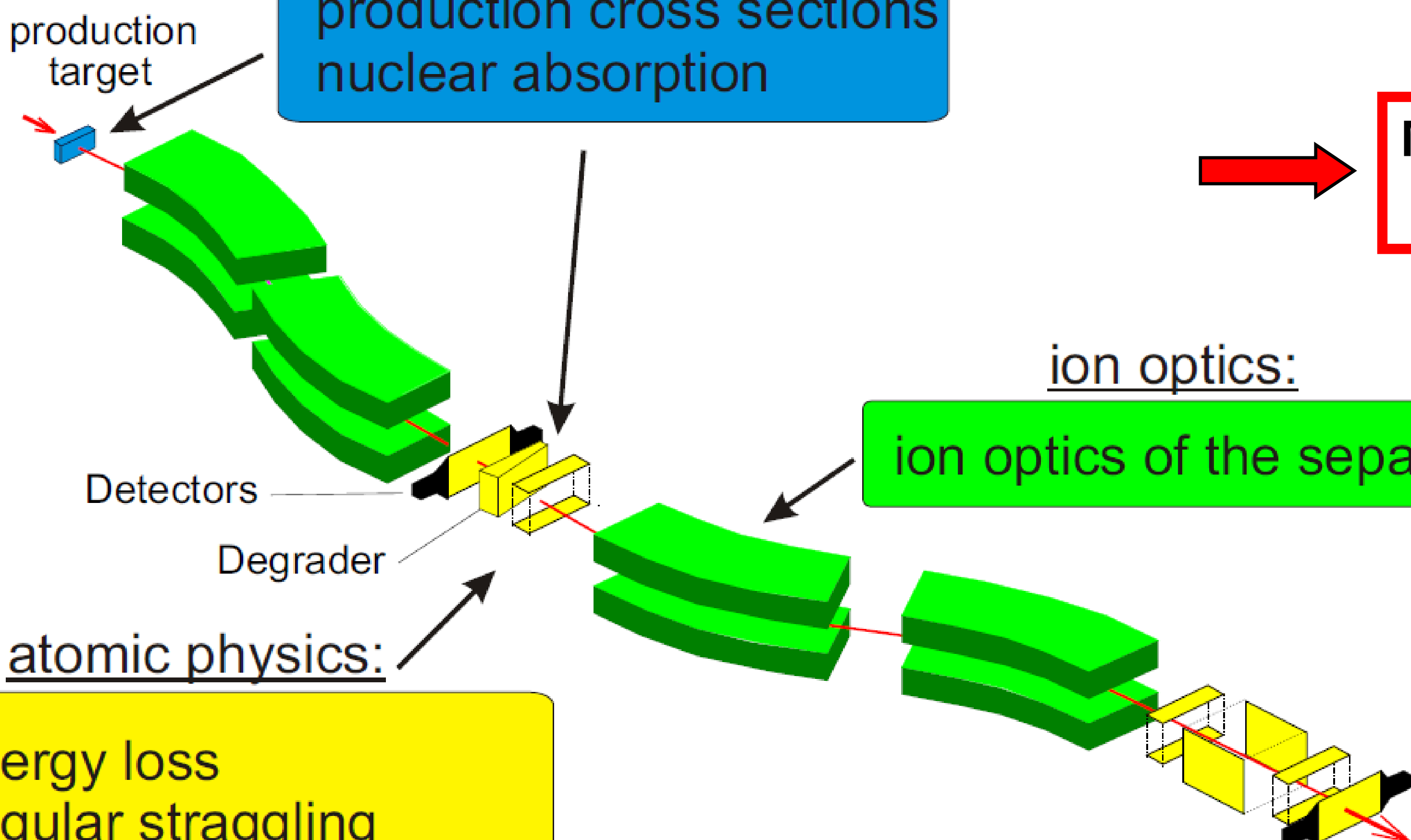

<u>ion optics:</u>

ion optics of the separator

<u>atomic physics:</u>

energy loss
angular straggling
charge state distribution

Monte Carlo
MOCADI / LISE^{++} MC

<u>MOCADI/LISE^{++} MC are optimized for beamlines with matter:</u>
ion always fly in forward direction, no multiplicity,
physics routines adjusted for beamline needs,
GEANT would be orders of magnitude slower and
more complicated to setup.

<u>Speed:</u>
Do not evaluate physics for each ion,
use parametrizations (Goldhaber, Morrissey, EPAX)
and precalculated results (ATIMA spline tables for energy loss),
optics parametrized by transfer matrices, no magnetic fields.

<u>Biasing:</u>
10^{10} ions/s like in reality are impossible for MC,
Do not create fragments with probability like in reality.
Calculate a certain statistics for one nuclide and biasing
is done by the very different production cross sections.

Example MOCADI

Bρ distribution after target
^{68}Ni fragments from ^{86}Kr

PAW: nt/plot 1.brho(1)
Root: T->Draw("brho[0]")

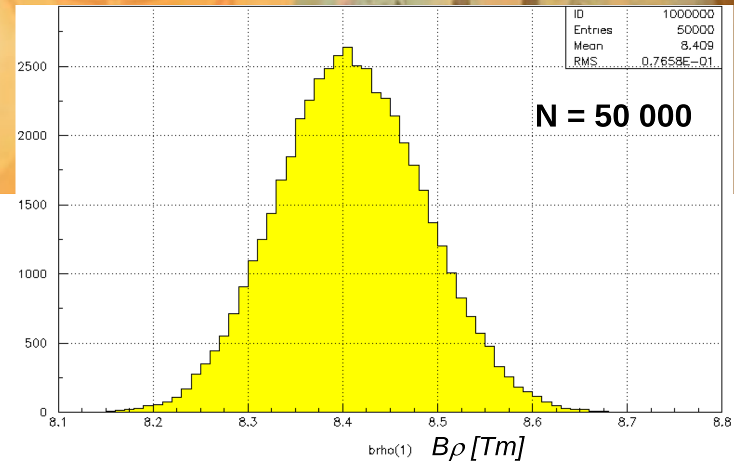

list of variables in output

```
N
X(N)
A(N)
Y(N)
B(N)
ENERGY(N)
TIME(N)
MASS(N)
Z(N)
ELNUM(N)
TOF(N)
DE(N)
BRHO(N)
WEIGHT(N)
RANGE
tpos
```

x position at dispersive focal plane S2

nt/plot 1.x(2)
T->Draw("x[1]")

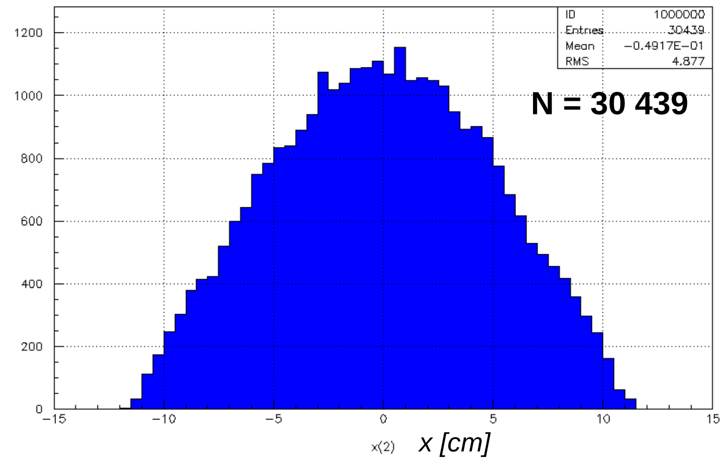

Correlation

nt/plot 1.x(2)%brho(1)
T->Draw("x[1]:brho[0]")

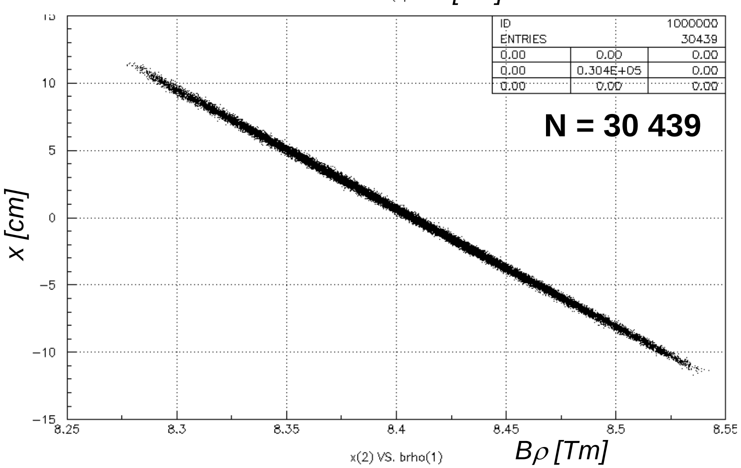

Convolution Technique

Each target, each piece of matter in beamline, each collimator reshapes the distributions in position, angle, energy of an ion species

Example:

Energy distribution after thin target,
Goldhaber distribution, Gaussian shape, $f(E)$

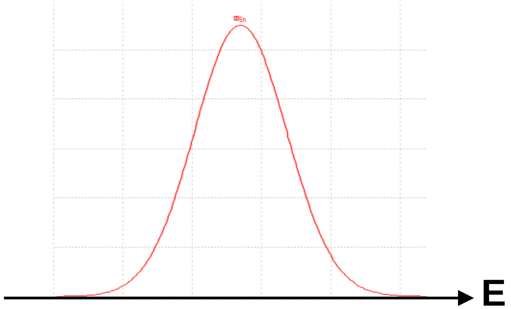

Energy difference by slowing down in thick target,
difference in dE/dx for projectile and fragment
depending on Z_p vs. Z_f and reaction position, $g(E)$

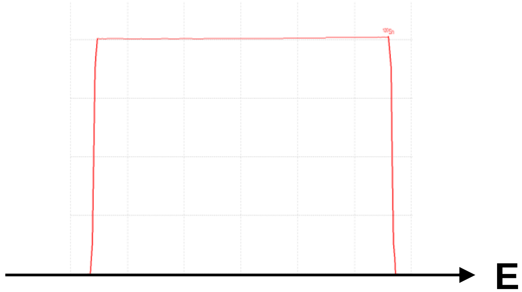

Combined effect given by the convolution of the two distributions

$$h(E) = (g * f)(E)$$

$$= \int_{-\infty}^{\infty} f(E-E')\ g(E')\ dE'$$

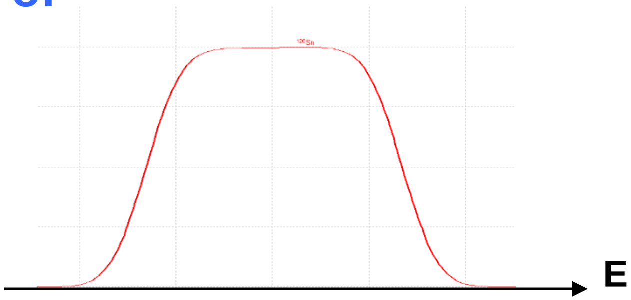

Convolution Technique (2)

programs:
LISE^{++} or LIESCHEN

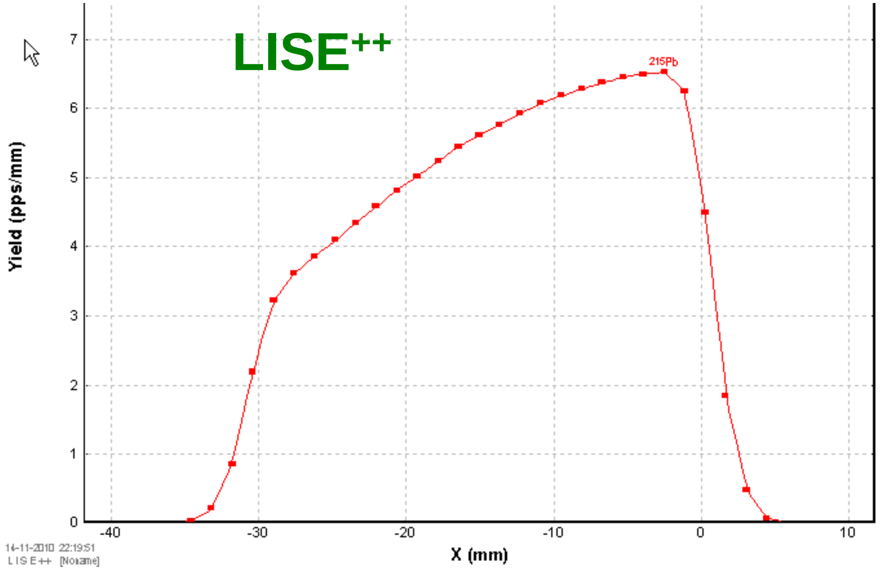

x-distribution described by 32 points

- **+ Fast as only a low number of points has to be calculated. Calculation of all fragments possible while watching.**
- **+ Parametrization on log scale, even small tails are still visible**
- **- Becomes very difficult with many cross correlations.**
- **- Usually limited to linear transformations (only 1st order optics).**

Simplifications for Convolution

Example in FRS:
star shaped vacuum chamber is difficult to describe in convolution technique. Only use independent cuts in x or y distribution.

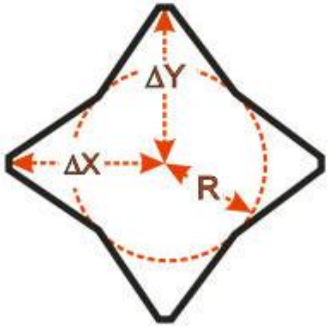

Details cannot be taken into account, so we do not try.
This also means more simplifications are allowed.
Replace single aperture cuts by effective cut for whole section.

One cut (x, y) after each separator stage,
one angular acceptance (a, b) for each stage (TA-S1, S1-S2, S2-S3, S3-S4).

FRS-TA2-S4_2014.lcn

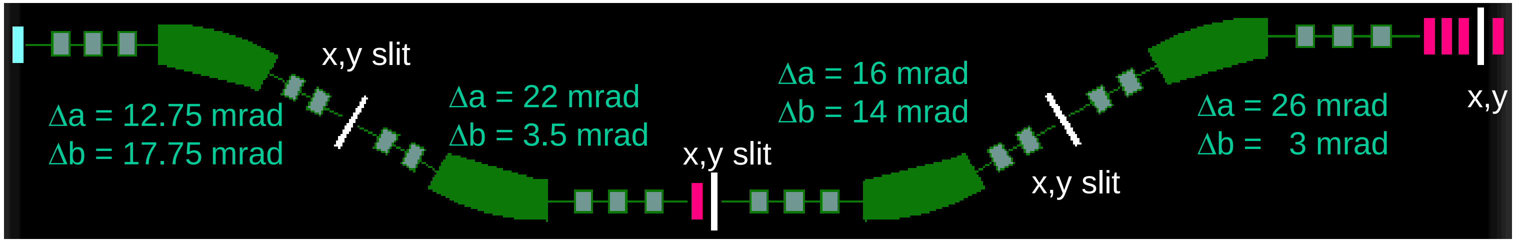

Values used in LISE are adjusted to values of a MOCADI simulation.
In normal FRS operation agreement of transmission within 20%

Goals

We can separate to single nuclide species (exception very high Z and A), but we do not have to !

The goal is to reduce the count rate enough so that detectors will work. Separation will always cause additional losses, slits or nuclear reactions in degraders, angular scattering, …

Typical limits:
DAQ (kHz), MUSIC (10 kHz), Sci(<MHz), TPC (10-100 kHz), Si implantation (100 Hz)

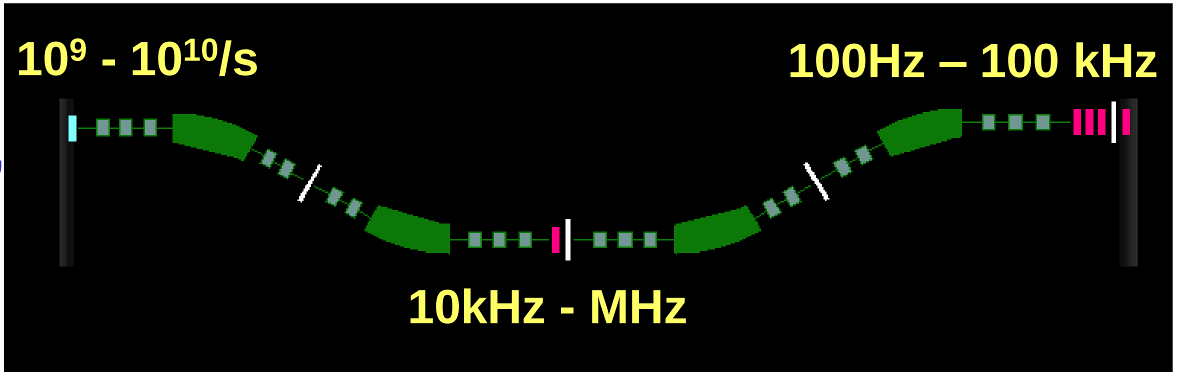

Predict the degrader settings to get beam at the wanted energy or to implant ions.
Provide input of beam sizes, energy spread, also for further simulations with more detectors.

Separator Setting for ^{212}Pb

from older FRS experiment

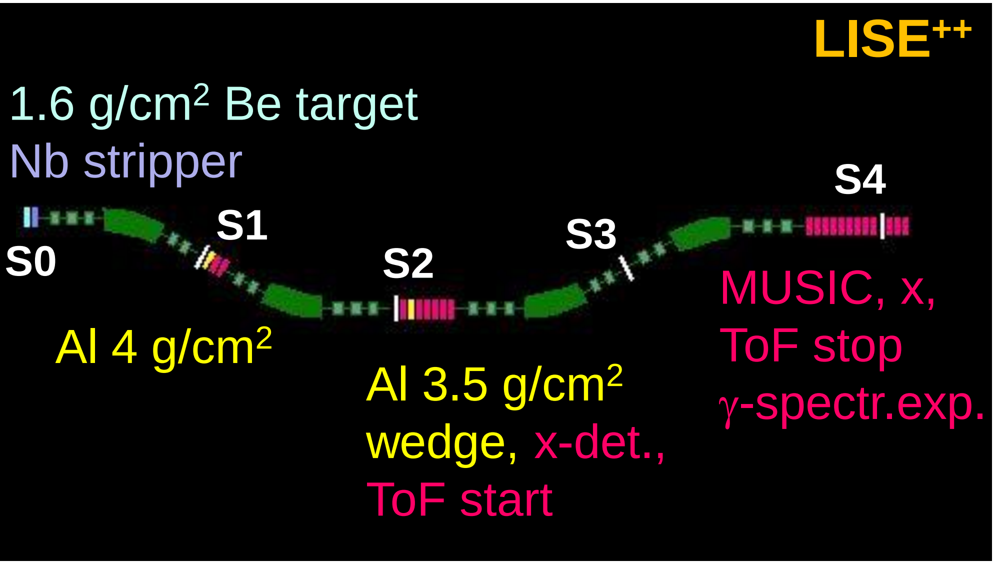

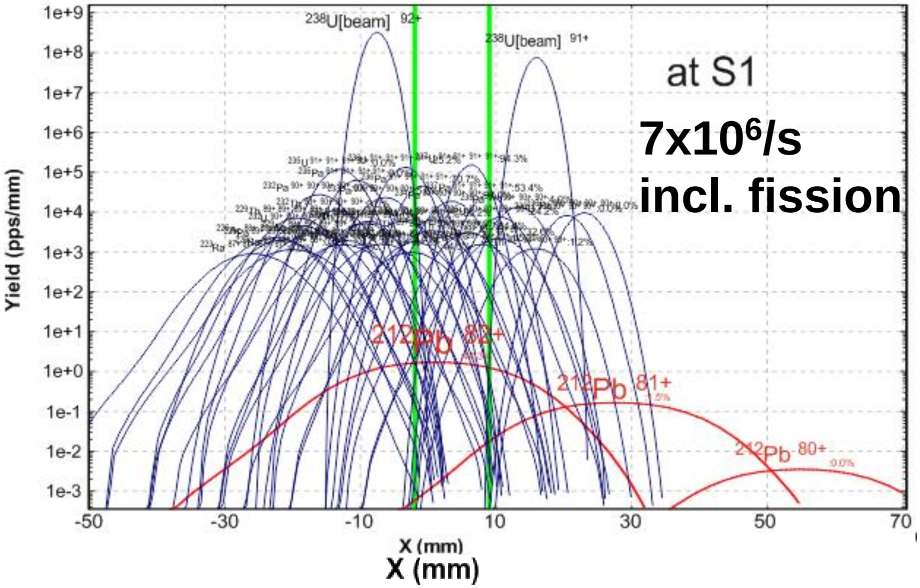

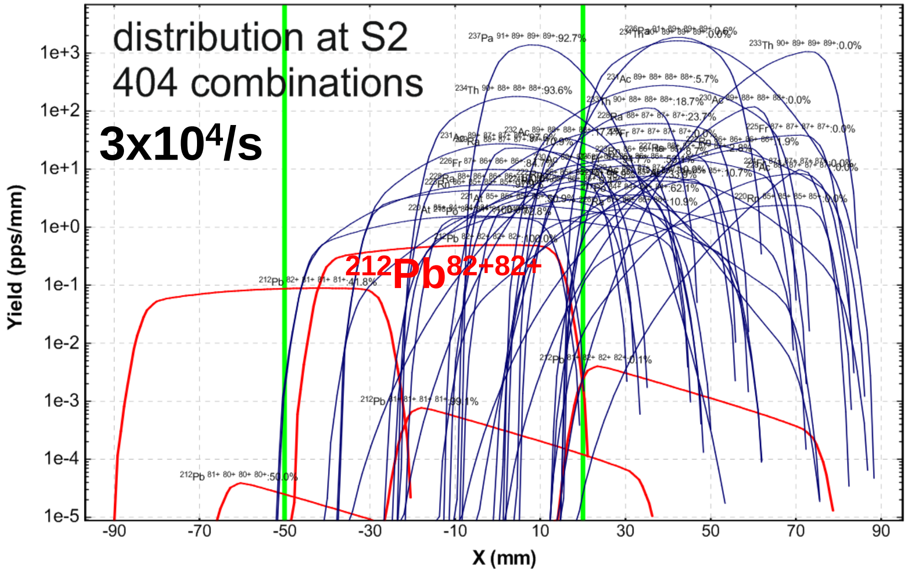

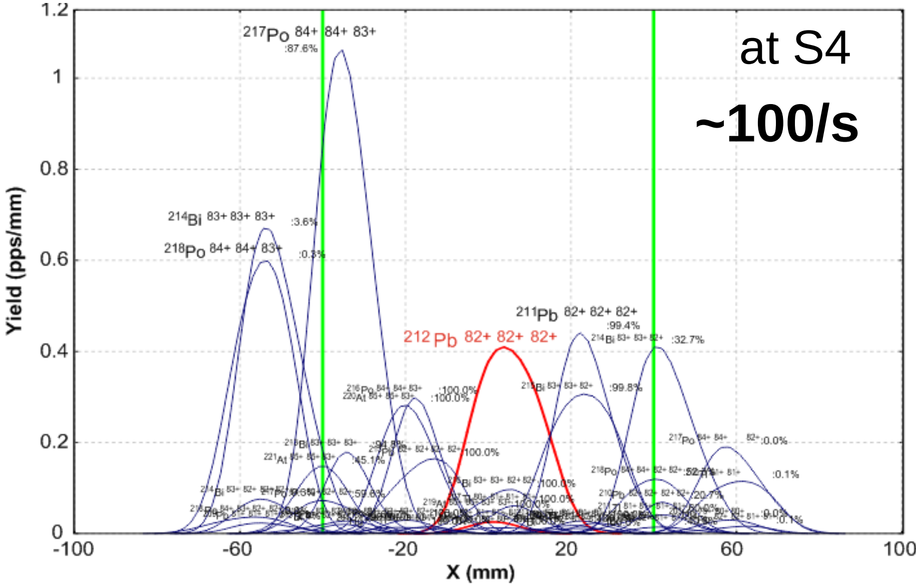

Details with Monte-Carlo

primary U beam at S1

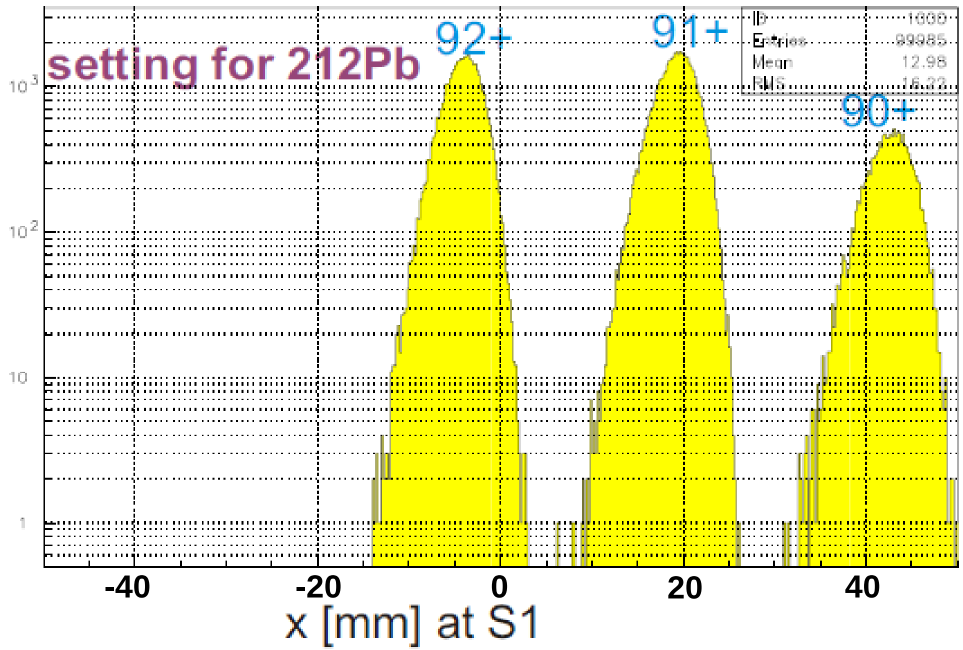

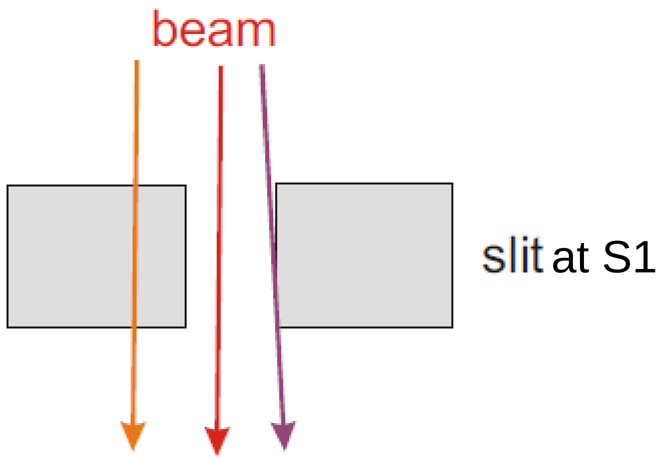

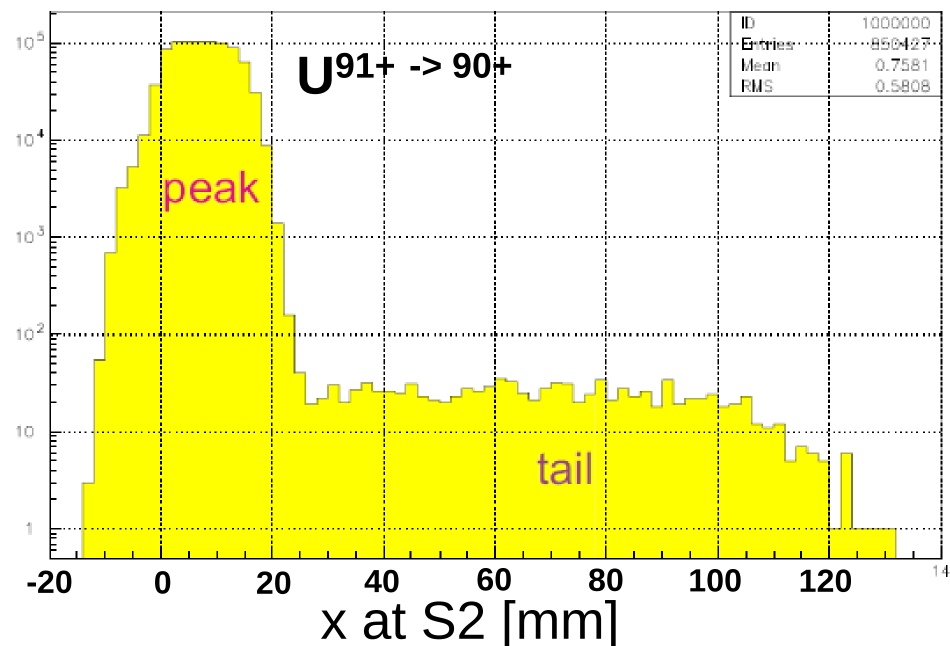

MOCADI

Really the END

Requirements / Boundaries

High nuclear production cross section for fragmentation, ~ $A_t^{2/3}$
Not too high energy loss in target, less electrons (low Z_t)
➔ best fragmentation yield for low Z_t materials (Li, Be, C).

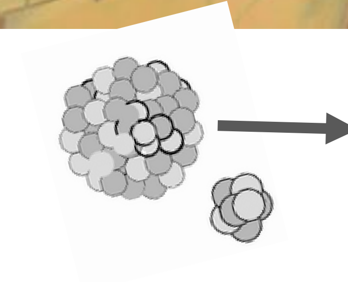

No big difference between projectile and fragment, at best $Z_p^2 / A_p \sim Z_f^2 / A_f$
Or increased energy spread by location straggling inside thick target.

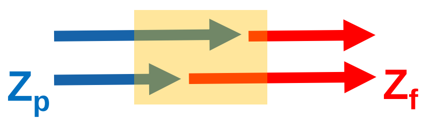

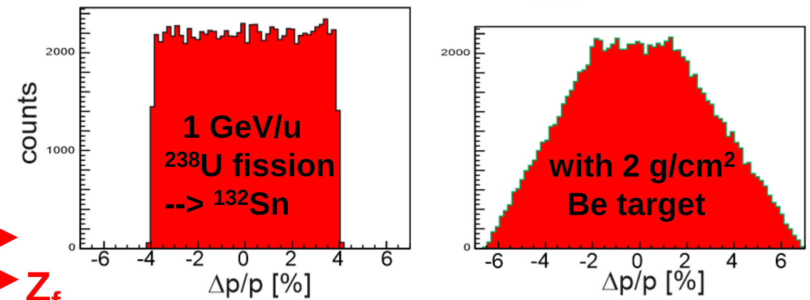

Thicker target → lower energy → larger emittance → lower transmission
Very thick → destruction of wanted fragment, but also possibility of enhancement via intermediate fragments.

Small beam spot on target to keep emittance increase low.
→ Not too large longitudinal target extension, otherwise not all in focus.

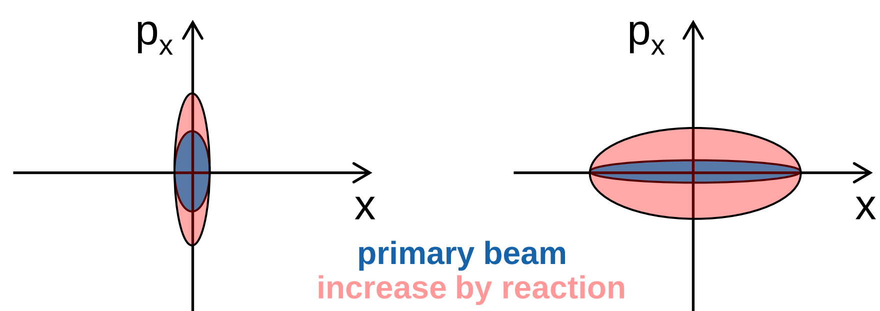

Production of Rare Isotopes

(Reactions, kinematics in-flight)

Projectile Fragmentation

Projectile Fission

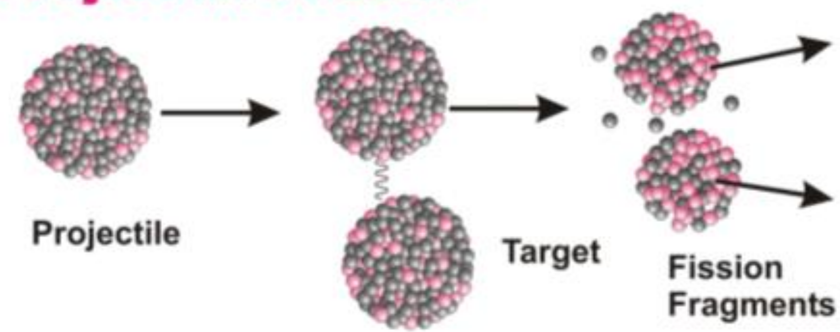

$$^{238}U + 0.1\ mg/cm^2\ {}^{12}C \longrightarrow {}^{132}Sn$$

$$^{124}Xe + 0.1\ mg/cm^2\ {}^{12}C \longrightarrow {}^{100}Sn$$

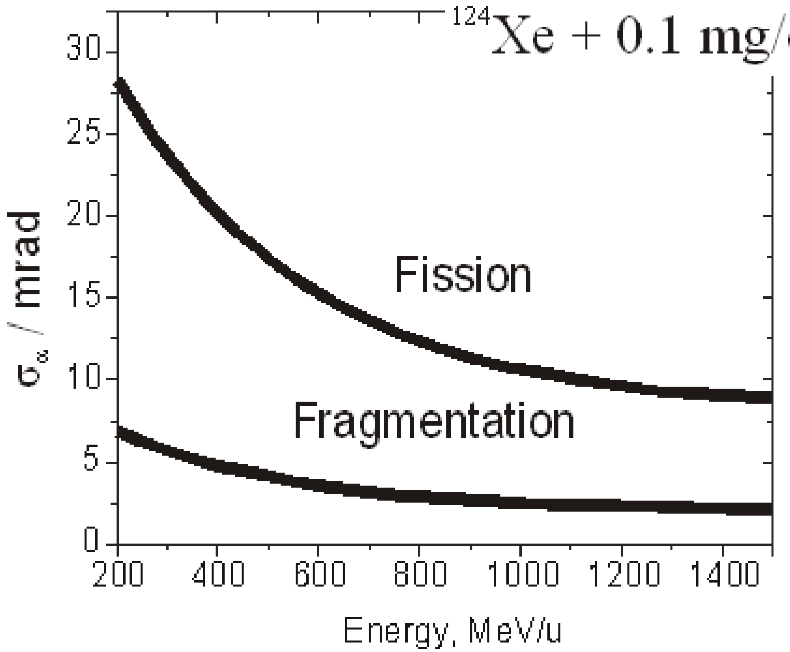

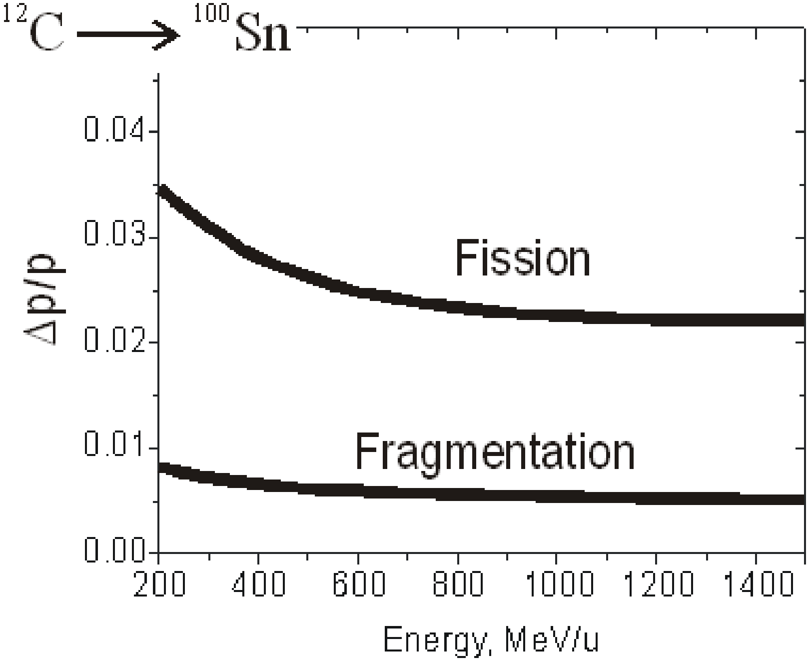

Production Cross sections

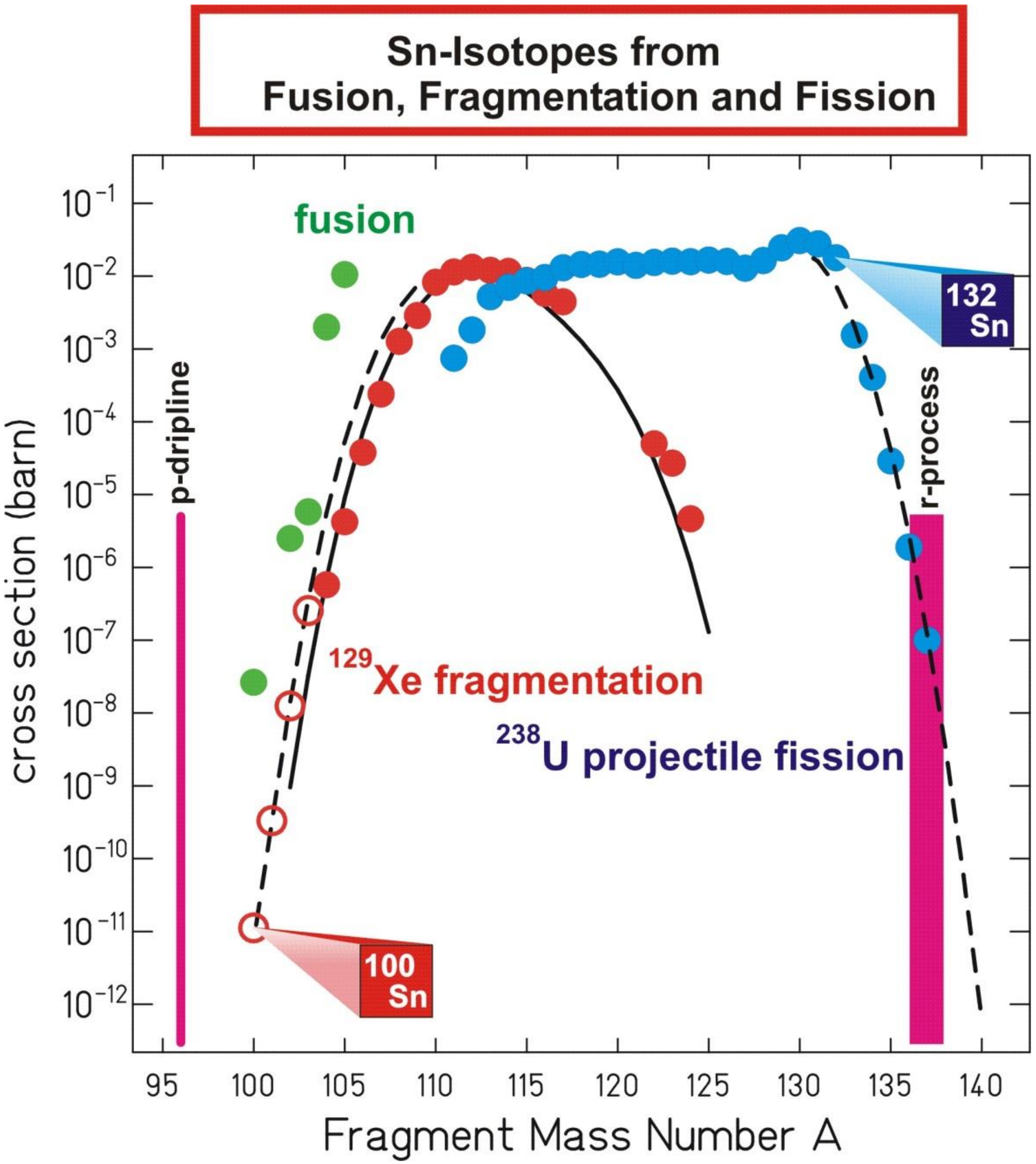

codes:

EPAX 3

parametrization of cross sections
K. Sümmerer, B. Blank

ABRABLA

J. Benlliure, K.H. Schmidt, et al.

LISE Abrasion/Ablation

O. Tarasov

+ Experimental data

Material in Fast Pulsed Beam

a simple temperature and stress calculation

Instantaneous energy deposition

$$\frac{dQ}{dm} = \frac{dE}{\rho dx} \frac{n}{\Delta x \, \Delta y}$$

stopping power
number of ions
spot size

$$\Delta T = \frac{dQ}{dm} \frac{A}{c_{mol}}$$

molar mass
heat capacity

at high T

$$c_{mol} \sim 25 \frac{J}{mol\,K}$$

low A ➔ low ΔT

$$P = K \; \alpha \; \Delta T$$

bulk modulus
thermal expansion coeff.

polycrystalline graphite, more nuclear x-section less slowing-down by electrons.

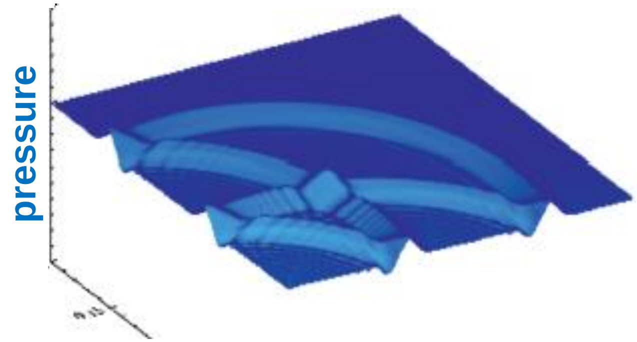

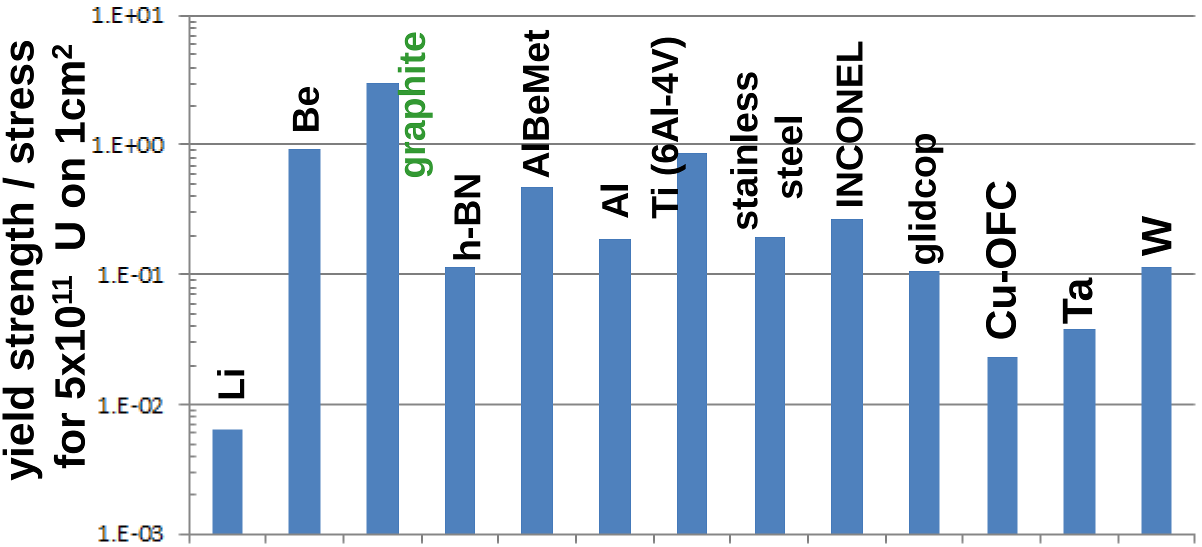

Initial compressive pressure, wave propagates to boundary → tensile stress.

plastic deformation not exactly elastic, cyclic stress, cracks?

Optical Elements of FRS

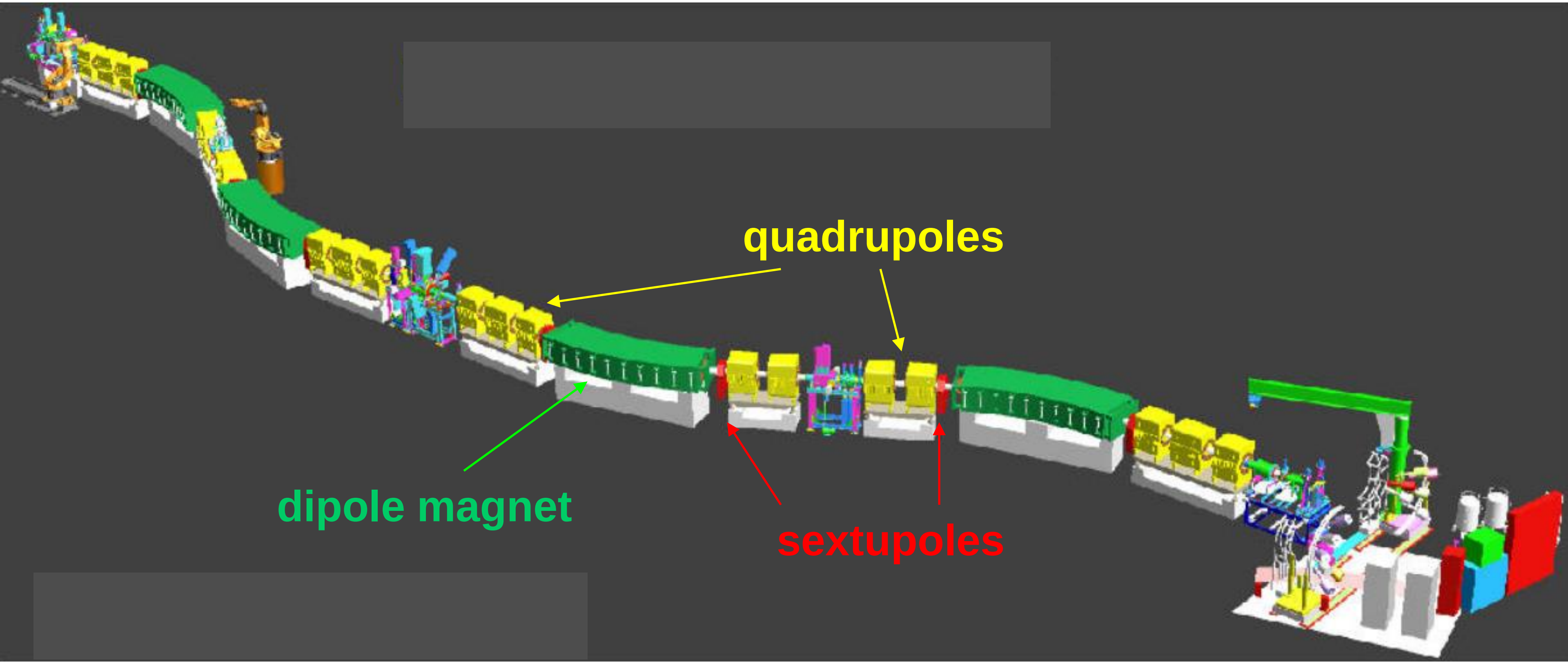

Steps

Choose target, primary beam, initial energy

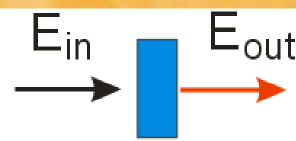

Scale magnets of 1st half of FRS

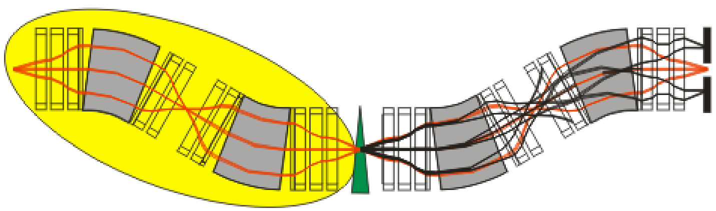

Scale magnets of 2nd half of FRS

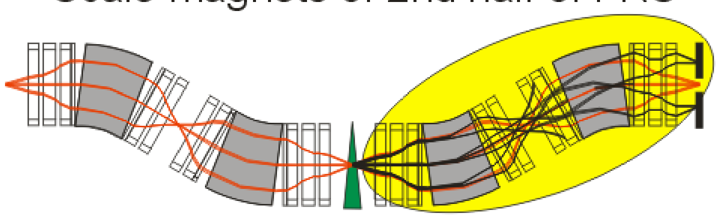

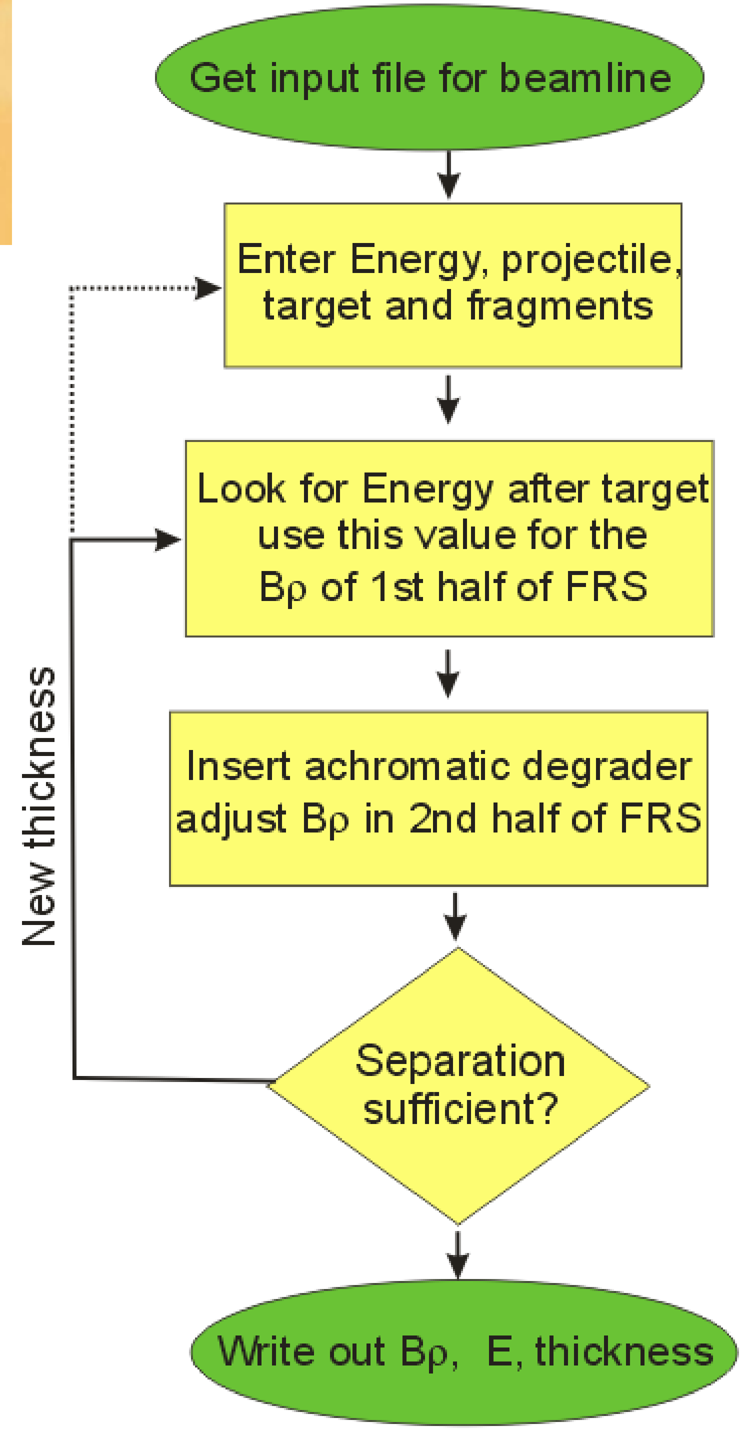

Effect on Fragment Separator

Separation of ^{213}Fr

optimal combination of q-states and stripper materials at different energy, FRS with achromatic S2 degrader in LISE^{++}

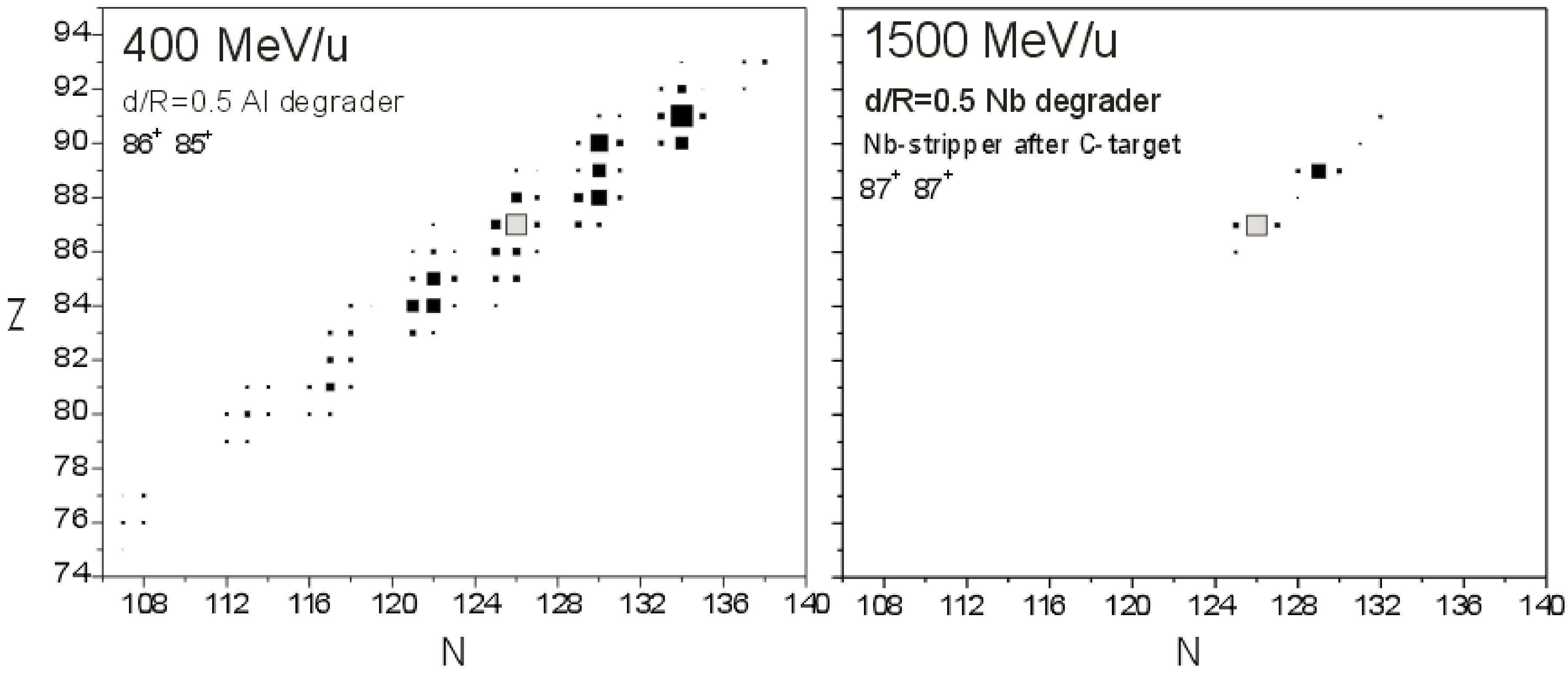

change in q at S2 fools the Bρ-ΔE-Bρ separation